AUTOMATIC SHIP HULL SURFACE MODELING AND HYDRODYNAMIC OPTIMIZATION

TANMOY DAS

Automatic Ship Hull Surface Modeling and Hydrodynamic Optimization

by

©Tanmoy Das

A thesis submitted to the School of Graduate Studies
in partial fulfillment of the requirements for the degree of
Master of Engineering

Faculty of Engineering and Applied Science
Memorial University of Newfoundland

April 2013

St. John's Newfoundland

Abstract

Engineers have always been fascinated by the optimality of an objective function of interest. Hydrodynamicists in the ocean and naval architectural engineering field have always sought to improve the hydrodynamic performance of any floating structure. For a moving vessel, wave resistance is one of the most important properties of hydrodynamic performance, and it influences a ship voyage economically by significant effect on EHP or fuel consumption. Therefore, reduction in wave resistance of any ship will help in reducing fuel cost.

The present study investigates the scope for optimization of ship hulls based on wave resistance by modifying their geometries. During modification, there are geometric constraints to be maintained required by design and operational criteria.

The calculation of wave resistance is based on a numerical solution, where ship hull surface discretization is required. An automatic hull generation and discretization system was developed, where a table of offsets or general coordinates of ship hull can be used as input. Then, the process proceeds with the BFGS (Broyden-Fletcher-Goldfarb-Shanno) optimization algorithms integrated with three different hull geometry modification methods. MAPS Resistance Version 2.0 was utilized to calculate wave resistance (the objective function) inside the algorithm.

An integrated program employing FORTRAN 90 was developed, which is able to represent a ship hull mathematically and graphically utilizing B-spline surface and IGES format, respectively. This system is also able to process an optimization algorithm with direct feedback

from the resistance evaluation unit. It will produce different sets of modified ship hull shapes with improved wave resistance. Therefore, it can serve a variety of interests determined by needs of a project.

Several types of ship hulls were developed and checked for geometric validation, and results were satisfactory. Two basic ship hulls (Wigley and Series 60 Hulls) were further investigated for their wave resistance coefficients with published experimental data, and the convergences of results were quite acceptable. The optimum hull forms obtained from the software show improved wave resistance with significant differences in coefficient of wave resistance (C_w) values for all the selected Froude numbers. This program has been prepared in such a way that it can be adopted to search for the minima of other objective functions.

Acknowledgements

I would like to express my utmost gratitude to my supervisor, Dr. Heather Peng, under whose enduring guidance and positive directions this research was carried out. I would also like place my sincere thanks to Dr. Wei Qiu for his suggestions and technical supports in carrying out the program operation.

This work was conducted at Memorial University through the funding provided by CREATE Offshore program and financial support provided by School of Graduate Studies. I would like to acknowledge CREATE Offshore program and fellows from School of Graduate Studies, Memorial University of Newfoundland. I would like to acknowledge the help provided from the Queen Elizabeth II Library and the Engineering Associate Dean's Office the Memorial University of Newfoundland.

I would also like to express my thanks to Dr. Saoyu Ni for his suggestions and help in using the MAPS Resistance program. I would also like to express my warm appreciations to all my colleagues in the Advanced Marine Hydrodynamics Laboratory for not only their help in various aspects, but also for making the place such a friendly hub. It has been a great adventure and pleasure living in St. John's, thanks to all my friends from graduate studies and outside the school.

My deepest appreciation to my parents and sister, far away, for their love, patience and support. They were always the encouragement in pursing my goal. I would also express my apologies for not being able to be always there for them when needed.

Table of Contents

Abstract ii

Acknowledgments iv

Table of Contents viii

List of Tables ix

List of Figures ix

Nomenclature xvi

1 Introduction 1

1.1 Motivation 1

1.2 Goals 4

1.3 Concept and Workbench 5

1.4 Thesis Outline 8

2 Literature Review 9

2.1 Numerical and Graphical Hull Development 10

2.1.1 Ship Hull Design with B-Spline Surfaces 10

2.1.2 Grid Generation 13

2.2 Hull Shape Modification and Optimization 16
2.2.1 MAPS-Resistance Version 2.0 26

3 Mathematical Formulation **27**
3.1 Global Curves and Surface Interpolation 27
3.1.1 Curves Interpolation to Offset Data 28
3.1.2 Generation of the Surface through the Stations 34
3.2 Hull Surface Grid Generation 39
3.3 Hull Form Variation 44
3.4 Optimization 47
3.5 AMECRC high-speed monohull 52

4 Numerical **54**
4.1 Organization of Input File 54
4.1.1 Shape of Centerline Profile Curves 55
4.1.2 Input Files 57
4.2 Flat Bottom Ships 60
4.3 Transformation of an Offset Table to a Row×Column Data Set 60
4.4 Transom Stern Discretization Algorithm 62
4.5 Geometrical Properties 64
4.6 Input File for MAPS Resistance 65

5 Geometric Validation **66**
5.1 Series 60, $C_b = 0.6$ 67
5.1.1 Principal Properties 67
5.1.2 Coordinates of Original Ship Hull Nodes 69
5.1.3 Body Plan and Centerline Profile 70
5.2 AMECRC High Speed Monohull Model # 1 71

5.2.1 Principal Properties 72
5.2.2 Body Plan and Centerline Profile 73
5.3 Wigley Hull: Principal Properties, Body Plan, and Centerline Profile 74
5.4 US Navy Combatant DTMB 5415 76

6 Modified Hull and Wave Resistance **80**
6.1 Series 60, C_b = 0.6 80
6.1.1 Series 60, C_b 0.6: Stations Shift 82
6.1.2 Series 60, C_b 0.6: Change in y-coordinates of Stations 84
6.1.3 Series 60, C_b 0.6: Changing the Vertical Location of Nodes on Stations 87
6.2 Wigley Hull, L/B = 10 and L/T = 16 91
6.2.1 Wigley Hull: Stations Shift 92
6.2.2 Wigley Hull: Change in y-coordinates of Stations 95
6.2.3 Wigley Hull: Changing the Vertical Location of Nodes on Stations . . . 97

7 Conclusions and Recommendations **100**

Bibliography **103**

A Fibonacci Search Method **110**

B Input Files **113**
B.1 Offset Table Format in Excel 113
B.2 *.csv File for Offset Table Format 115
B.3 x-y-z Format in Excel 116
B.4 *.csv File for x-y-z Format 117

C Cubic Spline Interpolation Code **118**

D Transom Stern Discretization **122**

E 3D Model Sample Views **124**

E.1 Series 60, C_b = 0.6 124

E.2 AMECRC Series: Model # 1 129

E.3 Wigley Hull: L/B = 10, L/T = 16 133

E.4 US Navy Combatant DTMB 5415 137

List of Tables

5.1 Series 60, C_b = 0.6: Geometric Properties Comparison 67

5.2 Series 60, C_b = 0.6: Coordinates Comparison for the Table of Offsets 69

5.3 AMECRC Model # 1: Geometric Properties Comparison 72

5.4 Wigley Hull: Geometric Properties Comparison 75

5.5 DTMB 5415: Geometric Properties Comparison 78

6.1 Series 60, C_b = 0.6: Longitudinal Shift - Changes in Properties 82

6.2 Series 60, C_b = 0.6: Change in y-coordinates- Changes in Properties. 84

6.3 Series 60, C_b = 0.6: Vertical Shift of Waterplanes - Changes in Properties . . . 89

6.4 Wigley Hull: Longitudinal Shift - Changes in Properties 93

6.5 Wigley Hull: Change in Y-coordinates - Changes in Properties 96

6.6 Wigley Hull: Vertical Shift of Waterplanes - Changes in Properties 97

List of Figures

1.1 Resistance Components and Ship Speed : Typical Curve 3

1.2 Program Structure with Optimization Loop 7

2.1 Mapping: computational space to physical space. *Courtesy: Thompson et al. (1999)* 15

3.1 Ship Hull Coordinate System for The Present Study 28

3.2 Coordinate System Followed in Wave Resistance Calculation 29

3.3 Conventional Table of Offsets' Coordinate System (e.g. Series 60) 29

3.4 B-spline Surface Interpolation 37

3.5 Series 60 Hull Surface Expressed by B-spline Surface (Port Side) 38

3.6 Grid Generation Process Step-by-step. 41

4.1 Profile Curves Plot (disregard the values) 56

4.2 Series 60 Profile. *Courtesy, Todd (1963)* 57

4.3 Manual Drawing of Series 60 Ship from Offset Table. 61

4.4 Interpolated Station. 62

4.5 Discretized Transom Stern. 63

4.6 Transom Stern Including Freeboard (IGES file output). 63

4.7 MAPS Resistance Coordinate System (z-positive upwards). 65

5.1 Series 60 Ship Hull Body Plan Comparison. 70

5.2 Series 60 Ship Hull Profile Curves Comparison. 71
5.3 AMECRC Model # 1 Body Plan Comparison. 73
5.4 AMECRC Model # 1 Forward Profile Curve Comparison. 74
5.5 Wigley Hull: Body Plan Comparison 76
5.6 DTMB 5415 Sharp Change in Geometry 77
5.7 DTMB 5415: Geometric Output with Smoothened Sharp Corners 77
5.8 DTMB 5415: Geometric Output 78
5.9 DTMB 5415: Body Plan Comparison 79

6.1 Series 60 $C_b = 0.6$ Wave Resistance Coefficient, C_w 81
6.2 Series 60: Longitudinal Shift- Forward. 83
6.3 Series 60: Longitudinal Shift- Middle. 83
6.4 Series 60: Longitudinal Shift- Aft. 84
6.5 Series 60: Variation of Y- Body Plan Comparison. 87
6.6 Series 60: Variation of Y- Body Plan Comparison. 88
6.7 Series 60: Shift of Waterplanes - Body Plan Comparison. 89
6.8 Series 60: Shift of Waterplanes - Profile Aft. 90
6.9 Series 60: C_w comparison - Various Modification Methods. 91
6.10 Wigley Hull: Wave Making Resistance Coefficient, C_w 92
6.11 Wigley: Longitudinal Shift - Forward. 94
6.12 Wigley: Longitudinal Shift - Middle. 94
6.13 Wigley: Longitudinal Shift - Aft. 95
6.14 Wigley: Variation of Y- Body Plan Comparison. 96
6.15 Wigley: Shift of Waterplanes - Body Plan Comparison, Iteration 6. 98
6.16 Wigley: Shift of Waterplanes - Body Plan Comparison, Iteration 12. 98
6.17 Wigley: C_w comparison - Various Modification Methods. 99

B.1 *.xls File: Offset Table Format 114
B.2 *.csv file: Offset Table Format 115
B.3 *.xls file: x-y-z Format 116
B.4 *.csv file: x-y-z Format 117

E.1 Series 60, C_b = 0.6, 3D Model, View 1 125
E.2 Series 60, C_b = 0.6, 3D Model, View 2 125
E.3 Series 60, C_b = 0.6, 3D Model, View 3 126
E.4 Series 60, C_b = 0.6, 3D Model, View 4 126
E.5 Series 60, C_b = 0.6, 3D Model, View 5 127
E.6 Series 60, C_b = 0.6, 3D Model, View 6 127
E.7 Series 60, C_b = 0.6, 3D Model, View 7 (flat bottom) 128
E.8 Series 60, C_b = 0.6, 3D Model, View 8 128
E.9 AMECRC Model # 1, 3D Model, View 1 130
E.10 AMECRC Model # 1, 3D Model, View 2 130
E.11 AMECRC Model # 1, 3D Model, View 3 (bottom) 131
E.12 AMECRC Model # 1, 3D Model, View 4 (bottom) 131
E.13 AMECRC Model # 1, 3D Model, View 5 132
E.14 AMECRC Model # 1, 3D Model, View 6 132
E.15 Wigley Hull: L/B = 10, L/T = 16; 3d Model View 1 134
E.16 Wigley Hull: L/B = 10, L/T = 16; 3d Model View 2 135
E.17 Wigley Hull: L/B = 10, L/T = 16; 3d Model View 3 (bottom) 135
E.18 Wigley Hull: L/B = 10, L/T = 16; 3d Model View 4 136
E.19 DTMB 5415; 3d Model View 1 138
E.20 DTMB 5415; 3d Model View 2 138
E.21 DTMB 5415; 3d Model View 3 139
E.22 DTMB 5415; 3d Model View 4 139

E.23 DTMB 5415; 3d Model View 5 140
E.24 DTMB 5415; 3d Model View 6 140

Nomenclature

BFGS	Broyden-Fletcher-Goldfarb-Shanno optimization method
B-Spline	Basis spline
CASHD	Computer aided ship design
CFD	Computational fluid dynamics
csv	Comma separated values
DFP	Davidon–Fletcher–Powell optimization method
EHP	Effective Horse Power
IGES	Initial graphics exchange specification
NURBS	Non uniform rational basis spline
TFI	Transfinite interpolation
L	Load waterline length of a ship
B	Breadth of a ship
T	Design draft
AP	Aft perpendicular of a ship
FP	Forward perpendicular of a ship
C_b	Block coefficient of a ship
C_p	Prismatic coefficient
C_m	Midship section coefficient
∇	Volume of displacement

$\mathbf{X}(u)$	Set of points on a B-spline curve in Cartesian coordinates [chapter 1]
$\mathbf{S}(u, v)$	Set of points on a B-spline surface in Cartesian coordinates
u, v	Parameters of B-spline curve and surface
$f_{i,p}(u)$, $g_{j,q}(v)$	Basis function of a B-spline surface
$P_{i,j}$	Control points on a B-spline curve or surface
$\mathbf{Q}_k$	Ship hull data points [chapter 3]
$\mathbf{X}(\bar{v})$	Points on B-spline curve [chapter 3]
$\bar{v}$, $\bar{u}$	Parameters of B-spline surface [chapter 3]
v, u	Knots for B-spline surface [chapter 3]
V, U	Knot vectors for B-spline surface
X, Y	x and y coordinates of control points of a B-spline curve
P_X, P_Y, P_Z	x, y and z coordinates of control points of a B-spline surface, sometimes defined by X, Y and Z
x, y, z	x, y and z coordinates of the points surface net
$N_{i,p}, N_{j,q}$	Vertical and horizontal basis functions for B-spline surface
$\mathbf{x}$	General variables in optimization algorithm
$[H]$	Hessian matrix
α	step length of variables
α^*	Optimum step length of a variable
∇f	Gradient vector in optimization
C_w	Wave making resistance coefficient
R_w	Wave resistance
$\mathbf{S}$	Product of gradient vector and Hessian matrix

ϵ	Convergence criteria for optimality
$\mathbf{d}$	Product of optimum step length and $\mathbf{S}$
d	Chord length
$\mathbf{g}$	Difference between the gradients of two consecutive optimization iterations
k	Number of optimization iterations

Chapter 1

Introduction

Improved hydrodynamic performance is one of the most important features of ship operation. In general, hydrodynamic performance depends mostly on the ship hull geometry. The hydrodynamic optimization generally aims to find a feasible hull geometry(s) for a particular ship type with best possible hydrodynamic properties.

1.1 Motivation

In the process of ship design, geometry development and evaluation of the ship hull accurately and efficiently, are initially the most important stage. Generally, in the ship geometry modeling field, the design team is supported in its task of determining a vessel's geometry by hydrodynamic performance prediction simulations. Hydrodynamic performance will be the first determinant for optimum ship hull geometries.

Computer Aided Ship Design (CASHD) and Computational Fluid Dynamics (CFD) are utilized one after the other to perform the above mentioned operations. These two media usually do not receive any direct feedback from each other. First, a ship's complicated hull geometry is developed based on an iterative process to meet all design criteria (i.e. displacement, block coefficient, etc.). In the next stage, the hydrodynamic performance is calculated based

on numerical fluid field analysis and model tests. Depending on the results, the ship geometry may be modified. After the first set of hull geometries, the interactive modification of a hull is performed based on hydrodynamic performance. These processes are not completely integrated, i.e., CFD results are passed to the CASHD group for evaluation of the geometry, and necessary modification are made and passed to the CFD group for a new set of evaluations.

At the end of twentieth century, Harries (1998) integrated CASHD and CFD to develop a system to produce optimum ship hull form(s). The initial hull design was performed based on the form parameters (e.g. prismatic coefficient for run, tangent of run, block coefficient, etc.) of a ship. In this design process, a set of geometric coefficients and angular values are calculated as the input for the geometric design. The complete process will first meet the design criteria with acceptable fairness (no discontinuity) of a ship's surface. Then it passes through an interactive optimization process to find an optimum hull form with the necessary variables.

Reanalysis of an existing ship hull form with the optimization committed to continuity of the ship's principal dimensions and properties, has yet not been investigated significantly. Here continuity of ship's principal dimensions means to keep the principal dimensions (length, breadth, draft) etc. to keep unchanged. There is always a scope for improvement in an existing ship hull form with tolerable changes in the hull shape without compromising the principal dimensions and properties.

To a researcher, the initial hull information available is usually the vessel's geometry in the form of a conventional table of offsets, a set of coordinates or a reference drawing with her principal particulars. In order to develop an optimization system based on numerical ship hull analysis, a complete coordinate descriptor of the hull geometry is usually required.

An integrated system with automatic hull generation, grid generation capabilities, and an integrated optimization process will minimize a significant amount of effort in investigation for a better performing hull form. Different strategies of hull form modification can be chosen in the integrated optimization procedure, and results due to them can be compared. These results

will be the decisive factors for the target ship hull in the optimization loop.

The best choice for the objective function in the optimization is wave making resistance. Wave making resistance has a great effect on vessel operating cost. Figure 1.1 shows components of hull resistance and their typical relation with ship speed.

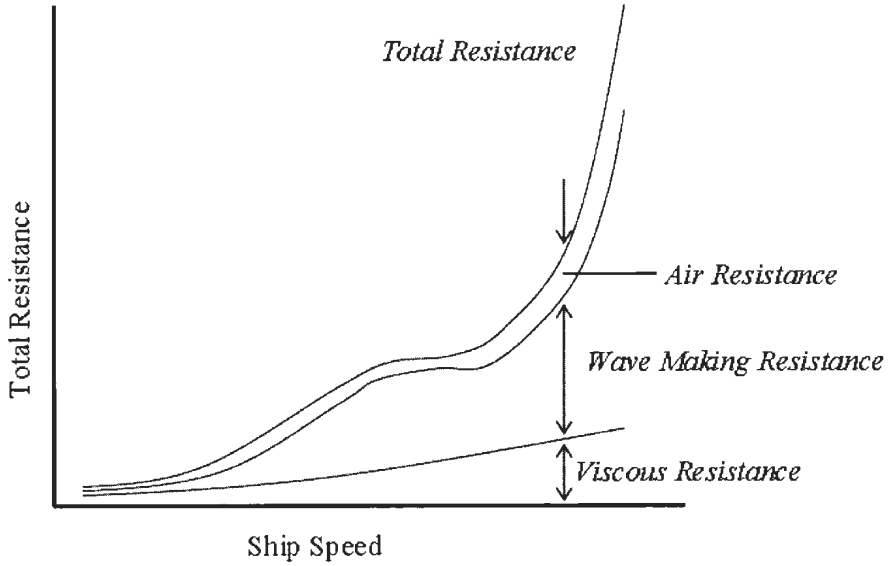

Figure 1.1: Resistance Components and Ship Speed : Typical Curve

It shows that wave resistance dominates among all other resistance components as the speed increases. If an operator is planning a voyage with higher speed, the ship will obviously require more power than with a slower speed. The relation between effective horse power and total resistance is simply an increasing trend. A ship's fuel consumption curve is similar in shape to its horsepower and total resistance curves. Clearly, reduction in wave resistance will significantly reduce the fuel consumption, and the cost of operation.

Referring to a sample voyage estimation (Makkar, 2002) for a very poor market in 2001, the expense for fuel oil was $300 per ton, for a bulk carrier carrying 52,000 MT of iron ore. For a voyage of 24.5 days, the total fuel oil cost will be around $94,650. EHP is generally the product of total resistance and ship speed, wave resistance is dominant in total resistance.

Therefore, a significant improvement of wave resistance will reduce a decent amount of the collective fuel cost for multiple voyages.

1.2 Goals

In this study, an optimization procedure is developed to obtain a ship hull form with minimum wave making resistance. The process starts with mathematical and graphical representation of an existing ship hull utilizing a table of offsets (or available node coordinates), followed by the hull surface discretization. Then, changes in the hull are performed with different dependent and/or independent variables and evaluated based on wave making resistance inside an optimization algorithm. This optimization algorithm searches for the best combinations of variables to produce a feasible modified ship hull form(s) expected to experience minimum wave resistance.

This study aims to contribute to the field of ship design in two ways:

1. Application of a comparatively simple mathematical method of curves and surfaces generation to the field of mathematical ship hull generation. Curves and surfaces are described by the coordinates of nodes of ship hull surface.

2. Interactive and integrated approach to hydrodynamic optimization, where the hydrodynamic performance is evaluated by potential flow techniques among CFD approaches, using a Rankine panel method.

Therefore, the research areas of highest importance to this work are:

1. Automatic mathematical and graphical ship hull surface modeling.

2. Computational Fluid Dynamics (CFD).

3. Hydrodynamic Optimization.

4. Constraint based ship hull variation (constraints: principal dimensions and form parameters)

1.3 Concept and Workbench

In general, an optimization procedure commences with an initial set of free parameters, i.e., ship's data and a choice of free variables of the optimization problems. In the first stage of ship hull generation, coordinates of the ship's surface nodes are utilized as input and ship hull geometry is developed and graphically represented. If no geometric constraints are violated, the ship hull shape is analyzed based on the hydrodynamic performance, which is the measure of merit assessing the ship geometry.

Then, an optimization subroutine is started, which it starts with hydrodynamic evaluation (wave resistance). An initial hull form variation is performed, and the measure of merit is checked at to decide if the variation is a promising change of the free variables according to the chosen optimization strategy. Taking into account the geometric constraints and bounds (i.e., length, beam, etc.), a new set of variables is devised and transferred for hydrodynamic evaluation. Based on these results, the optimization strategy performs a step length search for a new set of optimum variables. If a new set of possible variables are available a new loop of optimization starts. Optimization loops continue until there is no further improvement in the wave resistance. In case of a minimization problem, this conclusive point is decided by the difference between the objective function values of two consecutive iterations. A very small value will be set as the lowest difference between two wave resistance coefficients from two consecutive iterations. If the difference is lower than that value, the process will be terminated. Once that point is reached, a new set of variables is found, which generates the optimum ship hull geometry and the optimization process is terminated.

In principal, this strategy follows the manual design process. In the automatic procedure,

however a more rigid format is observed and a higher number of alternative shapes can be systematically investigated. Of course, intuitive shape variations that would be undertaken by an experienced designer in an interactive process might achieve similar results with less computational effort, though the manual labor will likely be much higher.

The optimization workbench implemented in the present study was in accordance with the optimization loop as in the flowchart in Figure 1.2. Models selected to perform in each steps in the optimization process are:

Hull Form Generation - Mathematical and graphical representation of hull shape were completed by a simple B-spline curve and surface generation method - global curve and surface interpolation, and graphically represented with the aid of "*.igs" file formed with control points and knots of the B-spline surface. B-spline curves and surfaces are usually defined by equations 1.1 and 1.2 respectively.

$$\mathbf{X}(u) = \sum_{i=0}^{n} f_{i,p}(u)\mathbf{P}_i \tag{1.1}$$

$$\mathbf{S}(u,v) = \sum_{i=0}^{n}\sum_{j=0}^{m} f_{i,p}(u)g_{j,q}(v)\mathbf{P}_{i,j} \tag{1.2}$$

Here, $\mathbf{P}_{i,j}$ are control poins, u and v are parameters which forms the knots, see, Chapter 3.

Measure of Merit - Integral resistance coefficient, i.e., wave resistance.

Fluid Dynamics - CFD analysis by means of MAPS Resistance version 2.0, see section 2.2.1, Chapter 2 and Ni et al. (2011).

Optimization - Multidimensional conjugate gradient optimization method, Broyden-Fletcher-Goldfarb-Shanno (BFGS), integrated with three different modification methods.

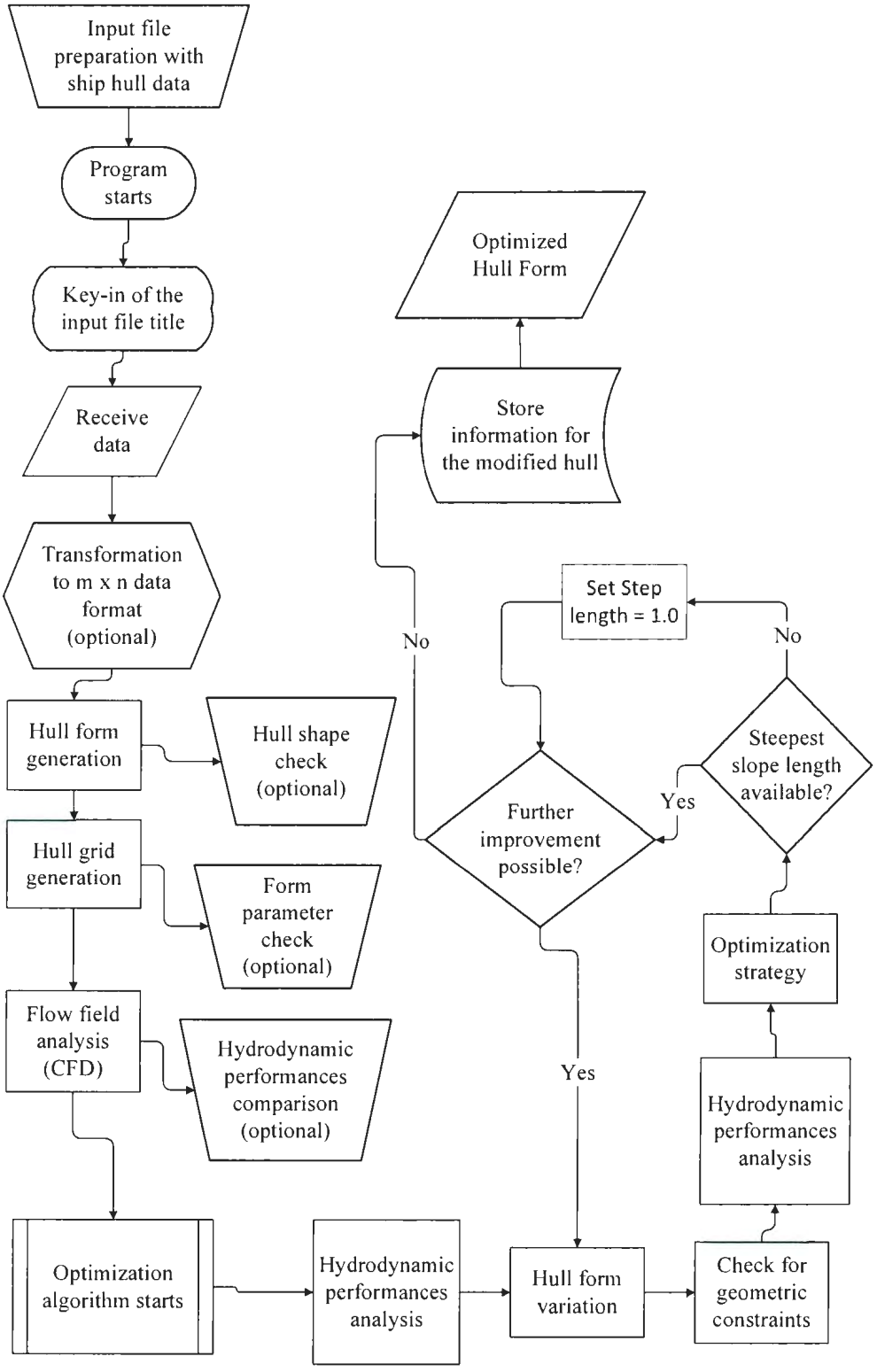

Figure 1.2: Program Structure with Optimization Loop

1.4 Thesis Outline

The scope of this work includes development of a program which performs a complete process starting from automatic hull generation to hydrodynamic optimzation. A FORTRAN 90 code was developed integrated with a library code to evaluate wave making resistance. This thesis is subdivided into seven different chapters to logically present the rationale behind the research, mathematical formulation, and the results, and validation based on results obtained from the study.

Chapter 2 (Literature Review) will illustrate a timeline of past work related to the current work. Chapter 3 (Mathematical Formulation) presents the mathematical background behind the methods adopted to develop the program. In chapter 3, there are subdivisions based on categories of individual tools which are integrated to build the complete program unit. Chapter 4 (Numerical) describes the input and output files, and some additional logical and mathematical accessories utilized in the program.

Chapter 5 and 6 present and explain the results. Chapter 5 aims to validate the geometric output from the program with the sample ships available for this study. Chapter 6 explains hydrodynamic performances (wave making resistance) of series 60 hull (C_b = 0.6) and Wigley hull, and studies the output from the optimization algorithm. Chapter 7 draws a summary of achievements and shortcomings of the study, and discusses further improvement and possibilities for new features in the main structure of methodologies.

Chapter 2

Literature Review

Ship designers and hydrodynamicists have always sought to find optimum ship forms with improved hydrodynamic performance, especially resistance. For a particular ship type, the most economic hull shape has always been a great concern among ship designers without intolerable alteration of the principal characteristics. For simplification, ship resistance may be divided into two parts: a frictional resistance and a wave-making resistance. Generally, for conventionally shaped ship hulls, frictional resistance is related to the wetted surface area, and frictional resistance cannot be reduced significantly by redesign of the hull. Thus optimal designs are those whose wave patterns contain the least energy. The approach followed here is to search for optimum design of ship hull form by numerical analysis based on wave resistance, starting from numerical hull form generation and graphical representation. First, the review looks at different approaches to automatic parent ship hull development and discretization. Then, different optimization methodologies along with hull shape variation strategies are discussed. The review extends to the resistance calculation methods adopted by MAPS Resistance Version 2.0.

2.1 Numerical and Graphical Hull Development

There are different approaches to represent hull surfaces mathematically. The following section discusses several methods adopted by researchers. Methods of discretization of the hull surface are discussed later.

2.1.1 Ship Hull Design with B-Spline Surfaces

There has been a significant amount of research aimed at automatic ship hull generation based on numerical constraints related to geometric features and hydrodynamic coefficients. Francisco L. Pérez Arribas's publications on ship hull modeling, parametric ship design and geometric modeling gives quite an impression in this field. Arribas, along with his fellow researchers have numerous publications in automatic ship hull generation. First, Pérez-Arribas et al. (2006), developed a thorough procedure for automatic modeling with a fair NURBS surface, where lists of points on the stations of ship hulls were used as initial data in the form of an offset table. Approximation of spline curves fitting the point data on the stations was made. The method adopted in that work is suitable for general conventional ships. The choice of parameterization and the method of point interpolation have special effects on the accuracy of the splines fitting any set of data points. They adopted least-square approximation for construction of NURBS surfaces which fit the ships' data points. As the choice of parameterization, centripetal parameterization was applied. A set of uniform weights for the NURBS surface was used, which in fact converts it to a B-Spline surface. An automatic faring process was used which deals with the local faring by reducing local bumps on the surface.

Pérez-Arribas et al. (2008) works on parametric designing of simple hull lines which meet hydrodynamic coefficients imposed by designers. Their method is based on the mathematical definition of the sectional area curve and the waterplane half-breadths curve of a vessel. These will return the main parameters and hydrodynamic coefficients of the ship. The next

stage is to develop the longitudinal profile without appendages, and for the sake of simplicity, it is a selected option of this study. After completion of these processes and basic mathematical fairing, a wire model of the ship hull is developed. Then, the whole hull is represented with one surface by means of NURBS surfaces, which is the present study's primary interest. Again in this paper, hull surface is defined using a uniformly weighted NURBS surface. Each station of hull lines has been approximated with mean square approximation with a cubic B-spline (power of B-Spline = 3) curve. By means of a linear system solver, the approximation problem was solved for each set of data points on the ship hull lines, and control points of the B-spline were acquired. The parameters and knot vector were calculated by centripetal parameterization and averaging method respectively.

In a later work (Pérez-Arribas and Clemente, 2011), a numerical constraints based method to obtain ship hull form, directly related to geometric features, was developed, where the final hull surface representation was produced by B-spline fitting of points on analytical curves. Finally, the hull surface is obtained by turning the control points to a control net and using two sets of parameters and knots, which is a general practice in transition of a spline curves to spline surface.

Stefan Harries (Harries, 1998) adopted a more complex method to develop ship hull form based on global and regional form parameters (principal dimensions, coefficients, centroids, etc.). After parametric design of suitable *basic curves* and parametric modeling of a set of *design sections* derived from basic curves, a small set of surfaces was generated interpolating the design sections. In the final stage of representation of a hull surface, Harries used the B-spline surface with fairness criteria. A set of cubic B-spline curves with eight vertices (or, control points) was used to represent the sectional curves of the ship hull. Afterward, interpolation of those curves at the nodes in horizontal direction with another set of B-splines produced the surface net of the ship hull form. As an advancement of the previous work, Abt et al. (2001) presented a parametric modeling approach to the design of ship hull forms which

allows creation and variation ship hulls quickly and efficiently. A design-oriented parametric definition language was introduced which features high-level descriptors of hull characteristics well-known in naval architecture. A modeling system was presented that produces a complete mathematical description of the hull via geometric optimization, enabling effective shape variations by keeping selected parameters constant while adjusting others automatically. The modeling technique presented in that paper was based on a parametric curve generation approach developed by Harries and Abt (1997), which has successfully been utilized for the generation and automated optimization of bare hulls by Harries (1998), as discussed above.

Many other publications are available, which investigate general approaches to designing ship hulls with different modification tools or partially new approaches (integrated with conventional methods) dedicated to improve the output surface quality. Rogers and Satterfield (1980) and Kouh and Chau (1993) stand as examples from early stage studies when scope for implementation of B-spline surfaces and rational cubic Bézier curves/ surfaces (respectively) in design of ship hull surface were investigated, combined with computer aided applications. On the other hand, Wen et al. (2006) search for a more accurate, fair and speedy process to fit a ship hull surface with NURBS by means of simulated annealing optimization on cross sectional area curves. Cang and Le (2011) attempt to represent complicated ship surface with non-uniform B-spline (NUB) surface fitting where fairness of interior surface is also improved with the help of a real-coded Generic Algorithm (GA) introduced by Yoshimoto et al. (2003).

Furthermore, for designing a bulbous bow using NURBS surfaces, Pérez et al. (2007) proposed a wire model of bulbous with B-spline curves (which satisfy few form parameters of the bulb) following by a B-spline surface fitting these splines. To obtain typical concept on design of new bulbous bow, one can always refer to Kracht (1978).

In general, B-spline or NURBS has been a very useful tool to generate a ship hull surface with provided data points (local parameters) or form parameters (global and/or regional). But accuracy of the outcome depends on the choice of the B-spline or NURBS property and meth-

ods of curve and surface fitting. Most of the above mentioned works focused their interest in parametric ship design, and approximation of the hull surface with fairing was mostly adopted method. Nowacki et al. (1995) provides an effective guideline on form parametric design of basic curves for ships.

The present study's interest is to optimize an existing ship hull form, where, the available information on a ship hull is expected to be the offset table or lines plan, i.e., data points. To fit an arbitrary set of geometric data points with B-Spline or NURBS, there are two different approaches (Piegl and Tiller, 1997, Chap. 9), *interpolation* and *approximation*. In *interpolation*, a curve or surface is constructed which satisfies the given data precisely. In *approximation*, it does not necessarily satisfy the given data precisely but only approximately. Moreover, in approximation it is often desirable to specify a maximum bound on the deviation of the curve of surface from the given data, and to specify certain constraints (Pérez-Arribas et al., 2006; Piegl and Tiller, 1997, Chap. 9). Therefore, interpolation method has been chosen to create B-Spline or NURBS to represent an existing ship hull form in the current work. As the discretization of the whole surface follows in the next step, it saves the complication of surface fairing process. This is because, in grid generation, a new set of local parameters for the curves is produced and the interpolation curve fitting methods follows them precisely, reducing the possibility of local discontinuity on the line or surface. Still, any unwanted local distortion or discontinuity on the surface can be treated numerically following the trend of each curve. Namely, *Global Interpolation* was the method chosen for curve and surface interpolation using uniformly weighted NURBS curves and surface.

2.1.2 Grid Generation

The hydrodynamic performance evaluation method adopted here is based on the panel method which demands attention to the accuracy of the hull body discretization. There has been a number of works on mathematical grid generation of any geometric surface. Unfortunately, from

technical point of view, grid generation is partly art, as well as science; though implementation of mathematics provides the base for science in grid generation, there is always art involved as no intrinsic equations or laws apply to this process. However, different generalized methods or individual case-based grid generation have been studied throughout time. The geometry in this study is available as a *parametrically defined surface*, i.e. B-spline surface or NURBS surface. Therefore, the surface geometry is defined in the form of a mapping $\{x(u, v), y(u, v), z(u, v)\}$ from a *parametric* (u, v) domain to a *physical* (x, y, z) domain. In structured grid generation, the actual grid generation process is the grid generation by mapping from the discrete rectangular computational (ξ, η) domain to parametric (u, v) domain, which results in the composite map $\mathbf{x}(\xi, \eta) = \{x(\xi, \eta), y(\xi, \eta), z(\xi, \eta)\}$ (see figure 2.1.2).

"Handbook of Grid Generation" (Thompson et al., 1999) collects most of the works published up to the year of publication and is necessary basic literature on grid generation. In the chapter of surface grid generation (Thompson et al., 1999, Chap. 9), Ahmed Khamayesh and Andrew Kuprat discuss two types of structured surface grid generation : Algebraic and Elliptic. Implementations of these methods with NURBS surfaces are also covered in the later part of that chapter. Elliptic grid generation using NURBS surfaces was first introduced in Khamayesh and Hamann (1996). These methods complement each other and both are typically used in a complete grid generation system.

The algebraic mesh generation proceeds step by step, starting with grid construction on the boundary curves of a surface. The surface grid is then constructed by algebraic interpolation between the boundary curves. A certain type of interpolation such as cubic Hermite interpolation can be used to generate surface meshes that provides boundary orthogonality required in certain numerical simulations. But the simplest method like linear transfinite interpolation (Thompson et al., 1999, Chap. 3, 9) is generally used to produce a valid initial mesh. Then, if required by the simulation process, the surface can be smoothed by another method to satisfy possible grid line orthogonality or grid point distribution.

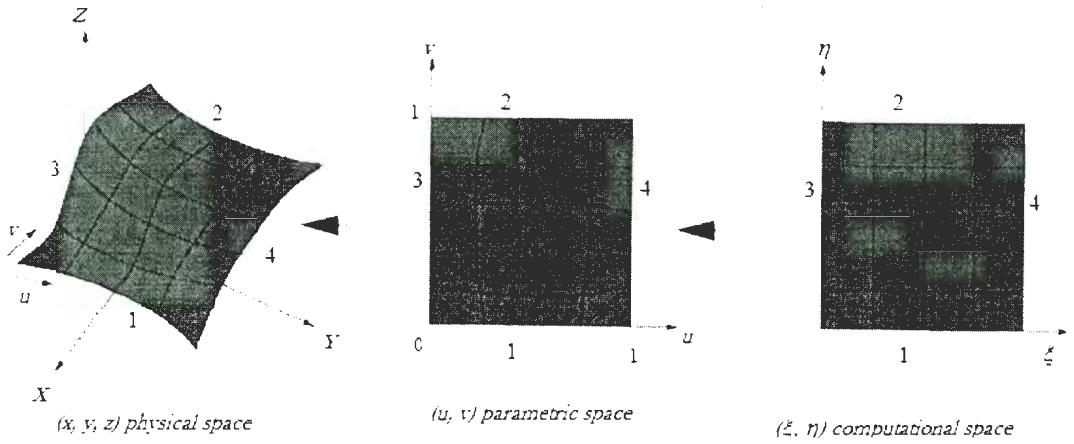

Figure 2.1: Mapping: computational space to physical space. *Courtesy: Thompson et al. (1999)*

Elliptic grid generation (Thompson et al., 1999, Chap. 6, 9) is the natural complement to the above process. Grids produced by the algebraic method are smoothed by iteratively solving the system of partial differential equations that relate the physical (x, y, z) and computational (ξ, η) variables. Desired orthogonality properties and desired point distributions in the physical domain are effected by imposing appropriate boundary conditions and/ or source terms in the elliptic system of equations.

In this study, the hull surface is expressed by uniformly weighted NURBS surface which converts itself to a B-spline surface. Therefore, from this point it will be referred to as B-spline curves or surface. The grid generation has been performed by introducing intermediate parameters in between consecutive points on horizontal and vertical boundary lines and mapping them to physical space to obtain physical coordinates of discretized points. This process follows the algebraic grid generation method as it discretize the boundary lines first. Instead of following transfinite interpolation, intersecting points are simply obtained from B-spline surface function.

2.2 Hull Shape Modification and Optimization

In the procedure for an optimal ship hull search, the optimization method and modification methods of the hull form are commonly inseparable. There has been an enormous number of works on ship hull optimization performed, with different hydrodynamic approaches. Along with those optimization processes, different methods of hull modification have been developed.

Nowacki (1993) conducted a useful introductory study on general approaches to hull form variation in optimization. Nowacki reviews the subjects of hull form variation and evaluation, which are traditionally two distinct stages of the ship design process. Different categories of hull form variables, variation methods and performance evaluation processes have been summarized in that study, which can be a helpful study before starting a ship hull optimization process.

Different systematic ship hull variations have been investigated as tools in different optimization studies. Similarly, some new or modified hull form variation methods have also been adopted and automated with hull form generation and/ or optimization. In this section, some basic methods of ship hull form variation are reviewed followed by a collection of ship hull form optimization approaches integrated with hull modification schemes.

A pioneer systematic work on hull form variation by H. Lackenby, in the *written discussion* based on the work of the British Shipbuilding Research Association (Lackenby, 1950), discusses the ship sections shifting method to modify the prismatic coefficient, the longitudinal center of buoyancy, and the parallel mid-body of the original/ parent hull. This method is commonly referred as the *Lackenby* method. A common practice was to make the spacing of the ship sections from the ends of the ship proportional to the difference between the respective prismatic coefficients and unity, which is known as "one minus prismatic" method. Lackenby extended this method of systematic sectional area curves variation, by introducing quadratic

shift functions to the change of a section's former position to a new one. Keeping the fore and aft perpendiculars unchanged, the quadratic shift functions for forebody and afterbody, changes four independent parameters, namely, prismatic coefficient (C_P), longitudinal centre of buoyancy (LCB), length of parallel middle body of the entrance (LPE) and length of parallel middle body of run (LPR).

Hollister (1996) developed a hull variation method to change the midship region. This method is independent of the beam and depth of each station and uses a factor called $C_m fact$. $C_m fact$ is defined by the intersection of the maximum beam and depth of the station and allows shape change of each station diagonally in the direction of the bilge corner. Though $C_m$fact is related to midship coefficient (C_m), it is actually based on the overall maximum beam and depth of the vessel, rather than the design waterline beam and the draft.

Hsiung (Hsiung, 1981) introduced a set of "tent" functions to approximate the ship hull function (geometry). By means of this "tent" function, Mitchell's (Michell, 1898) integral for wave resistance was reduced to a standard quadratic form in terms of ship offsets. By solving a quadratic programming problem for minimum wave resistance a set of subvectors was obtained which gave ship hull forms. Then applying various conditions of constraints in terms of linear combinations of the ship hull-form offsets, modified hull forms were obtained, which are in this case the optimal ship hull forms.

Janson and Larson (1997) proposed a optimization method for ship hulls from a resistance point of view. They used the SHIPFLOW program (Larsson, 1997) for computing the flow around ship hulls which was linked to a program called OCTOPUS (Esping et al., 1990) for solving non-linear optimization problems. The resistance components including wave resistance from a potential flow solution and the viscous resistance from a boundary layer and a Navier-Stokes solution, were included in their computation. The Method of Moving Asymptotes (MMA) was used as the optimization method for solving the non-linear optimization problems was developed in the optimization program, OCTOPUS. In the same work, they in-

cluded a geometry program, ALADDIN, which performed variation of the hull forms. As the hull form was defined by offset-points on the hull surface, for varying the hull form, the points were moved along certain directions. Two different variables were defined : Master and Slave variables. The latter ones are linear combination of the former ones. Master and slave variables are attached to the offset-points in ALADIN, and a basic shape together with a number of variations was created.

As discussed before, Harries (Harries, 1998) developed a geometric system for an automated ship hull form design based on form parameters, which is called *FRIENDSHIP Modeler*. The final goal of that work was to develop a system to automatically optimize a ship hull. The SHIPFLOW system was integrated for zonal CFD computation and wave resistance was the measure of merit for design evaluation. A multidimensional conjugate gradient method was used as the model of optimization. The conjugate gradient method is a standard deterministic optimization strategy, and the algorithm developed comprises two steps, which are alternately repeated until convergence. In the first step, the gradient of the measure of merit is computed with respect to the free variables at a base point. In the second step, a promising search direction is identified and a one-dimensional optimization is undertaken, setting out from the base point into the direction of improvement. In order to serve the search, Harries (1998) employed Golden Section search method.

In this optimization system usually form parameters (global and regional) related to sectional area curve (SAC) and/ or design waterline (DWL) were chosen as the free variables to modify the hull form. From the set of variables of an optimized hull form, the parametric ship hull design system would produce the optimized hull form. For an example, the set of variables Harries used to optimize the wigley hull were : longitudinal position of center of buoyancy (x_{CB}/L), tangent angle at the beginning of entrance of the sectional area curve (α_{AEE} of SAC), tangent angle at the beginning of run of SAC, (α_{ABR} of SAC), longitudinal center of flotation ratio (x_{CF}/L), tangent angle at the beginning of entrance of the design waterline (α_{AEE}

of DWL) and tangent angle at the beginning of run of DWL, (α_{ABR} of DWL). This complete method is outstanding if development and optimization of a parent hull based on her global or regional parameters are desired.

Markov and Suzuki (2001) presented a control points and parameters based method of hull form modification based on B-spline properties. Although, the method of ship hull development is not discussed in the paper, a single B-spline patch was used to represent the ship hull. Therefore, the mathematical representation of the hull consists a set of coefficients (control points), $\mathbf{P}_{i,j} = (P_{X_{i,j}}, P_{Y_{i,j}}, P_{Z_{i,j}})$ (equation 1.2). They introduced three schemes of hull form modification: shift of parametric sections, shift of real ship section and shift and deformation of real ship sections. All of these schemes were based on variation of B-spline control points $(P_{X_{i,j}}, P_{Y_{i,j}}, P_{Z_{i,j}})$ and parameters (u, v).

The first scheme directly changes only the $P_{X_{i,j}}$ which conveyed that ship sections represented by the B-spline were being shifted forward and back along the longitudinal direction of ship length. With an initial shift of ship sections and the effect on the wave resistance coefficients as the input in a optimization method, the first category optimization loop was proceeded. DFP (Davidson-Fletcher-Powell) optimization procedure found its engagement in their study. DFP controlled the amount of shift in every iteration.

The second scheme shifted the real ship sections instead of the parametric ones. A function with a parameter of optimization (b_k) and a basis function ($B_k(u)$) was introduced which is similar to a one dimensional B-spline function. The summation of these two parameters' product produces the longitudinal positional shift (x-coordinates) of ship sections (equation 2.1).

A similar method appeared in the third scheme with deformation of sections in the z-direction, where shift of ship sections were performed at the same time. In this case, product of one parameter of optimization ($b_{k,l}$) and two basis function ($B_k(u)$ and $B_l(v)$) developed a two dimensional B-spline function (equation 2.2). In equation 2.2, $x = x(u, v)$ is a transformation of the type $x = f(x, z)$. Again, DFP optimization procedure varied the optimization parameters

$b_{k,l}$ and evaluate the minimum wave resistance coefficient, C_w.

A higher-order Rankine source panel method fully based on B-spline (Markov and Suzuki, 2000) was integrated with the optimization operation to evaluate wave resistance.

$$x = x(u) = \sum_{k=1}^{N_u} b_k B_k^3(u) \tag{2.1}$$

$$x = x(u,v) = \sum_{l=1}^{N_v} \sum_{k=1}^{N_u} b_{k,l} B_k^3(u) B_l^3(v) \alpha \tag{2.2}$$

Researchers in pursuit of methods to modify shape of B-spline surfaces or NURBS surfaces can refer to Piegl (1989) and Hu et al. (2001).

Majumder, M. with Akintürk, A. and Çalişal, S. M. (Majumder et al., 2002) follow an optimization procedure where they optimize different cost functions based on some constraints like, displacement, stability and some or all safety rules. Seakeeping criteria are also involved in their study to produce a more comfortable vessel, where the initial cost had a marginal increment. Therefore, new design nodes such as crew safety or acceleration levels were proposed to be included at the preliminary design stage. In addition, a design process referred as "MATSHIP" was brought into discussion, which showed that an integrated technical computing system (in this case, MATLAB) can be included in preliminary small craft optimal design.

In the same year, in a later publication (Çalişal et al., 2002), Çalişal, S. M. along with Gören, Ö. and Danişman, D. B., expressed their interests in resistance reduction by increasing beam and converting a parallel middlebody to a non-parallel middlebody (parabolized waterlines) of a conventional ship. Motivated by wave resistance reduction in numerical computation due to addition of a sponson to a hull, a conventional coaster tanker was chosen for numerical and experimental wave resistance evaluation. Although, this study was not quite systematic, the increment in beam with parabolized waterlines showed reduction in EHP (effective horsepower) requirement at modest Froude numbers.

Another optimization approach can be found in Valorani et al. (2003), where gradient based optimization appeared in a different terminology, the sensitivity derivatives. The optimization approach was integrated with hull representation by a Béizer perturbation surface and hull form modification Béizer surfaces. The change in control points of the Béizer surfaces changed the hull shape in the y-direction, which is similar to the ideas in Janson and Larson (1997) and Markov and Suzuki (2001). The figure of merit or cost function was total drag coefficient, C_t.

After preliminary successful implementation of *FRIENDSHIP-Modeler* and being inspired by the technical improvement in optimal design, a consortium of fourteen European partners conducted a three year European R & D Project called *FANTASTIC* (Manisonneuve et al., 2003), in the year 2003. The principal objective of that project was to improve ship design by applying parametric shape modeling and state-of-the-art CFD analysis tools to predict ship hull performance. These functional aspects were integrated in an optimization environment. A larger coverage of design alternatives and improvement of the quality of final optimal design by using the most recent CFD analysis tools, were brought into the project. The article presenting that project is a good reference to an introduction to certain established tools on different sectors, such as, ship parametric modeling (FRIENDSHIP), ship design system (NAPA), shape deformation function (GMS/Fscet), graphical user interface unit (GiD), non-linear panel codes for wave resistance predictions (RAPID, SHIPFLOW, etc.) etc.

Grigoropoulos (2004) studied an asynchronous optimization of seakeeping and calm water resistance of a conventional reefer ship and a naval destroyer. As for initial hull building, it was built using form parameters and variation of hull form was based on Lackenby method (Lackenby, 1950). An initial optimization of the parent hull form for seakeeping was performed. Then the study continues to the improvement of calm water resistance. The Hooke and Jeeves algorithm (Hooke and Jeeves, 1961) was utilized to acomplish the optimization. This optimization method is based on the direct search method where no derivatives or gradi-

ents are required (Hooke and Jeeves, 1961).

Simultaneous optimization of multiple hydrodynamic performances has also been investigated (Zalek et al., 2009). Typically, existence of the global optimum for both seakeeping and powering performances in calm water is not possible, because a trade-off exists between both of them and the design constraints. Considering these competing criteria, Zalek et al. (2009) investigated a set of nondominated (*best trade-off*) by navigating the multimodal search space for calm water powering and seakeeping operability, using a multicriterion population- based evolutionary algorithm for the optimization process. They have adopted a nontraditional objective function formulation based optimization process, where the need for tuning the penalty function parameters for each new problem formulation has been eliminated, and appears to provide a more thorough representation of the nondominated solution (or Pareto front). A multicriterion optimization problem contains several conflicting objectives synchronized, where single optimal solutions are not available, but a set of different trade-offs called nondominated or Pareto optimal are available. The solution has objective criterion values, no worse than the associated values in the other solution, and one of the objective criterion values is better than the associated values in the other solutions. The set of all Pareto solutions, known as a Pareto front, can be represented in such a manner which is very useful aid in decision making (Branke et al., 2008; Zalek et al., 2009; Legriel et al., 2010).

Researchers from different fields have also found interest in ship hull shape optimization. Martineli and Jameson (2007) borrowed from control theory of systems constrained by partial differential equation to approach shape optimization. This approach has become a powerful tool for aerodynamic optimization for transonic wings, and has been extended to incompressible flow, and successfully applied to shape optimization of marine propellers.

Kim and Yang (2010) studied new approaches to hull modification in the scope of hull form optimization. Following the Lackenby method of ship section shifting, Kim and Yang (2010) expressed the sectional area curve (*SAC*) in a polynomial form which control the mod-

ification. In addition, to perform local modification, a radial basis function interpolation was developed. Kim et al. (2010) implemented these two hull form modification methods to acquire optimal resistance and improved seakeeping based on CFD. Bao-ji et al. (2009) also adopted a new hull variation method based on a function determined by cross sectional area at ship stations and some design variables. Reduced wave making resistance based on Rankine source method was the goal of the study and unconstrained nonlinear programming was adopted as optimization tool.

Hynul Kim, Chi Yang and Francis Noblesse, with co-author(s) have shown interest in practical design-oriented CFD tools while searching for optimal ship hull forms based on hydrodynamic performance (Kim et al., 2008; Yang et al., 2008; Kim et al., 2010). Kim et al. (2008) and Yang et al. (2008) have their common features on the practical design-oriented CFD tool which is based on Neumann-Michell (NM) theory. The significant difference in the second work is the optimization method. Both gradient-based and genetic algorithm have been implemented instead of gradient-based only. Kim et al. (2010) adopts some additional hull modification strategies and Bale's seakeeping ranking method to evaluate objective function associated with seakeeping.

Recently, Kim and Yang (2011) extended their work to evaluation of the strong near-field interference effects between closely-spaced multihulls, and a hydrodynamic computational tool has been developed. That tool has been integrated to a CFD-based hull-form hydrodynamic optimization tool aiming to optimize the demihull shape for minimum total drag. A Catmaran model has been studied in that research.

There are some other earlier works worth mentioning, which have showed interest in optimization of special type vessels' hull forms: the R&D project for SWATH (Abt and Schellenberger, 2007) and CFD hull form optimization process for the *Glenn Edwards* (Hutchison and Hochkirch, 2007), which was the newest and largest hopper dredge in the U.S. fleet in 2007.

In 2005, under the leadership of the German shipyard Nordseewerke GmbH, FRIENDSHIP SYSTEM, MD GmbH, the model basin Hmburgische Schiffbau-Versuchsanstalt and the consultancies MTG Marinetechnik GmbH joined forces to develop an integrated computer aided design and optimization environment for SWATH ships, which they called OptiSWATH. The parametric modeling of the SWATHs was performed by FRIENDSHIPS SYSTEMS. As discussed before, this parametric model provides an excellent start point for the optimization (Harries, 1998; Harries et al., 2004). HSVA's CFD department provided the latest developments for non-linear potential flow calculations adapted to SWATH vessels on the basis of their code v-Shallo. This means, resistance and local flow phenomena were evaluated to an increasing extent by use of CFD. MTG (Hamburg based engineering consultant) provided their seakeeping code SEDOS to the consortium, which was developed for twin hull vessels. Finally, OptiSWATH became a newly developed SWATH design and optimization program suite for hull form modeling, resistance performance and seakeeping analysis, based on a holistic approach.

On the other hand, a more formal hull form optimization approach treated the dredge *G*lenn Edwards (Hutchison and Hochkirch, 2007), and produced measurable improvement in performance both in deep and shallow water operations. For parametric design of the ship hull form, *FRIENDSHIP-Modeler* was utilized with hull symmetry, length, volume and a few other geometric properties as the geometric constraints. For performance assessment, the well-known CFD code SHIPFLOW (Larsson, 1997) was employed with potential-flow module *xpan* to calculate wave making resistance. The Sobol sequence is used to provide a uniform distribution of hulls within the design space, and then, the Tangent search method handles the variable for optimal design. For details on Sobol sequence and Tangent search method refer to Press et al. (1988) and Hilleary (1966) respectively.

The present study targets a system where an existing parent vessel, at the preliminary design state, with proper information on hull coordinates (offset tables), finds possible opti-

mized hull form(s) based on wave making resistance. The only required information is the set of coordinates of hull geometry, and final output will be optimized hull form with coordinate information and graphical representation in IGES file format which is readable in most hydrodynamic software. A complete automatic system with minimum manual 'in process' interaction is set to be another goal. As discussed in section 2.1.1, *global interpolation* for B-spline curves and surfaces has been chosen for mathematical representation of the ship hull. As observed, gradient based optimization methods have been successful in most of the optimal ship hulls explorations, and the advanced unconstrained optimization technique BFGS (Broyden-Fletcher-Goldfarb-Shanno) has been adopted. This method can be considered as quasi-Newton, conjugate gradient and variable metric method.

Numerical experiences show that the BFGS method is less influenced by the errors in step length than DFP (Davidon-Fletcher-Powell) method (Rao, 2009, Chap. 6). Exact line searches do not seem possible in industrial practice which forces the use of numerical single-variable search methods. However, BFGS converges to the optimum of a convex function even when inexact line searches are used. The BFGS algorithm has demonstrated generally more satisfactory performance than other methods in numerical experiments, even though it is a more elaborate formula (Pike, 2001, Chap. 6). Again, quoting from (Ravindran et al., 2006, Chap. 3), " The method proposed by Broyden, Fletcher, Goldfarb, and Shanno has received wide acclaim and has in fact been strongly recommended by M. J. D. Powell".

In this study, the hull form modification is based on the control points of B-spline curves and surface. Janson and Larson (1997); Markov and Suzuki (2001); Valorani et al. (2003) observe the effect on the variation of hull from due to changes in control points. Modification due to control points has the advantage of maintaining the constraints (length, breadth, draft, etc.), as the maximum/ minimum values of control points at stations can easily treated as the boundaries. Moreover, effects on hull geometry due to changes in control points are easily predictable, which gives the benefit of maintaining the ship-like shape of the hull geometry.

Multiple variables inside the optimization algorithm are classified in longitudinal shift, athwart distortion (Beam) and vertical local points shift of the sections and combinations of two of the classes. The Lackenby ship section shift method with B-spline control points' application (Lackenby, 1950; Markov and Suzuki, 2001) adjusts the longitudinal variables. Athwart distortion (Y-coordinates) and vertical local points shift (z-coordinates) are varied by means of B-spline surface control point movements. During this process, similar effects on every stations and every waterline respectively, have been ensured to maintain ship-like look and to preserve the shape of the parent hull form. Finally, an optimized hull form with certain tolerance on volume of displacement is acquired, where MAPS-Resistance (version 2.0) evaluates the hydrodynamic performance of the ship in each iteration, based on wave making resistance.

2.2.1 MAPS-Resistance Version 2.0

In this single objective optimization study, wave resistance, as the only optimization objective, is calculated by MAPS-Resistance Version 2.0 (Ni et al., 2011). The MAPS-Resistance Version 2.0 is developed based on potential flow theory, which solves the steady wave-making problem of ships by using the alternative Dawson method. The hull surface up to the design waterline and a part of the still water surface around the ship need to be discretized in panels in a *row*×*column* format. Constant Rankine source singularities are distributed on each panel, and then, the Laplace equation is solved numerically using the Rankine panel method to compute wave resistance and wave pattern around the hull. The boundary condition is satisfied on the underwater body surface, and an alternative Dawson free surface condition (Dawson, 1977) is satisfied on the computational free surface. For more details refer to section 2 and 3 of Ni et al. (2011).

Chapter 3

Mathematical Formulation

The mathematical model for the complete system presented in this chapter has been divided into four parts:

1. Global Curve and Surface Interpolation: this section presents the mathematical method and formulae to fit a set of ship hull points using B-splines curves and surfaces.

2. Hull Surface Grid Generation: this section explains the method developed to discretize the hull surface by means of B-spline parameters and their mapping into physical space.

3. Hull Form Variation: describes the methods of hull form modification.

4. Optimization Procedure: explains the optimization methodology and modification inside the optimization algorithm due to the hull form variation and constraints setup.

3.1 Global Curves and Surface Interpolation

Development of a ship hull surface starts with producing the curves for each station of the hull, and then, interpolation of the station curves in the longitudinal direction produces the surface net for the ship.

3.1.1 Curves Interpolation to Offset Data

The initial curve is expressed using non-rational (uniformly weighted) B-spline curves. Offsets of the ship hull is the initial input. Figure 3.1 shows the basic coordinate system, based on which the whole calculation up to preparing input file for resistance calculation, is performed. Later, this coordinate system is transformed to the system required for the resistance calculation algorithm (Figure 3.2). Figure 3.1 illustrates that the origin is located at the bottom center line (keel line) of the hull where aft perpendicular (AP) is placed for conventional ship framing system. For conventional ship offsets (e.g. series 60), the origin is placed similarly, but at the forward perpendicular (FP). The input file is prepared as it is available for those ships i.e., origin at FP (Figure 3.3). After the input file has been read the coordinates are transformed to the present system. For this study, x is positive towards the forward, y-positive to the port side and z-positive upward of the vessel.

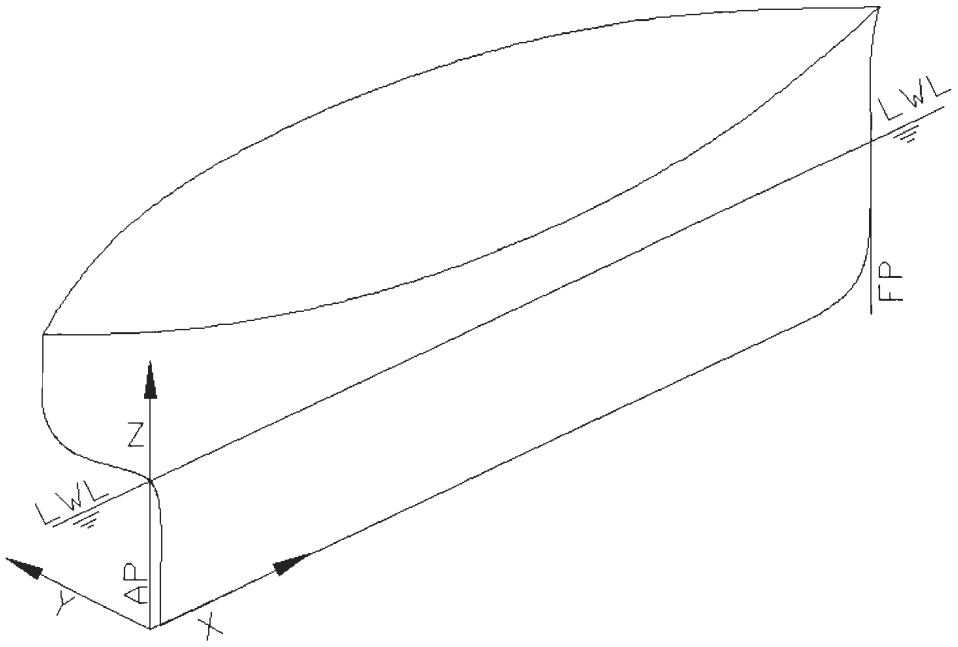

Figure 3.1: Ship Hull Coordinate System for The Present Study

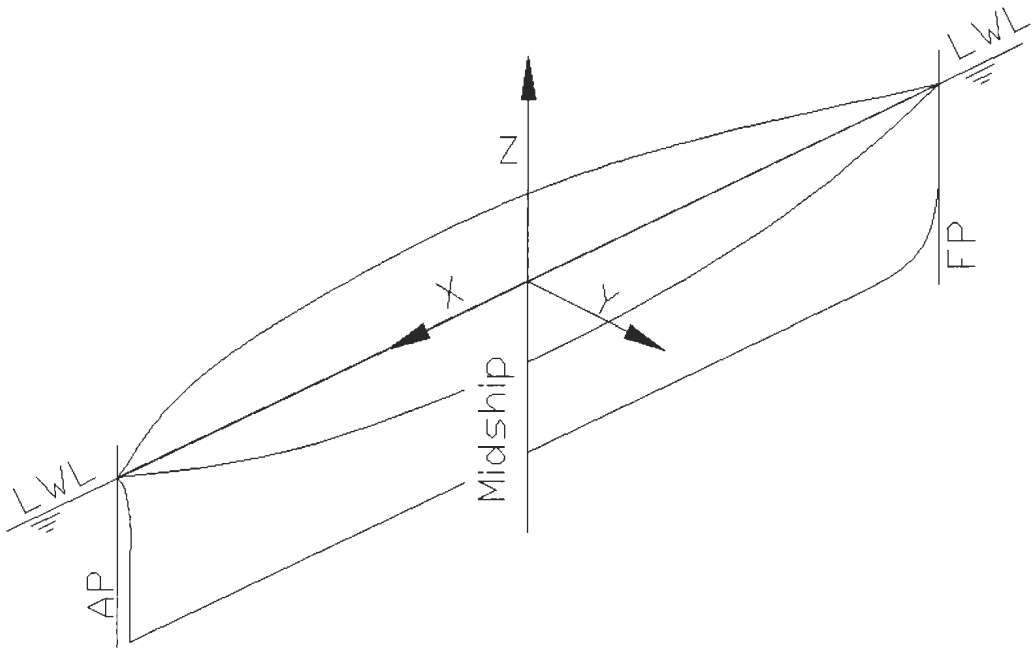

Figure 3.2: Coordinate System Followed in Wave Resistance Calculation

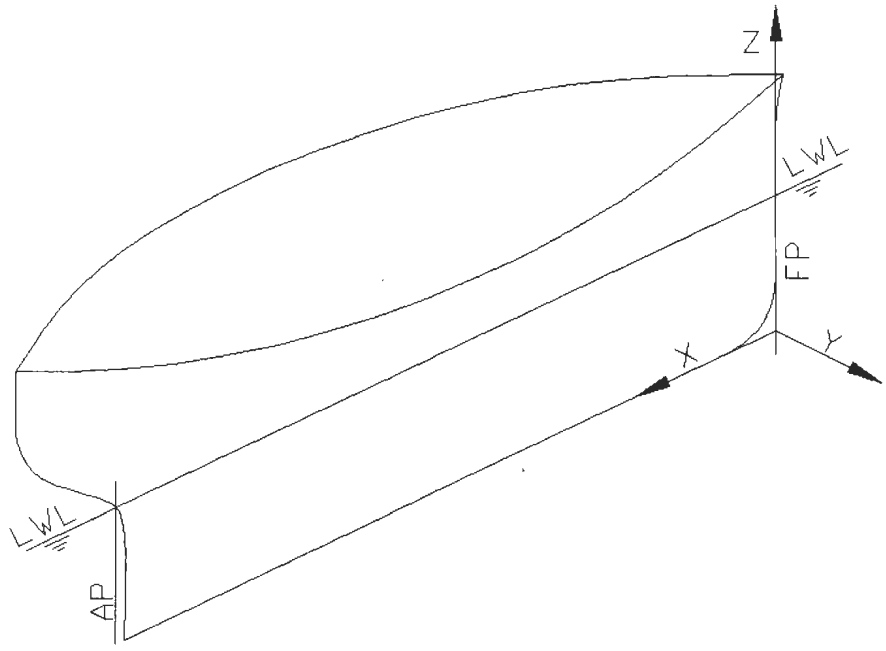

Figure 3.3: Conventional Table of Offsets' Coordinate System (e.g. Series 60)

Stations on the longitudinal half of the ship hull are developed using the *global curve interpolation* method to point data (Piegl and Tiller, 1997). The given set of points for a station is $\mathbf{Q}_k$, where, $k = 0, \ldots, n$, and $n+1$ is the total number of points on the curve. These points are to be interpolated with a p-th degree non-rational B-spline curve. The method, *global curve interpolation* is discussed below with the corresponding methods of calculation for parameters and knots of B-spline curves. In general, parameters and knots for vertical curves have been denoted by $\bar{v}$ and v, respectively. Similarly, for longitudinal curves, the parameters and knots are $\bar{u}$ and u.

The parameter value for the k-th point is $\bar{v}_k$, and a set of knots, known as the knot vector, for a curve is defined by $V = \{v_0, \ldots, v_t\}$, where, $t = n + p + 1$. $\bar{v}_k$ is to be assigned to each $\mathbf{Q}_k$, and $V = \{v_0, \ldots, v_t\}$ is to be calculated with a proper method. Then, for the $(n + 1)$ number of points on a curve, a $(n + 1) \times (n + 1)$ system of linear equations can be set up as in equation 3.1.

$$\mathbf{Q}_k = \mathbf{X}(\bar{v}_k) = \sum_{i=0}^{n} N_{i,p}(\bar{v}_k)\mathbf{P}_i \tag{3.1}$$

In equation 3.1, $\mathbf{Q}_k$ are the physical points on the curve of each ship station, the coordinates for each station being conventionally in the xy local coordinates system. The origin is set at the bottom of the middle line of the transverse section of each station, where y is positive upward and x is positive outward. $\mathbf{X}(\bar{v}_k)$ is the set of coordinates of the surface ponts, $\mathbf{X} = \begin{Bmatrix} X \\ Y \end{Bmatrix}$. $N_{i,p}$ (equation 3.8) is B-spline basis function and $\mathbf{P}_i$ is the set of control points $\begin{Bmatrix} P_{X_i} \\ P_{Y_i} \end{Bmatrix}$ (where, $i = 0, \ldots, n$). p is the degree of the B-spline curve. This *global interpolation* method is independent of the number of coordinates of a point.

The first task to develop the linear system will be to obtain appropriate parameters, $\bar{v}_k$ and knot vector, V. In general, the impact of the selected parameters and knots cannot be predicted easily. However, it is straightforward that, if the chord length distribution is about the same, all

parameter selection methods should perform similarly. Offset data of any ship is almost always in a certain order, i.e., the stations usually have common spacing and the waterlines also are in equal distance (there may be additional intermediate data). In the algorithm for parameter calculation all three methods for parameter calculation, as given in equations 3.2 to 3.6, have been utilized. After the first graphical output of the original ship hull, the best performing calculation method for parameters can be selected and utilized throughout rest of the process. The parameter values are set to lie in the range $\bar{v} \in [0, 1]$.

Here, three different methods of calculation of a B-spline curve parameters based on data points are observed: equally spaced, chord length and centripetal. Generally, the chord length and centripetal methods are chosen to determine, $\bar{v}_k$. For a set of data of a station with probable sharp turn, centripetal method performs more effectively. Calculation of knot vector, V is achieve by the technique of averaging.

Equally Spaced

$$\begin{aligned} \bar{v}_0 &= 0 \qquad & \bar{v}_n &= 1 \\ \bar{v}_k &= \frac{k}{n} \qquad & k &= 1, \ldots, n-1 \end{aligned} \tag{3.2}$$

This method is not usually recommended because it may produce erratic shapes (such as loops) when the data is unevenly spaced (Piegl and Tiller, 1997).

Chord Length

Total chord length, d is defined as,

$$d = \sum_{k=0}^{n} |\mathbf{Q}_k - \mathbf{Q}_{k-1}| \tag{3.3}$$

Then the parameter calculation is as follows:

$$\begin{aligned} \bar{v}_0 &= 0 \qquad \bar{v}_n = 1 \\ \bar{v}_k &= \bar{v}_{k-1} + \frac{|\mathbf{Q}_k - \mathbf{Q}_{k-1}|}{d} \qquad k = 1, \ldots, n-1 \end{aligned} \tag{3.4}$$

Centripetal Method

In this case, the total chord length, d is defined as,

$$d = \sum_{k=0}^{n} \sqrt{|\mathbf{Q}_k - \mathbf{Q}_{k-1}|} \tag{3.5}$$

Again, the parameter calculation is as follows:

$$\begin{aligned} \bar{v}_0 &= 0 \qquad \bar{v}_n = 1 \\ \bar{v}_k &= \bar{v}_{k-1} + \frac{\sqrt{|\mathbf{Q}_k - \mathbf{Q}_{k-1}|}}{d} \qquad k = 1, \ldots, n-1 \end{aligned} \tag{3.6}$$

Knots Calculation

The recommended method to calculate knots with these parameters calculation methods is *averaging*. The method appears in equation 3.7.

$$\begin{aligned} v_0 = \cdots = v_p &= 0 \qquad v_{t-p} = \cdots = v_t = 1 \\ v_{j+p} &= \frac{1}{p} \sum_{i=j}^{j+p-1} \bar{v}_i \qquad j = 1, \ldots, n-p \end{aligned} \tag{3.7}$$

In equation 3.7, t defines the number of knots where, $t = n + p + 1$ and $t + 1$ is the total number of knots. In this method, the knots reflect the distribution of $\bar{v}_k$.

Once the knot vector V and parameters $\bar{v}_k$ are obtained, equation 3.1 can be solved to obtain the set of control points $\mathbf{P}_i$, provided that the B-spline basis function $N_{i,p}(\bar{v}_k)$ is calculated first. A spline curve of pth-degree is a linear combination of B-spline basis functions of the same degree. These functions are constructed recursively from lower to higher degree in terms of the list of knots (in the present case, starting from v_0). These basis functions are

calculated using a recurrence formula due to deBoor, Cox and Manisfield, usually known as deBoor formula, and this is the most useful formula for the computer implementation. For the $t + 1$ number of knots and pth-degree (order $p + 1$) spline, the formula appears as shown in equation 3.8.

$$N_{i,0}(\bar{v}_k) = \begin{cases} 1, & \text{if } v_i \leq \bar{v}_k < v_{i+1} \\ 0, & \text{otherwise} \end{cases}$$
$$N_{i,p}(\bar{v}_k) = \frac{\bar{v}_k - v_i}{v_{i+p} - v_i} N_{i,p-1}(\bar{v}_k) + \frac{v_{i+p+1} - \bar{v}_k}{v_{i+p+1} - v_{i+1}} N_{i+1,p-1}(\bar{v}_k) \tag{3.8}$$

Equation 3.1 can finally be written as a system of linear equations as in equation 3.9.

$$\begin{bmatrix} N_{0,p}(\bar{v}_0) & N_{1,p}(\bar{v}_0) & \cdots & N_{n,p}(\bar{v}_0) \\ N_{0,p}(\bar{v}_1) & N_{1,p}(\bar{v}_1) & \cdots & N_{n,p}(\bar{v}_1) \\ \vdots & \vdots & \ddots & \vdots \\ N_{0,p}(\bar{v}_n) & N_{1,p}(\bar{v}_n) & \cdots & N_{n,p}(\bar{v}_n) \end{bmatrix} \begin{bmatrix} \mathbf{P}_0 \\ \mathbf{P}_1 \\ \vdots \\ \mathbf{P}_n \end{bmatrix} = \begin{bmatrix} \mathbf{Q}_0 \\ \mathbf{Q}_1 \\ \vdots \\ \mathbf{Q}_n \end{bmatrix} \tag{3.9}$$

B-spline basis functions form a $(n + 1) \times (n + 1)$ square matrix. Solution of this system will provide the control points for a particular station defined by a set of the coordinates of points, $\mathbf{Q}_k$. Now, for any coordinates set (x or y), the linear system is solved individually, as in equation

3.10.

$$\begin{bmatrix} N_{0,p}(\bar{v}_0) & N_{1,p}(\bar{v}_0) & \cdots & N_{n,p}(\bar{v}_0) \\ N_{0,p}(\bar{v}_1) & N_{1,p}(\bar{v}_1) & \cdots & N_{n,p}(\bar{v}_1) \\ \vdots & \vdots & \ddots & \vdots \\ N_{0,p}(\bar{v}_n) & N_{1,p}(\bar{v}_n) & \cdots & N_{n,p}(\bar{v}_n) \end{bmatrix} \begin{bmatrix} P_{X_0} \\ P_{X_1} \\ \vdots \\ P_{X_n} \end{bmatrix} = \begin{bmatrix} Q_{X_0} \\ Q_{X_1} \\ \vdots \\ Q_{X_n} \end{bmatrix} \quad \text{or,}$$

$$\begin{bmatrix} N_{0,p}(\bar{v}_0) & N_{1,p}(\bar{v}_0) & \cdots & N_{n,p}(\bar{v}_0) \\ N_{0,p}(\bar{v}_1) & N_{1,p}(\bar{v}_1) & \cdots & N_{n,p}(\bar{v}_1) \\ \vdots & \vdots & \ddots & \vdots \\ N_{0,p}(\bar{v}_n) & N_{1,p}(\bar{v}_n) & \cdots & N_{n,p}(\bar{v}_n) \end{bmatrix} \begin{bmatrix} P_{Y_0} \\ P_{Y_1} \\ \vdots \\ P_{Y_n} \end{bmatrix} = \begin{bmatrix} Q_{Y_0} \\ Q_{Y_1} \\ \vdots \\ Q_{Y_n} \end{bmatrix} \tag{3.10}$$

Conventional linear system solvers such as the Gaussian elimination, the LU decomposition, Iterative solvers, etc. can be applied to solve the linear equations. In the present study, the LU decomposition is adopted to solve the linear equations to calculate the control points $\mathbf{P}_i$.

Computation of a point on a B-spline curve

A point on a B-spline curve can be computed based on a fixed value of $\bar{v}_k$. To compute a point on a B-spline curve at a fixed $\bar{v}_k$, three steps are followed. They are:

1. to find the knot span where $\bar{v}_k$ lies (this is defined while calculation of $N_{i,0}(\bar{v}_k)$ is performed in the first portion of equation 3.8);

2. to compute the nonzero basis functions $N_{i,p}(\bar{v}_k)$ (equation 3.8);

3. to multiply the values of the nonzero basis functions $N_{i,p}(\bar{v}_k)$ with the corresponding control points $\mathbf{P}_i$ (equation 3.9).

3.1.2 Generation of the Surface through the Stations

Pérez-Arribas et al. (2006) followed the simple method of generalization of cubic spline curves to bicubic spline surface. The control polygon was substituted for a control net depending on

two indices, $\mathbf{P}_{i,j} = (P_{X_{i,j}}, P_{Y_{i,j}}, P_{Z_{i,j}})$. In this present work, general global surface interpolation method has been implemented. A surface produced using global interpolation has a special property: change in any point effect the nearby points and eventually the surface in a certain manner. Given a set of $(n + 1)\times(m + 1)$ offset points $\mathbf{Q}_{k,l}$, $k = 0, \ldots, n$ and $l = 0, \ldots, m$ and a non-rational (p, q)-th degree B-spline surface has to be constructed interpolating these points. The B-spline surface is given by equation 3.11.

$$\mathbf{S}(v, u) = \sum_{i=0}^{n} \sum_{j=0}^{m} N_{i,p}(v) N_{j,q}(u) \mathbf{P}_{i,j} \tag{3.11}$$

Since, it contains all the data points, and if the parameter $v = \bar{v}_k$ and $u = \bar{u}_l$ correspond to offset points $\mathbf{Q}_{k,l}$, equation 3.11 becomes,

$$\mathbf{Q}_{k,l} = \mathbf{S}(\bar{v}_k, \bar{u}_l) = \sum_{i=0}^{n} \sum_{j=0}^{m} N_{i,p}(\bar{v}_k) N_{j,q}(\bar{u}_l) \mathbf{P}_{i,j} \tag{3.12}$$

$N_{i,p}(\bar{v}_k)$ is independent of j, hence, it is separable from the summation dependent on j, as follows:

$$\mathbf{Q}_{k,l} = \mathbf{S}(\bar{v}_k, \bar{u}_l) = \sum_{i=0}^{n} N_{i,p}(\bar{v}_k) \left(\sum_{j=0}^{m} N_{j,q}(\bar{u}_l) \mathbf{P}_{i,j} \right) \tag{3.13}$$

As only $\mathbf{P}_{i,j}$ among the terms in braces in equations 3.13 has both i and j indices, the inner expression can be defined as,

$$\mathbf{R}_{i,l} = \sum_{j=0}^{m} N_{j,q}(\bar{u}_l) \mathbf{P}_{i,j} \tag{3.14}$$

More precisely, if i is fixed to the same value, $\mathbf{R}_{i,l}$ is the point evaluated at $\bar{u}_l$, on the B-spline curve of degree q defined by $(m + 1)$ unknown control points on row i of the $\mathbf{P}$'s

$(\mathbf{P}_{i,0}, \mathbf{P}_{i,1}, \mathbf{P}_{i,2}, \ldots, \mathbf{P}_{i,m})$. Finally, equation 3.12 turns into equation 3.15.

$$\mathbf{Q}_{k,l} = \sum_{i=0}^{n} N_{i,p}(\bar{v}_k)\mathbf{R}_{i,l} \tag{3.15}$$

Thus $\mathbf{Q}_{k,l}$ are the points, evaluated at $\bar{v}_k$ of a B-spline curve of degree p defined by $(n + 1)$ unknown control points $\mathbf{R}$'s (i.e., $\mathbf{R}_{0,l}, \mathbf{R}_{1,l}, \mathbf{R}_{2,l}, \ldots, \mathbf{R}_{n,l}$) on column l by repeating this for every k-th $(k = 0, \ldots, n)$ parameter $(\bar{v}_0, \bar{v}_1, \ldots, \bar{v}_n)$. Therefore, the global curve interpolation can be applied to each column of the data points to obtain a column of control points, $\mathbf{R}_{k,l}$. Since there are $m + 1$ columns of offset points (data points), $m + 1$ number of columns of $\mathbf{R}$'s are to be calculated.

Now, the same strategy can be applied to the equation of $\mathbf{R}_{i,l}$ (equation 3.15). In this equation, data points on row i of $\mathbf{R}$'s (i.e., $\mathbf{R}_{i,0}, \mathbf{R}_{i,l}, \mathbf{R}_{i,2}, \ldots, \mathbf{R}_{i,m}$) are the points on a B-spline curve, evaluated at $\bar{u}_0, \bar{u}_1, \ldots, \bar{u}_m$, of degree q defined by $m + 1$ unknown control points $\mathbf{P}_{i,0}, \mathbf{P}_{i,l}, \mathbf{P}_{i,2}, \ldots, \mathbf{P}_{i,n}$. Therefore, applying curve interpolation with degree q and parameters $\bar{v}_0, \bar{v}_1, \ldots, \bar{v}_m$ to row i of the $\mathbf{R}$'s gives row i of the desired control points. Figure 3.4 schematically shows the surface generation process from data point to B-spline surface net interpolations via B-spline curves interpolation.

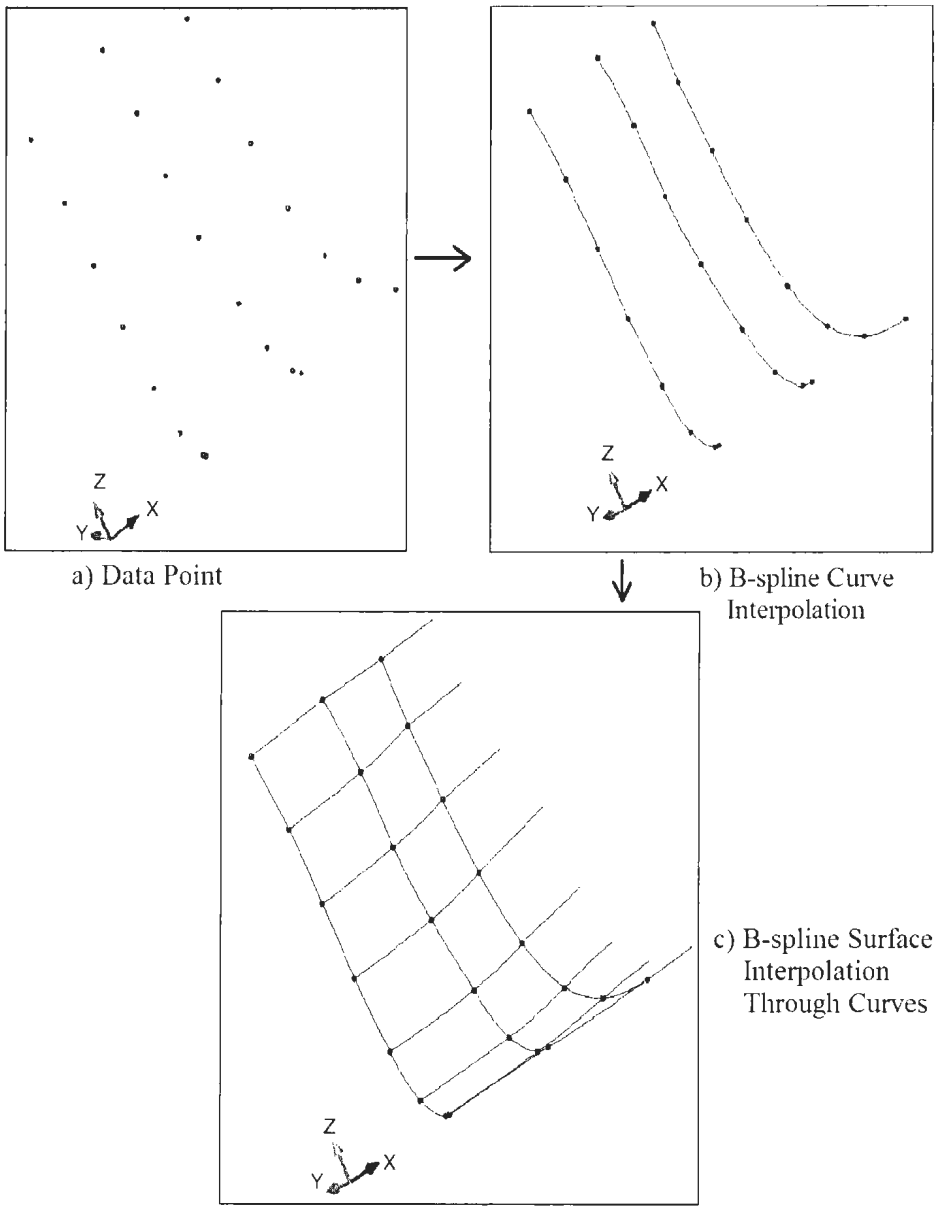

Figure 3.4: B-spline Surface Interpolation

Once all the rows of control points are found, these control points along with the two knot vectors and degree p and q define an interpolated B-spline surface of degree (p, q) of the given data points. Therefore, surface interpolation using B-spline consists of $(n + 1) + (m + 1)$ curve interpolations.

Once the ship hull surface has been defined, an algorithm to check the error in surface fitting can be employed. The first step will be to find out the minimum distance between the B-spline surface points $\mathbf{S}(v_i)$ and data points $\mathbf{Q}_i$. Then, if this minimum distance is a non-zero number, they can be minimized by changing the control points numerically. If the distance is considered as D, then the goal is to minimize the function, $D = \sum_{i=0}^{n} |\mathbf{S}(v_i) - \mathbf{Q}_i|$. This process will reduce the surface fitting error due to interpolation method, if there is any.

Figure 3.5 shows the port side of the original of the series 60 ($C_b = 0.6$) ship. The small white squares indicate the location of the control points for the surface net.

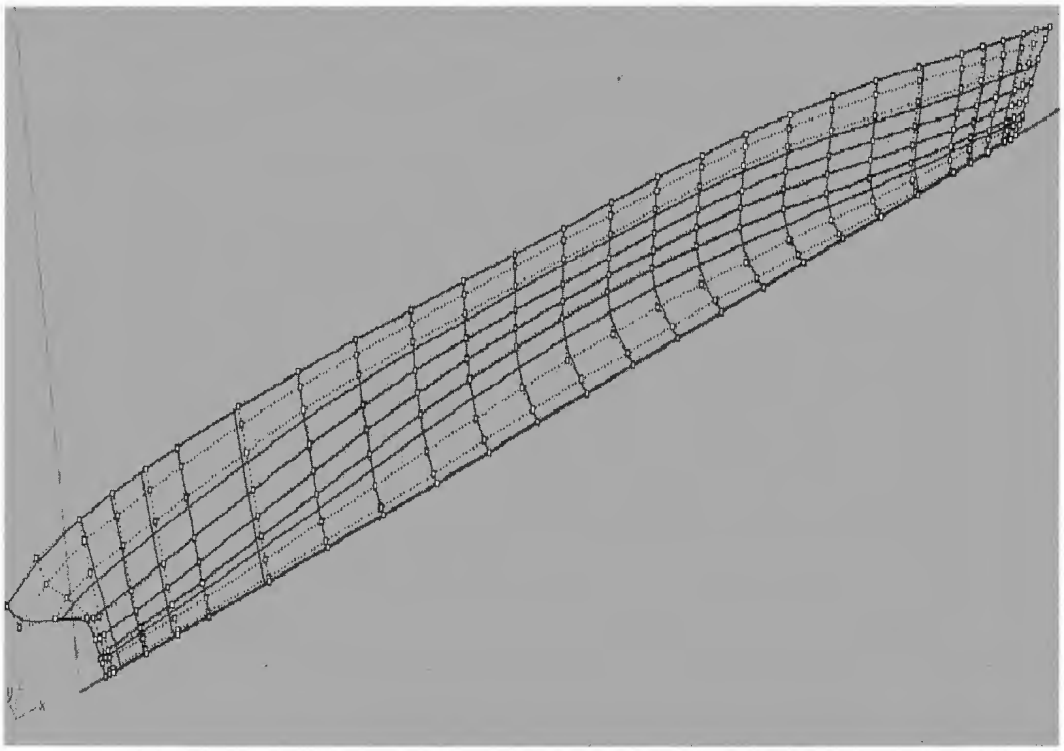

Figure 3.5: Series 60 Hull Surface Expressed by B-spline Surface (Port Side)

3.2 Hull Surface Grid Generation

As the B-spline surface function is a function of parameters ($\bar{u}_l$, $\bar{v}_k$), and it is mapped from the parametric domain to the physical domain by the B-spline function, discretization of the parameters ($\bar{u}_l$, $\bar{v}_k$) for each curve on the surface net will provide new grid points on the surface. Therefore, production of a $(\underline{m}+1)\times(\underline{n}+1)$[1] number of grid points on a physical surface starts with the specification of the boundary distribution along the parametric lines of the surface net. $\underline{m}+1$ is the total number of grid points on the rows and $\underline{n}+1$ is the same on the columns.

The discretization process divides the parameters on each horizontal and vertical curves, and calculates their corresponding coordinates in physical domain by means of the three steps mentioned in section 3.1.1 (page 34). The means of the parameter discretization are discussed in this section. Two different simple schemes have been attempted: the first one is depended on the span between two primary stations or waterlines and the other one is depended on the total number of final grid points.

Grid Generation Scheme 1

For the first method, each horizontal k-th waterline and each vertical l-th station are the boundary lines of the quadrilaterals of the surface net. This method starts with adding points between every two stations. The total number of additional points between every two stations will be defined by,

$$\underline{m}_l = Integer\{(\bar{u}_{l+1} - \bar{u}_l) \times m_u\}, \quad \text{here, } l = 0, 1, \ldots, m-1 \tag{3.16}$$

where, m_u is a selective integer ≥ 20 (changing this value total number of grid columns can be changed), $(\bar{u}_{l+1} - \bar{u}_l)$ is the difference between two parameters $\bar{u}$ in the horizontal direction.

[1] $\underline{m}$ and m or $\underline{n}$ and n denote different numbers. $\underline{m}$ and $\underline{n}$ are the total number of girds on a column and a row respectively.

Load waterline has been taken as the reference line to calculate $\underline{m}_l$.

The main objective of this parameter dividation process is to obtain a number of additional points based on the span between two primary stations. For an example: if $\bar{u}_1 = 0.1$, $\bar{u}_2 = 0.2$, $\bar{u}_3 = 0.4$ and $m_u = 60$, the number of new parameters (eventually, new grid points) between stations 1 and 2 will be $(0.2 - 0.1) \times 60 = 6$. Similary, points between stations 2 and 3 will be 12. If $m_u = 40$, these numbers will be 4 and 8 respectively.

$\bar{u}_l$ denotes parameters on the primary waterlines. Now, denoting $\bar{u}^g_{l_1}$ as the grid points' parameter on the waterlines, $\bar{u}^g_{l_1}$ will be obtained as,

$$\bar{u}^g_{l_1} = \bar{u}_{l_1} + \frac{(\bar{u}_{l+1} - \bar{u}_l) \times l_m}{\underline{m}_l}$$

This calculation continues in a loop, where, $l_m = 1, 2, \ldots, m_l$;

when, $l_m = \underline{m}_l$, $l = l + 1$; (3.17)

$l = 0, 1, \ldots, m - 1$ and $l_1 = 1, 2, \ldots, \underline{m}$

where, $\bar{u}^g_0 = \bar{u}_0 = 0.0$ and similarly, $\bar{u}^g_{\underline{m}} = \bar{u}_m = 1.0$.

In the next step, x-y-z grid points on the watelines are calculated utilizing the corresponding control points $\mathbf{P}_{i,j}$, following the three steps in 3.1.1 (page 34). Figure 3.6(b) shows new grid points on the waterlines in parametric space.

Addition of grid points along the vertical direction is obtained in the similar manner, i.e., introducing vertical parameters along each station. Computation of these parameters for each primary and new station is performed following the similar manner in equations 3.16 and 3.17. $\underline{n}_k$ will be the total additional number of parameters between two waterlines, and $\bar{v}^g_{k_1}$ will be the new parameters. Then,

$$\underline{n}_k = Integer\{(\bar{v}_{k+1} - \bar{v}_k) \times n_v\}, \quad \text{here, } k = 0, 1, \ldots, n - 1 \tag{3.18}$$

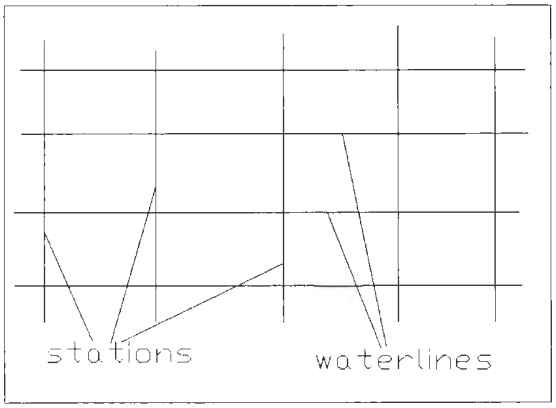

(a) Primary Surface Net

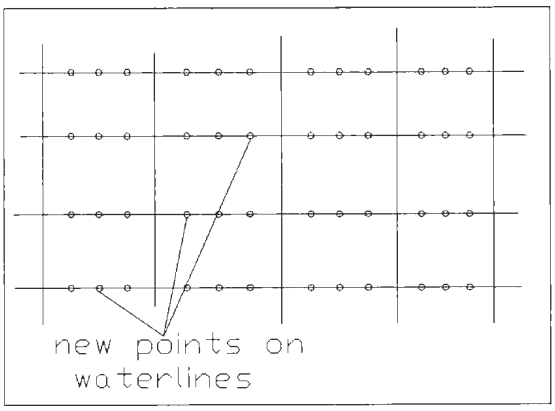

(b) Grid Points on Waterlines

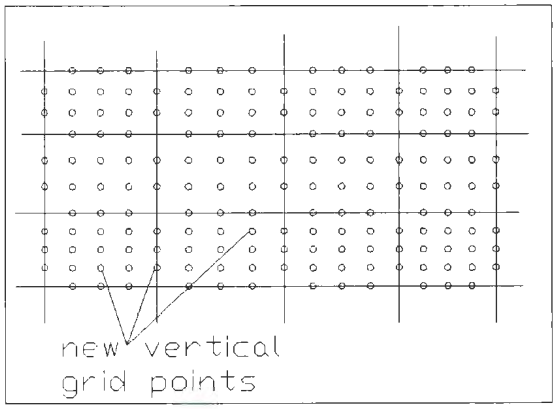

(c) Grid Points on Vertical Direction

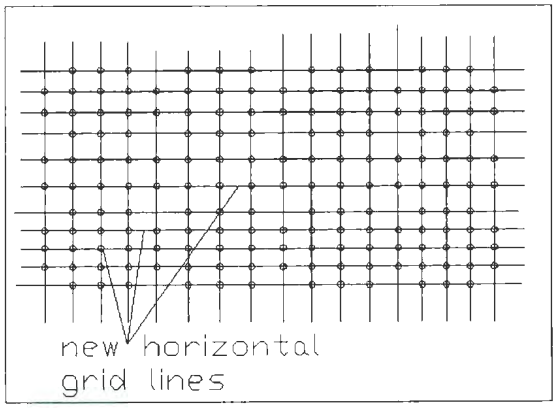

(d) New Grids and Lines

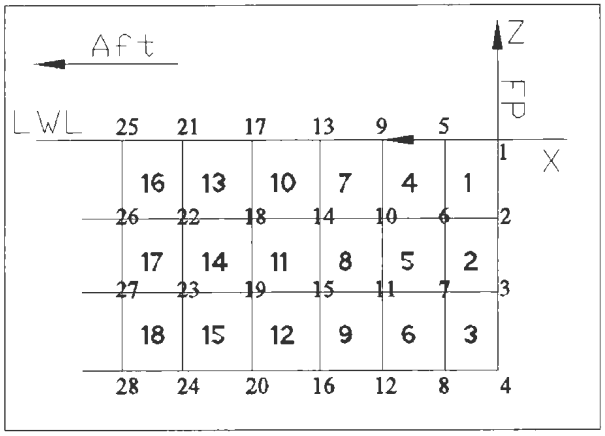

(e) Grids and Nodes Arrangement

Figure 3.6: Grid Generation Process Step-by-step.

where, n_v is a selective integer ≥ 20 (the total number of grid rows can be changed by changing this value), $(\bar{v}_{k+1} - \bar{v}_k)$ is the difference between two parameters $\bar{v}$ in the vertical direction.

Again,

$$\bar{v}^g_{k_1} = \bar{v}_{k_1} + \frac{(\bar{v}_{k+1} - \bar{v}_k) \times l_n}{\underline{n}_k}$$

This calculation continues in a loop, where, $l_n = 1, 2, \ldots, n_k$;

when, $l_n = \underline{n}_k$, $l = l + 1$;

$l = 0, 1, \ldots, n-1$ and $k_1 = 1, 2, \ldots, \underline{n}$ (3.19)

where, $\bar{v}^g_0 = \bar{v}_0 = 0.0$ and similarly, $\bar{v}^g_{\underline{n}} = \bar{v}_n = 1.0$.

Following the similar manner as before, the new grid points' coordinates are computed utilizing corresponding control points, $\mathbf{P}_{i,j}$ and basis functions. Figure 3.6(c) illustrates this stage, where all the grid points in the parametric space are introduced.

Figure 3.6(d) shows all the grid points and lines. Figure 3.6(e) gives an idea on the formations of panels used in the input file for the MAPS-Resistance program. The numbering of the nodes starts from the top of a station, increases till the bottom, and starts from the top of next station. The counting starts from the very first station (forward profile) at the forward end and continues to the aft.

Grid Generation Scheme 2

The B-spline parameters for the grid points are calculated in the following manner:

$$\bar{u}^g_{l_1+1} = \bar{u}^g_{l_1} + \frac{(\nabla \bar{u}_k) \times l_1}{\underline{m}} \text{ or,}$$
$$\bar{u}^g_{l_1+1} = \bar{u}^g_{l_1} + \frac{(\bar{u}_m - \bar{u}_0) \times l_1}{\underline{m}} \quad (3.20)$$

where, $l_1 = 0, 1, \ldots, \underline{m}$, $\bar{u}^g_0 = \bar{u}_0 = 0$, $\bar{u}^g_{\underline{m}} = \bar{u}_m = 1$ and $\underline{m}$ = total number of grids on a row.

Again,

$$\bar{v}^g_{k_1+1} = \bar{v}^g_{k_1} + \frac{(\bar{v}_n - \bar{v}_0) \times k_1}{\underline{n}} \tag{3.21}$$

where, $k_1 = 0, 1, \ldots, \underline{n}$, $\bar{v}^g_0 = \bar{v}_0 = 0$, $\bar{v}^g_{\underline{n}} = \bar{v}_n = 1$ and $\underline{n}$ = total number of grids on a column.

The main advantage of scheme 2 is that the density of the grids/ panels on any particular region can be controlled. By placing a comparatively higher number of parameters within a smaller length will produce denser meshes in the region. For an example, $\underline{m}$ can be divided in three parts, with $\frac{\underline{m}}{3}$ number of grids in each part. Then equation 3.20 will be divided in three parts, but the primary parameters $\bar{u}_k$ will be distributed depending on the requirement of the density of meshes. If the forward portion between first four primary stations needs denser grids, $\nabla\bar{u}_k = \bar{u}_3 - \bar{u}_0$, where, this portion is lower than $\frac{1}{3}$rd of the whole length (e.g. $\frac{1}{5}$th) of the ship.

Surface Regeneration for Grids

The introduction of grids to the surface shows a positive effect on the surface smoothness quality. It shows that, due to the introduction of close grid parameters, the surface gets rid of local bump produced due to inadequate data points. Thus, the graphical presentation and surface regeneration become an important task as well. Same method for primary hull generation is applied for the new grid points to model the grid lines and surface. Directly the global interpolation is applied on the new physical grid points to model the discretized surface.

In order represent geometric models of the B-spline surface geometries of the original hull and discretized hull, IGES 5.3 (Initial Graphics Exchange Specification) file format has been employed. To learn about the details on the requirements to prepare an IGES 5.3 format file for different models expressed with certain types of geometric tools (e.g., lines, parametric splines, B-spline surface, etc.), refer to the publication from *U.S. Product Data Association*, IGES 5.3 (IGE, 1996).

3.3 Hull Form Variation

The first method adopted here to change the hull form is similar to the first scheme practiced by Markov and Suzuki (2001). This scheme directly shifts ship hull sections. The hull sections shift is performed moving the control points assigned to each station in longitudinal direction. Equation (3.12) expresses the hull surface, where control points, $\mathbf{P}_{i,j} = (X_{i,j}, Y_{i,j}, Z_{i,j})$[2].

In the first scheme, the longitudinal variable is $X_{i,j}$, where, $X_{i,0}$ and $X_{i,m}$ are stationary. The optimization algorithm requires an initial change in the variables to calculate gradients of the objective function. The initial change is chosen to be dependent on ship length. $\frac{L}{400.0}$ seems to work properly as the change of $X_{i,j}$ in the gradient calculation. Therefore, the new location of control points are $(X_{i,j} + \frac{L}{400.0})$. This initial increment may vary depending on the vessel's principal dimensions and the type of modification. Once the first control point of each station is changed, every control point on the station in the vertical direction are changed in the same way.

Ship hull has been divided in n_l number of different regions along the length. One of the objectives is to maintain the ship shape similar to original as much as possible. Therefore, there have been constraints set up, so that consecutive stations do not exchange their positions. Denoting l_c as the variable to be modified by the optimization algorithm, the hull section shifting strategies follows the equation, 3.22[3].

$$
\begin{aligned}
& X^1_{i,j} = X^1_{i,j} \pm l_c \qquad \text{where, } c = 1, 2, \ldots, n_l, \text{and,} \\
& l_c \leq |X^1_{n,e+1} - X^1_{n,e}| \\
& \text{where, } e = c \times \frac{m}{n_l} - 1, \text{ and, } c = 1, 2, \ldots, n_l
\end{aligned}
\tag{3.22}
$$

[2]From this point, the control points will be denoted by $\mathbf{P}_{i,j} = (X_{i,j}, Y_{i,j}, Z_{i,j})$ instead of $\mathbf{P}_{i,j} = (P_{X_{i,j}}, P_{Y_{i,j}}, P_{Z_{i,j}})$ for convenience and clarity.

[3]For clarity and convenience $\underline{m}$ and $\underline{n}$ have been denoted as m and n in this section. All the m and n, in the rest of this chapter, stand for gird numbers $\underline{m}$ and $\underline{n}$. n_l, n_b and n_d are different numbers.

In equation 3.22, the first values for l_c starts with zero. After the first gradient calculation the change in the variables are set to zero again. Therefore, the limiting values for l_c is dependent on new control points X^1, which indicates that the regions are being shifted, and the stations are being shifted as well.

The second method of hull form variation is based on deformation of hull sections in the athwart direction (y-direction). Following the similar strategy of the first scheme, control points $Y_{i,j}$ are varied for each station. $Y_{0,j}$ and $Y_{n,j}$ are unchanged, as well as $X_{i,j}$ and , $Z_{i,j}$. The differential increment of $Y_{i,j}$ in gradient calculation of the optimization algorithm is dependent on breadth (B) of the vessel, which is $\frac{B}{300.0}$ (dependent variable). The ship hull has been again divided into n_b number of regions. For each region, the variable assigned for the change of $Y_{i,j}$ is b_c. b_c is the variable to be optimized, will change the control points, and eventually, modified hull form. The constraints set up for the control points $Y_{i,j}$ variation is given by equation 3.23. $Y^1_{i,j}$ is recurrently checked, where values of b_c start with zero.

$$
\begin{aligned}
Y^1_{i,j} &= Y^1_{i,j} + b_c \qquad \text{where, } c = 1, 2, \ldots, n_b, \text{ and,} \\
b_c &> \begin{cases} Y^1_{1,e} - Y^1_{0,e+1}\,, & \text{if } Y^1_{1,e} \geq Y^1_{1,e^1+1} \\ Y^1_{1,e^1+1} - Y^1_{0,e^1+1}\,, & \text{if } Y^1_{1,e} < Y^1_{1,e^1} \end{cases} \\
b_c &\leq \begin{cases} Y^1_{n-1,e^1+1} - Y^1_{n,e^1+1}\,, & \text{if } Y^1_{n-1,e} \geq Y^1_{n-1,e^1+1} \\ Y^1_{n-1,e} - Y^1_{n,e}\,, & \text{if } Y^1_{n-1,e} < Y^1_{n-1,e^1+1} \end{cases} \\
&\text{where, } e = c \times \frac{m}{n_d}\,, \\
&\qquad e^1 = c \times \frac{m}{n_d} - \frac{m}{n_d} \text{ and,} \\
&\qquad c = 1, 2, \ldots, n_b
\end{aligned}
\tag{3.23}
$$

The total number of b_c depends on the number of division in the ship hull, n_b. Hence, the number of variables to be optimized can be chosen. The final optimized variables, b_c will

produce the modified hull form with new control points $Y^1_{i,j}$.

In the similar manner, the stations can be modified by changing the z-coordinate of the control points. In this case, the total number of regions of the ship hull is divided along the draft. The total number of regions and the variables to be optimized are n_d and d_c respectively. The modification procedure satisfies equation 3.24. Similar to equation 3.23, $Z_{i,j}$ has been denote by $Z_{i,j}$ for convenience.

$$
\begin{aligned}
& Z^1_{i,j} = Z^1_{i,j} + d_c \\
& \text{where,} \\
& \quad Z^1_{e+1,j} \leq Z^1_{e,j} \text{ and,} \\
& \quad e = c \times \frac{n}{n_d} \text{ and,} \\
& \quad c = 1, 2, \ldots, n_d
\end{aligned}
\tag{3.24}
$$

All the modification schemes mentioned above are completely based on the control points of B-spline surfaces for each station point. m and n are the total number of control points in row and column respectively. Several conditional constraints has been applied to keep the ship likeness to her original hull form. Recurring modification of control points occurs, and in every complete modification the hull shape is checked. The modification variables l_c, b_c or d_c are updated, if required by the constraints. The design length, breadth and draft of the ship have been aimed to be unchanged.

Random combinations of the schemes defined in equations 3.22 to 3.24 can also be investigated. In that case, total number of variables to be optimized by optimization algorithm will be $(n_l + n_b)$ or $(n_d + n_b)$ or $(n_d + n_b)$. These will provide hull sections' shifts and deformation at the same time.

3.4 Optimization

In general, nonlinear multivariable optimization problems are stated as:

$$\begin{aligned} &\text{Minimize or Maximize:} \quad y = f(\mathbf{x}) \\ &\text{Subject to:} \quad g_{ii}(\mathbf{x}) = 0 \qquad \text{for } ii = 1, 2, \ldots, h \\ &\qquad\qquad\quad g_{ii}(\mathbf{x}) \geq 0 \qquad \text{for } ii = h+1, \ldots, mm. \end{aligned} \tag{3.25}$$

There will be nn number of variables, $\mathbf{x} = x_1, x_2, \ldots, x_{nn}$. If there are constraints, there will be mm number of constraint equations, where h is the number of equality constraints (Rao, 2009).

In this study, wave making resistance coefficient, C_w is set to be the objective function. C_w is a function of wave making resistance (R_w), forward speed (U), water density (ρ) and wetted surface area (S_B), expressed as, $C_w = \dfrac{R_w}{\frac{1}{2}\rho U^2 S_B}$. R_w is dependent on the ship geometry and the wave condition. In the panel method, ship geometry is defined by the panels and node coordinates of the panels. In the present surface modeling system, those nodes are dependent on B-spline control point, $\mathbf{P}_{i,j}$. Therefore, $\mathbf{P}_{i,j}$ are considered as the variables in the optimization problem, and C_w will be treated as the function of $\mathbf{P}_{i,j}$. Thus, the generalized optimization problem can be expressed as:

$$\begin{aligned} &\text{Minimize: } C_w = f(\mathbf{P}_{i,j}) \\ &\text{Subject to: } \left| L \times B \times T \times C_b - \int_0^L \left(\int_0^T y \, \mathrm{d}z \right) \mathrm{d}x \right| \leq tolerance \\ &\qquad\qquad \begin{bmatrix} x_{i,j} \\ y_{i,j} \\ z_{i,j} \end{bmatrix} \leq \begin{bmatrix} L \\ B \\ T \end{bmatrix} \end{aligned} \tag{3.26}$$

here, $i = 0, 1, \ldots, \underline{n}$ and $j = 0, 1, \ldots, \underline{m}$. L, B and T, are the length, breadth and draft of a ship

respectively, and C_b is the block coefficient. x, y and z are the x-y-z coordinates of the ship hull surface grids, which are dependent on control points, $\mathbf{P}_{i,j} = \{X_{i,j}, Y_{i,j}, Z_{i,j}\}$. The term *tolerance* is a selective number based on a particular case. *tolerance* is the amount of difference between the volume of a modified hull and the original one, that a researcher wants to maintain. The second set of constraints is designated to maintain the original length, breadth and draft of the ship. As explained in previous section of hull variation, $\mathbf{P}_{i,j}$ is the variable to change the hull form, and the variation methods have constraints set up, which are originally dedicated to maintain the length, breadth, draft and ship-like look of the ship.

There are four classes of procedures for multivariable optimization applicable to non-linear models. These are multivariable search methods, multivariable elimination procedures, random search, and stochastic approximation procedures. Multivariable search methods are the most important ones. These methods can be considered as encompassing the theory and algorithms of nonlinear programming along with the associated computational methods (Pike, 2001).

Multivariable search methods use algorithms which are based on geometric or logical concepts, and generates a sequence of values of $\mathbf{x}_k$ that move rapidly from the starting point $\mathbf{x}_0$ to neighborhood of optimum $\mathbf{x}^*$. Then in the algorithm, iteratively $\mathbf{x}_k$ should converge to $\mathbf{x}^*$, and terminates when a convergence test is satisfied. Therefore, an important theoretical strategy for an algorithm should be a theorem that proves the sequence of values $\mathbf{x}_k$ generated by the algorithm converge to a local optimum, for an example, steepest ascent method. All the algorithms involve a line search given by the equation 3.27.

$$\mathbf{x}_{k+1} = \mathbf{x}_k + \alpha[H_k]\,\nabla f(\mathbf{x}_k) \tag{3.27}$$

where, $\mathbf{x}_k$ is the variable to change in the optimization algorithm, α is the optimized step length between variables in two consecutive iterations, $[H]$ is the Hessian matrix to be calculated based on optimization method, k is the iteration number in the optimization algorithm and ∇f

is the gradient of the objective function (C_w) due to an inital change of the variables (explained in the following paragraphs for optimization steps).

Different algorithms, such as, Newton's method, quasi-Newton methods, gradient search, etc. have different ways of calculating the square matrix $[H_k]$. Gradient search method uses a unit matrix $[I]$ for $[H_k]$. Newton's method has the inverse of the Hessian matrix[4], $[H]^{-1}$ and α is one in equation 3.27. For quasi-Newton method $[H_k]$ is a series of matrices starting with unit matrix, $[I]$, and ends with the inverse of the Hessian matrix, $[H]^{-1}$.

In this study, the BFGS method of optimization has been practiced, which is an extended form of quasi-Newton method. This method updates the Hessian matrix by the BFGS formula which is considered to be the most effective method among the unconstrained multivariale search technique (Pike, 2001). The steps to develop the BFGS algorithm with the application of hull variation and performance evaluation are discussed as follows (according to Rao (2009)).

1. As mentioned before, it starts with an initial point $\mathbf{x}_1$, $\left(\text{where, } \mathbf{x} = \begin{bmatrix} x_1 \\ x_2 \\ \vdots \\ x_{nn} \end{bmatrix} \right)$ and a positive $nn \times nn$ symmetric matrix $[H_1]$, as an initial estimated of the inverse of the Hessian Matrix of target function f. Referring to equations 3.22 to 3.24, $\mathbf{x} = l_c$, b_c or d_c (which are dependent on control points, $(\mathbf{P}_{i,j})$, $c = 1, 2, \ldots, nn$, and $nn = n_l$, n_b or n_d, depending on the method of modification is in operation.

   In the absence of additional information, $[H_1]$ is taken as the identity matrix $[I]$. Gradient vector $\nabla f_1 = \nabla f(\mathbf{x}_1)$ is computed, and the iteration number is set as $k = 1$.

[4]Hessian Matrix is a square matrix of second order partial derivatives of a function.

$$\nabla f_1 = \nabla f(\mathbf{x}_1) = \begin{bmatrix} \dfrac{\delta f}{\delta(x_1)_1} \\ \dfrac{\delta f}{\delta(x_2)_1} \\ \vdots \\ \dfrac{\delta f}{\delta(x_n)_1} \end{bmatrix}$$

For an example, in the case of the second scheme of hull modification, if the initial change for gradient calculation is b_c then, the above equation for gradients becomes,

$$\nabla f(b_c)_1 = \begin{bmatrix} \dfrac{C_w(Y_{i,(1\times j)+1} + b_c) - C_w(Y_{i,(1\times j)+1})}{b_c} \\ \dfrac{C_w(Y_{i,(2\times j)+1} + b_c) - C_w(Y_{i,(2\times j)+1})}{b_c} \\ \vdots \\ \dfrac{C_w(Y_{i,(n_b\times j)+1} + b_c) - C_w(Y_{i,(n_b\times j)+1})}{b_c} \end{bmatrix} \tag{3.28}$$

here, $j = 0, \ldots, \dfrac{m}{n_b}$, and, $i = 0, \ldots, n$

where, $n_b =$ number of regions, the ship is divided into.

$m =$ number of horizontal grid points

$n =$ number of vertical grid points

In the above equation, Y is the y-coordinates of control points. During the modification it is necessary to maintain $Y_{i,0}$ and $Y_{i,m}$ as unchanged. While changing the coordinates, it should be confirmed that all the points in i-th direction (vertical direction) are modified at the same time.

2. The gradient of the function ∇f_k , at $\mathbf{x}_k$ is computed, and set $\mathbf{S}_k = -[H_k]\nabla f_k$.

3. The optimal step length α_k^* in the direction $\mathbf{S}_k$ is calculated, and set $\mathbf{x}_{k+1} = \mathbf{x}_k + \alpha_k^* \mathbf{S}_k$. Here, optimal step length α_k^* can be calculated by the Fibonacci search method of the Golden section search method. In the present study, the Fibonacci search method has been employed to find the optimal step length [Appendix A]. But, if the Fibonacci number inside the search algorithm is too high then, step length is set to 1.00.

4. The point $\mathbf{x}_{k+1}$ is tested for optimality. If $|\nabla f_{k+1}| \leq \varepsilon$, where ε is a very small quantity, $\mathbf{x}^*$ is considered as $\mathbf{x}^* \approx \mathbf{x}_{k+1}$ and the process is stopped. Otherwise, the whole method proceeded to step 5.

5. The Hessian matrix is updated as

$$[H_{k+1}] = [H_k] + \left(1 + \frac{\mathbf{g}_k^T [H_k] \mathbf{g}_k}{\mathbf{d}_k^T \mathbf{g}_k}\right) \frac{\mathbf{d}_k \mathbf{d}_k^T}{\mathbf{d}_k^T \mathbf{g}_k} - \frac{\mathbf{d}_k \mathbf{g}_k^T [H_k]}{\mathbf{d}_k^T \mathbf{g}_k} - \frac{[H_k] \mathbf{d}_k^T \mathbf{g}_k}{\mathbf{d}_k^T \mathbf{g}_k} \tag{3.29}$$

where, $\mathbf{d}_k = \mathbf{x}_{k+1} - \mathbf{x}_k = \alpha_k^* \mathbf{S}_k$, and

$$\mathbf{g}_k = \nabla f_{k+1} - \nabla f_k = \nabla f(\mathbf{x}_{k+1}) - \nabla f(\mathbf{x}_k)$$

6. New iteration number is set as $k = k + 1$ and proceeded to step 2.

For an example, in the second method of hull variation, $\mathbf{x}_k = (b_c)_k$, where, c is the number of variables ($c = 1, 2, \ldots, n_b$), and k is the number of iterations. Then, ∇f_k is defined as follows,

$$\nabla f_k = \begin{bmatrix} \dfrac{C_w(Y_{i,(1\times j)+1} + b_1) - C_w(Y_{i,(1\times j)+1})}{(b_1)_k - (b_1)_{k-1}} \\ \dfrac{C_w(Y_{i,(2\times j)+1} + b_2) - C_w(Y_{i,(2\times j)+1})}{(b_2)_k - (b_2)_{k-1}} \\ \vdots \\ \dfrac{C_w(Y_{i,(n_b\times j)+1} + b_{n_b}) - C_w(Y_{i,(n_b\times j)+1})}{(b_{n_b})_k - (b_{n_b})_{k-1}} \end{bmatrix} \tag{3.30}$$

here, $j = 0, 1, \ldots, \frac{m}{n_b}$; $i = 0, 1, \ldots, n$; n_b = number of regions in which the ship is divided into; m = number of horizontal grid points and n = number of vertical grid points.

The hull performance evaluation function will be calculated for every variable change and in each iteration. Inside the algorithm for the optimal step length (α_k^*), the target function will be evaluated several times depending on the calculated Fibonacci number. Therefore, the faster the objective function evaluation is completed, the faster each iteration is completed. At the final iteration, the optimization algorithm provides the optimum variables, which produces the optimum location of each stations coordinates. In this study, the final outputs are: the optimum hull form's coordinates, the intermediate modified hull forms' coordinates for all the iterations, a record of the C_w values for all iterations and the basic geometric information, and for the graphical representation IGES files for all iterations. MAPS Resistance 2012 is called every time for the calculation of the wave resistance coefficient, C_w.

3.5 AMECRC high-speed monohull

The method of ship hull geometry development has been attempted to apply on a model from AMECRC series for high-speed monohull. The AMECRC systematic series is based on the High-Speed Displacement Hull Form (HSDHF) systematic series developed at the Maritime Research Institute Netherlands (MARIN) (Sahoo et al., 2011). The parent hull forms of the AMECRC series was based on the parent hull form of HSDHF series and subsequently 13 more models were developed by systematic variation of L/B, B/T and C_b. These are the ship hull types with transom sterns.

Model # 1 from the series was chosen for the geometrical validation. Ship hull's coordinate information was available in a general format, where the coordinates of x, y and z are given in three common long columns for all the stations. Therefore, a new modified program was developed to facilitate the input file and transom stern hull representation. The input file

types are discussed in section 4.1 in chapter 4. The process of discretization of the transom stern is discussed in the following paragraphs.

It is not necessary to perform the discretization of the transom during the main hull body discretization. In this study, the transom has been considered as a flat surface, therefore, straight lines connecting grid points on the stern section will provide the panels on the transom surface. It can be performed just before the input file preparation for a ship hull performance evaluation. Also, for the graphical representation, the discretization can be performed inside the IGES format algorithm. Section 4.4 in chapter 4 discusses the algorithm of the transom stern discretization.

Chapter 4

Numerical

During the development of programs, different apposite techniques and tools have been utilized beside the main methodologies. Preparation of input files, checking for the zero tangency of ship bottom region, transformation of the input data to a data set of row $\times$ column format, discretization of transom stern, etc., require special concern and judicious techniques. This chapter lists varieties of practices similar to these, and their methodologies along with their algorithms (if applicable). It is expected that, this chapter will help for better comprehension of the programs developed for the ship hull generation and the optimization system.

4.1 Organization of Input File

Primarily, the input file type was based on conventional offset table. The geometric data points for Model # 1 ship from the AMECRC series were more in general forms. As mentioned in 3.5 in chapter 3, a new input file format was required to be prepared. A modified program was prepared too. The only modification in this new program was in the input file reading and the additions for transom stern. This program still can deal with cruiser or counter stern, but the type of the ship stern is needed to be declared in the input file. The rest of the program is the same as the first optimization program. In fact, both programs are the same except for

the requirements for the input files. But, the first program do not deal with transom or bulbous bow, and the second program does not read the table of offsets directly.

Input data requires the information for centerline profile curve at the bow and stern for both cases. The process of preparation of these data points is discussed in the first subsection. Then, the following subsection discusses on both of the input file types.

4.1.1 Shape of Centerline Profile Curves

In the present study, an existing ship with her hull coordinates is the target of investigation. For an existing ship type, there should always be some knowledge on the forward and after end shape of the ship, if no coordinate information are given for that regions. Prediction or drawing of forward or after end profile shape without any kind of relevant information is not possible, unless it is in the primary stage of a new ship design.

If there are no coordinates information for the centerline profile curves, there could be several ways to obtain the points on these curves. If there is a printed copy of the hull shape, scaled measurement from the drawing will provide approximate coordinates of the points. These points on the curves should be on the waterlines of the ship. A plot of these points against the waterlines distances (z-coordinates) will show schematic shapes of these curves (Fig. 4.1). Then, this can be compared with the original one. If there is a software copy of the ship given, the dimensions can easily be obtained. But, all z-coordinates will have to be on the given waterlines of the original ship data. The plotted curves need not to necessarily be exactly the same as the original profile. If the points' coordinates are close enough, B-spline curve interpolation will produce the best possible shape.

One of the models from the well known series 60 ship hull was the first one investigated in this study. The model was the one with block coefficient, $C_b = 0.6$. Todd (1963)'s experimental report provides a common detail on the centerline profile curves for series 60 hull in chapter 4. Figure 4.2 demonstrates contour of the forward and after end of the series 60 ships.

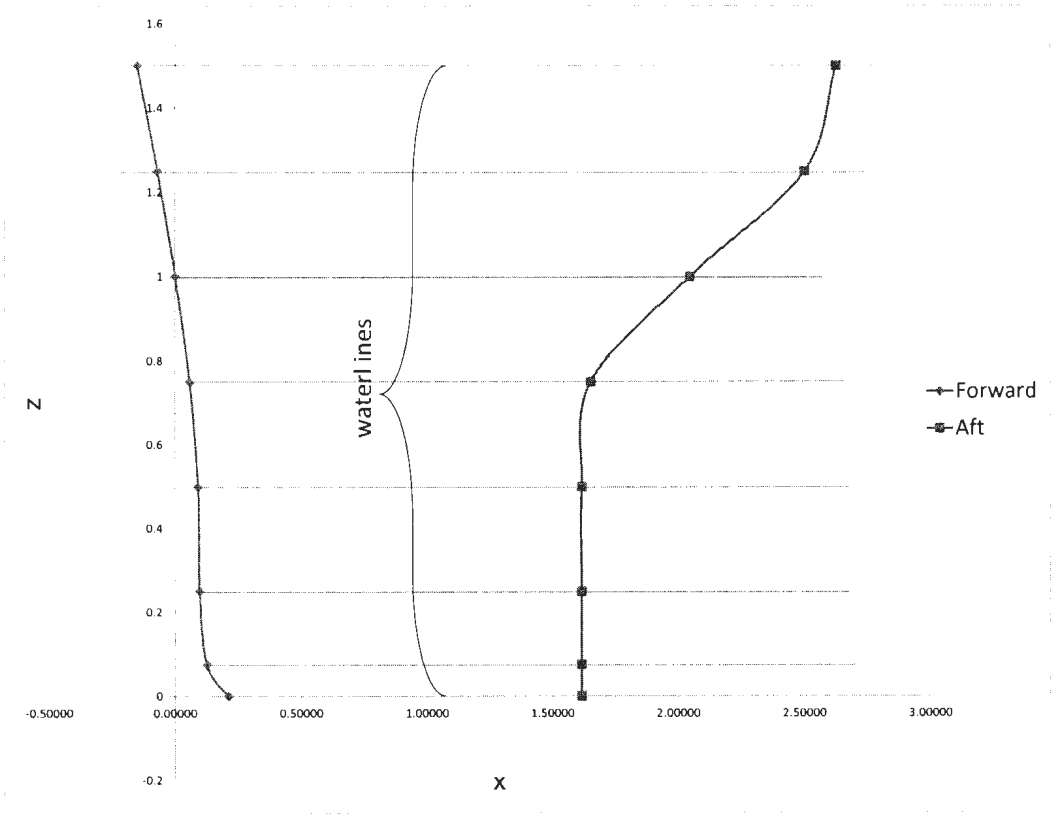

Figure 4.1: Profile Curves Plot (disregard the values)

To obtain the required coordinates, it just needs to be divided into the waterlines according to the studied ship' offset table.

On the contrary, the numerical information provided for the AMECRC ship hull was not good enough to draw the forward region above the design waterline. The coordinate information is only up to forward perpendicular. But, there was a reference drawing for the ship hull model # 1. Therefore, obtaining forward profile information was not an issue. But, the points given for each station were not the same in number, which means, the numbers of the given nodes on the ship hull surface were not the same for each row. The necessary changes made in the input data format, to develop the hull surface automatically, will be explained in following sections.

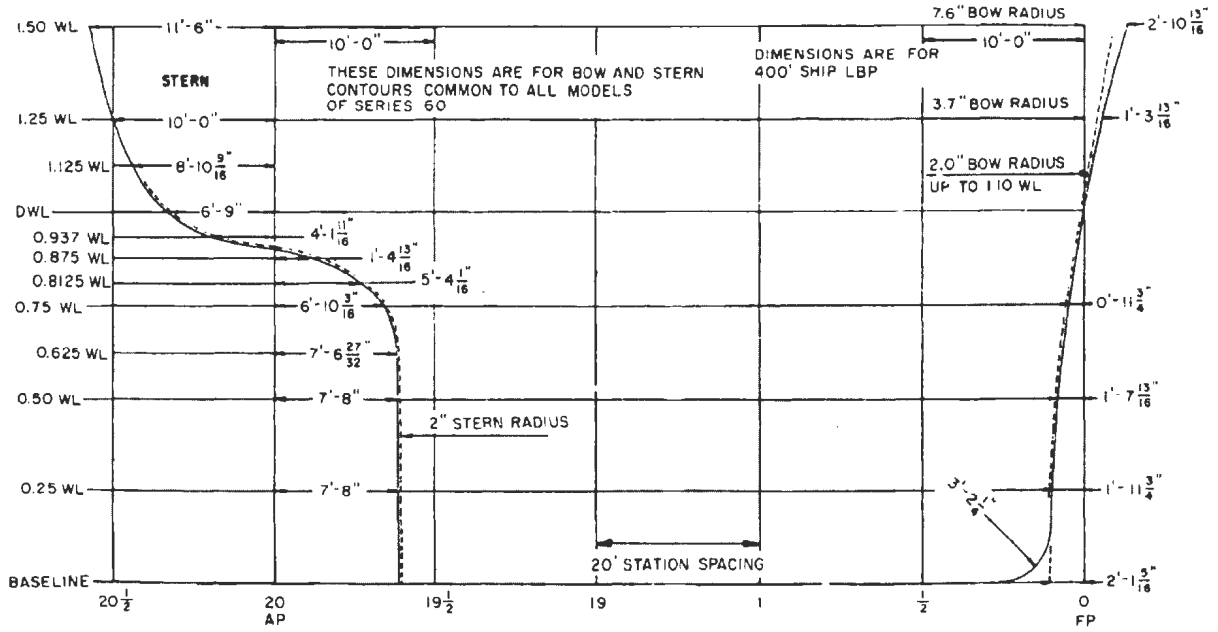

Figure 4.2: Series 60 Profile. *Courtesy, Todd (1963)*

4.1.2 Input Files

The process of the preparation of these two different input files has different goals of their own. The input file in offset table format requires additional information on profile curves. On the other hand, the input file for general *x*-*y*-*z* format requires the data set to be in a $m \times n$ (row $\times$ column) format, along with the profile curves' information.

Appendix B shows the two different types of the input files. The first one is for offset table format. The file will be prepared in Microsoft Excel, and then needs to be saved in "*.csv" (comma delimited) format file. In excel, "save as" command has different options for file output to be saved, and "CSV (comma delimited, *.csv)" is the option needs to be chosen. Figure B.1 in appendix B shows a partial image of a sample of an offset table format input file in MS Excel. The items inside the input file are listed below with details, according to the number of rows (the number on the left is the row number in the excel file).

1. In this row a title for the input file can be given or kept blank.
2. Name of the ship or blank.
3. Total number for the stations[1] is provided on this row on fourth column (column D).
4. Total number for the waterlines[1] is written on this row on fourth column (column D). If there is a flat bottom, this number will be (total waterlines + 1).
5. Load Water Line length[1] (LWL) of the ship.
6. Maximum beam (breadth)[1] of ship at load waterline.
7. Maximum draft[1] up to load water line.
8. Intentionally kept blank.
9. No action required on this row.
10. Location of waterlines including bottom line, the values start from bottom to top. If there is a flat bottom, the first number is repeated in column C [2].
11. x-coordinates of the points on the bow profile curve intersected by waterlines [3]. If there is a flat bottom, the first value is repeated in column C. An insignificant increment can be given in this second value.
12. x-coordinates of the points on the aft profile curve intersected by waterlines [3]. If there is a flat bottom, the first value is repeated in column C. The first value can be insignificantly smaller than the second one (difference in third decimal point).
13. Intentionally kept blank.

[1]The number shall only be written on column D, everything else remains unchanged on this row.

[2]All the values start from column B, column A is intentionally kept blank.

[3]In this case, x is zero at forward perpendicular (FP), positive to the aft direction. Refer to section 3.1.1 for coordinate systems.

14. Repeats row 10.

15. From this row through the next suitable rows, the coordinate information is borrowed from the offset table. First column (column A) gives the stations' locations (x-value) [3]. Column B contains the bottom centerline information with all zeros. The rest of the columns contain the remaining values from a conventional offset table as in series 60. If the values are given in the form of ratios of the maximum beam, actual coordinates should be obtained first.

As mentioned before, this file will be saved as *.csv file. Figure B.2 in appendix B shows a partial image of a sample *.csv file for offset table format input file.

The difference in the structure of the input file for x-y-z format is given below.

- Row 1 is the same. Row 2 to 6 are same as row 3 to 7 for the offest table format file.
- Row 7 is intentionally kept blank.
- Row 9 reads if there is a transom stern. If there is a transom hull TR = 1 in column 9, otherwise, TR = 0.
- Row 13 reads if there is a bulbous bow in the profile.
- From row 11 to the end row the ship hull's coordinates are given. Column A, B and C contain the values for x, y and z coordinates respectively [4].

Figure B.3 and B.4, in appendix B, show partial images of the *.xls file and the *.csv file, respectively, for this type of input file. These files can be saved in any name. At the start of the program the name has to be provided on the screen, when asked. Next, total numbers of required grid rows and columns should be provided.

[4] x is zero at forward perpendicular (FP), positive to aft direction. Refer to section 3.1.1 for coordinate systems.

4.2 Flat Bottom Ships

This section is about the analysis of the zero tangency of the ship hull bottom i.e., flat bottom. Depending on the flatness of the hull bottom, the total number of vertical nodes will be defined. After the data input in the program, it first calculates the sum of column B and C seperately. If the sum of column B is zero, nodes' count starts from column B which indicates that the ship has a flat bottom hull. Otherwise, the nodes' count starts from column C. In either case, the first node is always the point on bottom center line (keel line) for each station. Later, the first point is set to the top water line. This process is only applicable to the program where offset table format is the input file.

4.3 Transformation of an Offset Table to a Row×Column Data Set

This process applies to the program with offset table format input file. In the other case, the iput file is prepared in row×column type data set. In the following paragraphs both of these cases are discussed.

Figure 4.3 shows a manual drawing of the series 60 ($C_b = 0.6$) hull. This ship hull form has been drawn using only the coordinates' information available in the offset table. The coordinates for station 20 (AP) have only 3 nodes, i.e., the y-value for the top 3 water lines. An automatic hull form development always requires a $m \times n$ (row×column) number of points. The development of IGES file format and the input file for MAPS resistance also have the same requirements. Therefore, all the stations requires same number of points, i.e., nodes on every water line.

To solve this problem for the stations similar to 20 (AP), different techniques could be implemented. In the program, first, there is a search for these kinds of stations. Stations'

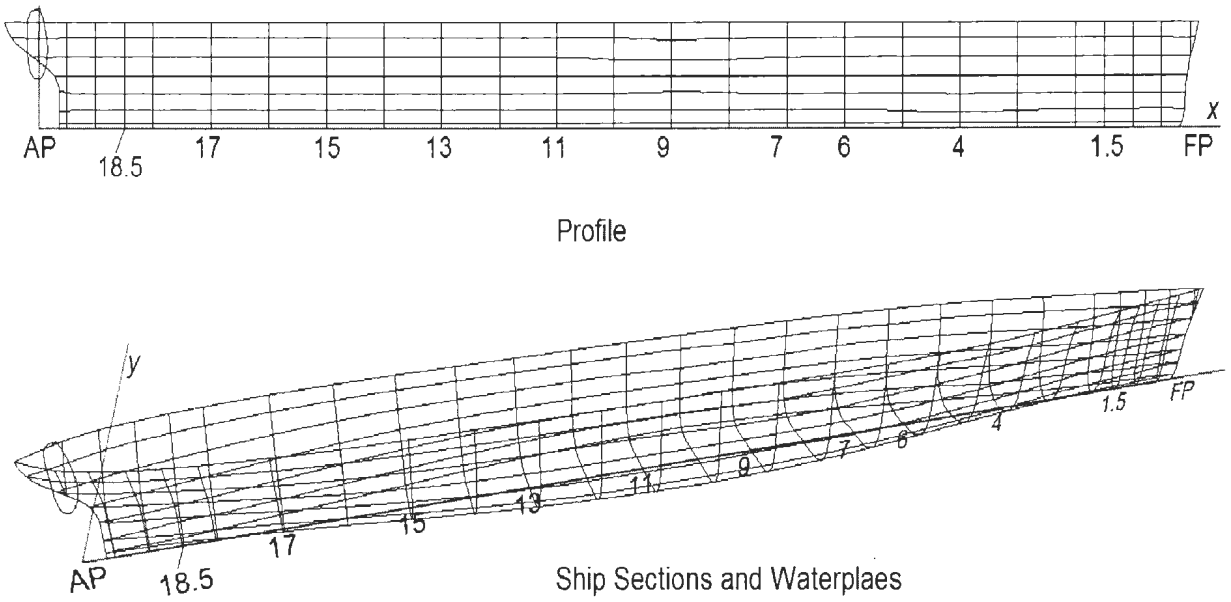

Figure 4.3: Manual Drawing of Series 60 Ship from Offset Table.

locations and total number are investigated. Possible solutions to obtain a $m \times n$ of data set are listed below.

1. Elimination of these stations. In this case, hull form will not be smooth enough near these region.

2. Elimination of these stations, and linear interpolation between the points on the last station and the profile curve. In this case, the lines connected those points are straight lines, which may not satisfy the hull shape's continuity.

3. Elimination of these stations, and cubic spline interpolation between the points on the last station and the profile curve. This technique is expected to produce better result.

The cubic spline interpolation code (appendix C) provides the intermediate line as shown in figure 4.4. This new interpolated station may have variable x-values. In the cubic spline interpolation, choice of the number of total points influences the interpolation result. Therefore, the

total number of points, $N + 1$ (appendix C) needs to be varied until a satisfactory shape at the location of interest is obtained.

As mentioned earlier, in the x-y-z type input files, the data set are prepared in $(m \times n)$ format before read by the program. For the AMECRC ship hull's input file, necessary points were added and removed to make the total points on each station as the same number. Evidently, this operation should not alter the final shapes of the stations.

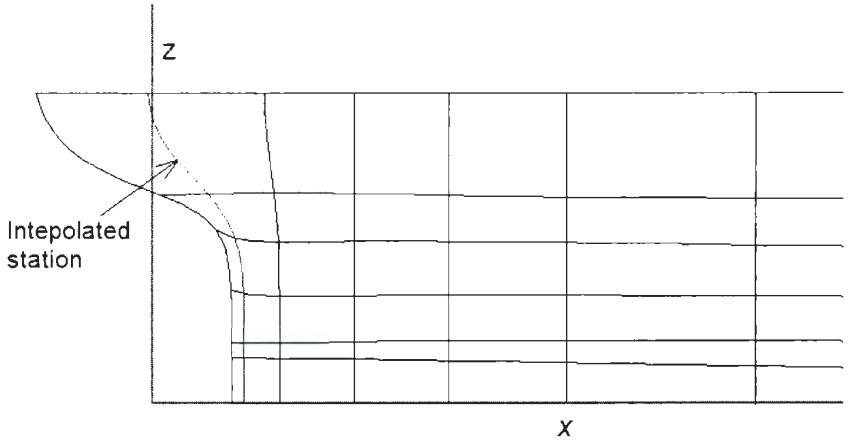

Figure 4.4: Interpolated Station.

4.4 Transom Stern Discretization Algorithm

As transom stern is a flat surface, it does not essentially need to be uniformly discretized or very small meshes. In the present study, the grid generation for transom is dependent on the total grid points on a station of the main hull. The transom is divided in a $n^1 \times n^1$ of panels, i.e, $n^1 + 1$ number of nodes on the boundary curves. $n^1 = \text{integer}\left(\frac{n}{2}\right)$, where n is the number of panels on each column, i.e. on each station. The panels distribution is shown in figure 4.5, which shows that (10×10) number of panels are distributed on the transom surface up to load waterline. In this case, total number of nodes on the transom stern station is 21. (9×10) number

of panels are distributed down to node number 10, and in the rest, (1×10) number of panels are located. Appendix D shows the short algorithm employed to serve this purpose.

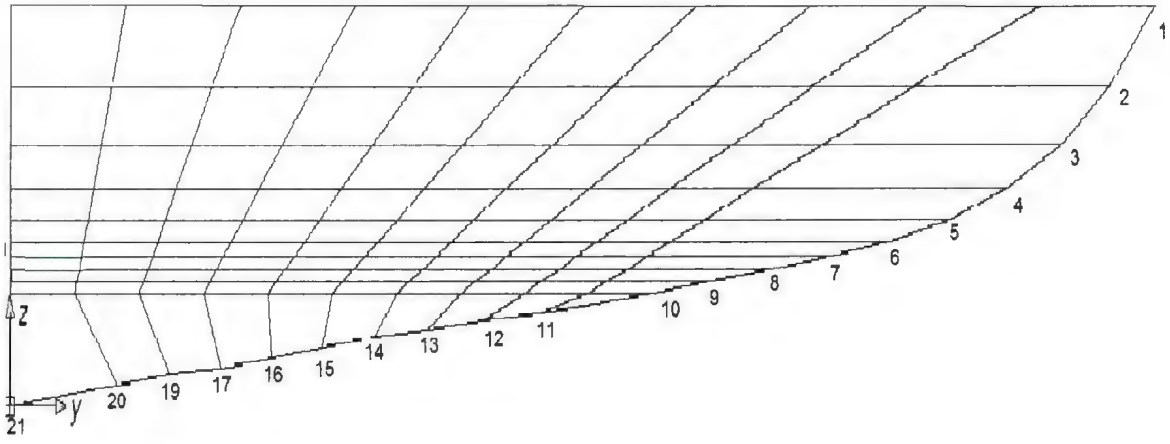

Figure 4.5: Discretized Transom Stern.

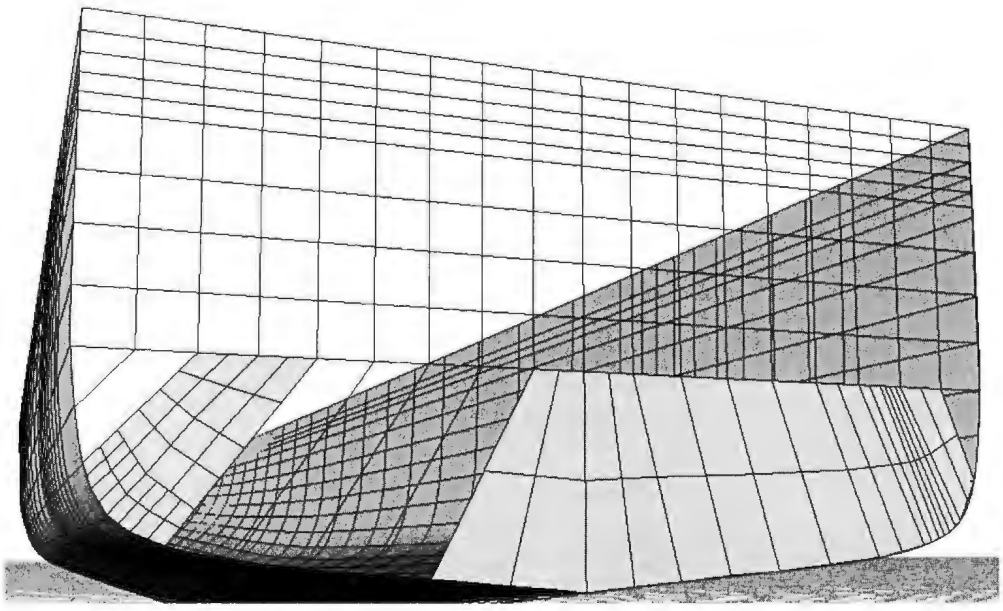

Figure 4.6: Transom Stern Including Freeboard (IGES file output).

Figure 4.6 shows an *.igs output of the transom of the model # 1 from AMECRC high

speed ship series. This discretization of the transom is done including freeboard section, unlike figure 4.5 where the discretization is only done up to load water line (LWL). If the ship hull performances are required to be evaluated in any kind of software capable of reading IGES files, this output could be utilized as the input. In figure 4.6 the initial transom representation is provided by lines. It is recommended that, before using this file as an input, one should connect those grid points to produce a surface. Several surface patches on the transom can be created from the corner point of the grids, and joined to make one or two full surface(s). Depending on the curvature of boundary lines, smaller or bigger patches can be created by drawing more lines in between the primary lines. The figure shows few sample surface patches on the transom.

4.5 Geometrical Properties

For the basic geometrical properties' validation, volume of displacement, wetted surface area, block coefficient, prismatic coefficient, etc., were calculated. To perform the numerical integration of the discretized points and stations, general trapezoidal rule was implemented. There was a modification inside the integration algorithm, which needs to be explained.

After the cubic interpolation, the profile projection of the station may not be perpendicular to the waterlines. Therefore, the surface plane of this station's sectional area is not parallel to the next one. The trapezoidal integration rule calculates between two parallel ordinates. Therefore, first, an analysis for the orthogonality of the interpolated station is performed. If the station is not perpendicular to the waterlines, a perpendicular sectional area is approximated at the center of the line connecting closest consecutive points (usually keel line points), and integrated. This process does not have any effect on the hull geometry representation or on the hydrodynamic performance.

4.6 Input File for MAPS Resistance

The coordinate system for the MAPS resistance is different from the frame of reference of the developed program. Figure 4.7 shows a schematic diagram defining the coordinate system for MAPS Resistance input files. Here, the origin is at the load water line (water surface) intersecting with the ship center line and the midship section. The ship hull information is only given up to the load water line. x-value is positive toward the aft of the ship length. z-value is positive upwards, i.e., all the z-values are less than or equal to zero in the input file. The panels are numbered from top to bottom for each column, starting from the forward most panel. For more details on the MAPS Resistance input file preparation, refer to Saoyu et al. (2012).

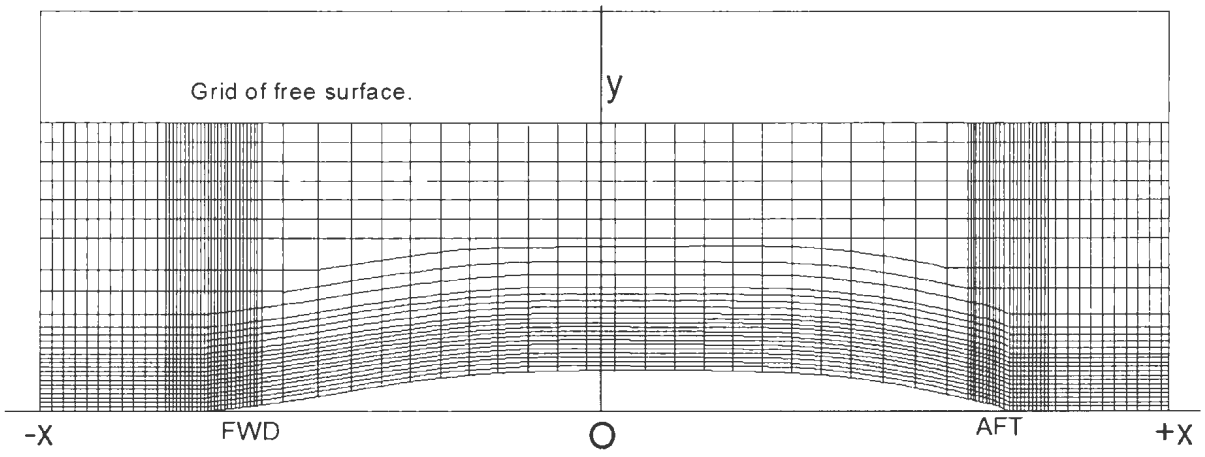

Figure 4.7: MAPS Resistance Coordinate System (z-positive upwards).

Chapter 5

Geometric Validation

The global curve or surface interpolation method is expected to construct curves or surface through data points effectively. For a globally interpolated surface patch, changes in one node on a curve influence the whole curve and nearby regions of the surface. This is because the global interpolation puts a parametric value on each point of a curve reflected by the trend of all the points on the curve. The control points on a B-spline curve are significantly away from the constructed curve where the curve has higher bends. Again, to maintain the physical shape of the curve, some points on B-spline curves change positions sometimes. For a surface, the ordinates shift to produce a suitable surface net. Finally, the global interpolation fits the data points forming the best possible curves or surface depending on the trend of available data points.

In order to check the geometric output of ship hulls, first, principal geometric properties are investigated, then, the numerical output for nodes on ship hulls will be compared with the original ships' coordinates. In the end, the body plan of the ship hull will be compared, following by the comparison of the bow and stern curves (forward and aft profile curves), if needed.

5.1 Series 60, $C_b = 0.6$

In this section, geometric properties, offsets, sectional curves and center buttock line (profile curves) for series 60 hull ($C_b = 0.6$) will be checked with original ship hull information.

5.1.1 Principal Properties

Todd (1963) provides the basic information on series 60 ship hull in its chapter 5. The table of offsets provides principlal dimensions ratios and coefficients for the ship models, beside the half breadth of water line at different stations. For the model with block coefficient, $C_b = 0.6$, table 5.1 compares the ratios and coefficients with the original ship hull form. The load water-line length (LWL) in this example is 20 units (generally meters).

Table 5.1 shows that depending on the schemes of grid generation there are differences

Table 5.1: Series 60, $C_b = 0.6$: Geometric Properties Comparison

	Grid Generation Scheme 1 : 31×53 Panels					
Type	L/B	B/T	C_b	Total C_p	Fwd C_p	Aft C_p
Original Ship (Todd, 1963)	10.0	2.0	0.60	0.614	0.581	0.648
Calculated Ship Hull	9.98	2.02	0.60	0.615	0.581	0.650
	Grid Generation Scheme 2: 20×60 Panels					
Type	L/B	B/T	C_b	Total C_p	Fwd C_p	Aft C_p
Original Ship (Todd, 1963)	10.0	2.0	0.60	0.614	0.581	0.648
Calculated Ship Hull	10.0	2.0	0.599	0.614	0.581	0.647

among the results for geometric properties. The numerical integration is influenced by the

spacing between consecutive ordinates (stations or waterlines). Scheme 2 for grid generation seems to produce better combination of principal properties. L/B and B/T are supposed to be exactly the same as defined by the table of offsets. This is because in the second scheme of the grid generation, the geometry development is only performed up to LWL excluding freeboard. Therefore, the length and breadth are predefined, and the parameters of B-spline surface are set to zero at this waterline. At the beginning and the end points of a B-spline curve are 0 and 1 (sec. 3.1.1), which means in this case, load waterplane and bottom centerline are fixed. There will not be any effect due to the surface fitting process.

As it has been mentioned in the first paragraph of this chapter, in global interpolation curves on a surface net may be influenced by other neighboring curves. For the grid generation scheme 1, LWL seems to be reduced by 2% and beam increased by 2%. This is because the freeboard is taken into account, i.e., zero parameter for B-spline curve is set at the top deck line of the ship. This might affect its neighborhood underneath this line, apparently, the load waterline is influenced. The rest of the properties agree quite well to the original one's.

As for the scheme 2 of grid generations, the coefficients are same as in the table of offsets, except for the block coefficient, which is 0.1667% lower. This seems tolerable considering other properties' convergence.

The method adopted to calculate the resistance requires ship hull panelization only up to load waterline. Denser meshes at the neighborhood of ship's forward and aft end and the water surface are required for better numerical evaluation. These can be performed in scheme 2 of the grid generations. Acknowledging all these, scheme 2 was employed in the optimization procedure in the present study.

5.1.2 Coordinates of Original Ship Hull Nodes

Global surface interpolation section (sec. 3.1.2) simply imply that, the backward calculation of equation 3.15 will return exactly the same values as in the table of offsets, if there are no numerical errors in the process. Comparison of all the output values with the original value from the table of offset show that all the values are exactly the same except those five values in Table 5.2. The values which are different from the original offset points are shown in italic text.

Table 5.2: Series 60, C_b = 0.6: Coordinates Comparison for the Table of Offsets

Ship Type		Waterlines (m)							
Original Hull		0.0000	0.0750	0.2500	0.5000	0.7500	1.0000	1.2500	1.5000
Calculated Hull		0.0000	0.0750	0.2500	0.5000	0.7500	1.0000	1.2500	1.5000
Type	St (m)	Half Beam at Stations & Waterlines							
Original	3.0	*0.0391*	0.1697	0.2896	0.3460	0.3680	0.3910	0.4400	0.5310
Calc. Hull	3.0	*0.0390*	0.1697	0.2896	0.3460	0.3680	0.3910	0.4400	0.5310
Original	18.0	*0.0462*	0.1316	0.1901	0.2360	0.3210	0.5360	0.7090	0.8340
Calc. Hull	18.0	*0.0461*	0.1316	0.1901	0.2360	0.3210	0.5360	0.7090	0.8340
Original	18.5	0.0227	0.0883	*0.1281*	0.1560	0.2160	0.4250	0.6260	0.7690
Calc. Hull	18.5	0.0227	0.0883	*0.1280*	0.1560	0.2160	0.4250	0.6260	0.7690
Original	19.5	*0.0061*	0.0197	*0.0327*	0.0220	0.0410	0.1930	0.4180	0.5790
Calc. Hull	19.5	*0.0062*	0.0197	*0.0337*	0.0220	0.0410	0.1930	0.4180	0.5790

The maximum difference is only 2.9%, all other values are exactly the same, which implies that the global interpolation method has been successfully implemented. The possible

reason of this difference could be due to the involvement of cubic spline interpolation which was utilized to predict the intermediate data (chapter 4). Now, if the geometry of the ship hull physically appears to be similar to original hull and smooth enough, primary geometric output of the ship hull can be considered as an adequate output.

5.1.3 Body Plan and Centerline Profile

Figure 5.1 shows a body plan of series 60, C_b = 0.6 ship hull. In this figure, dashed lines show the sectional curves at different stations, which are developed mathematically. Solid lines represent curves from original hull. These solid lines have been drawn manually on a digital image of series 60, C_b = 0.6 ship hull's body plan (Todd, 1963), using splines in *AutoCAD*.

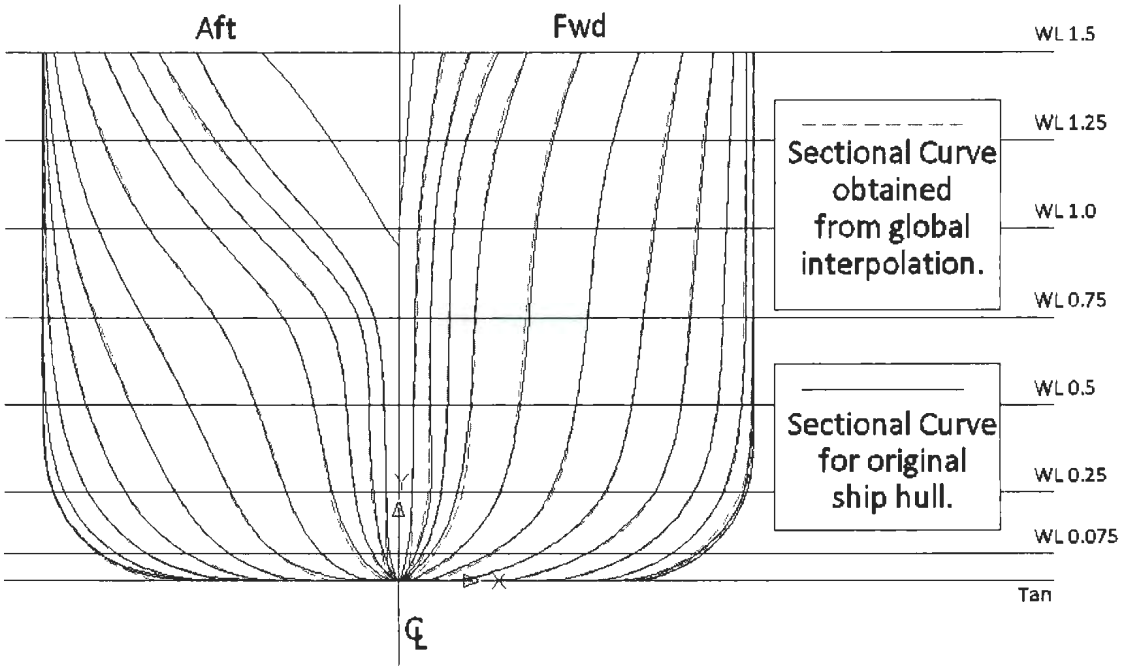

Figure 5.1: Series 60 Ship Hull Body Plan Comparison.

Both types of these lines are close enough to each other, especially follow same shapes. The maximum gap recorded between mathematical and original stations is 0.0131 units. This

gap has been found at station 0.5, nearby waterline 0.075, which is cubic spline interpolated. This can be considered as a tolerable error. It can be simply minimized by changing y value at this particular point after the interpolation, if precise match is required.

In the similar manner figure 5.2 shows bow and stern shape for original and mathematical ship hulls.

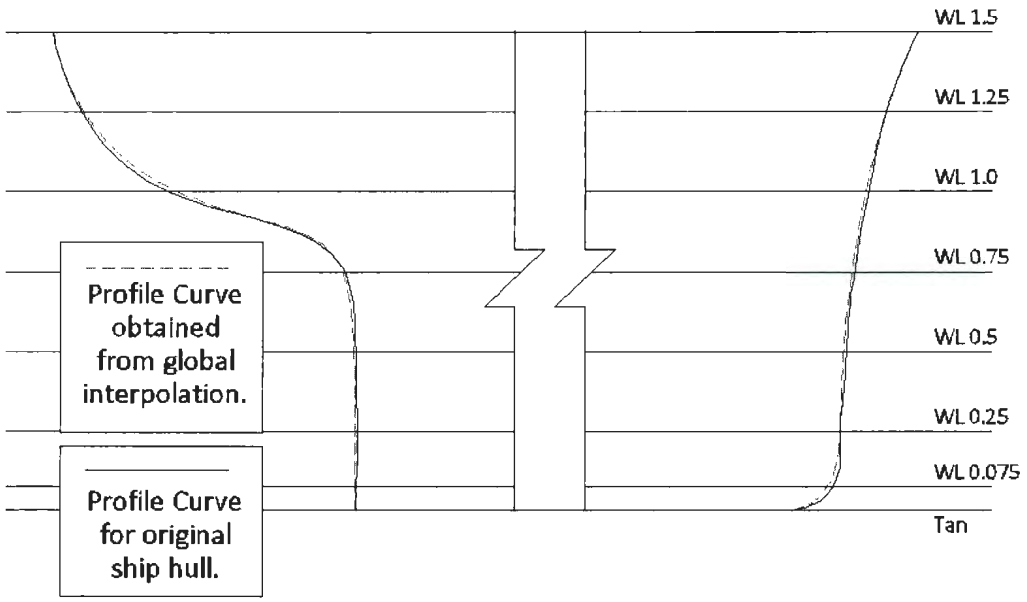

Figure 5.2: Series 60 Ship Hull Profile Curves Comparison.

To check the smoothness of the hull surface, one can check appendix E, where different views of 3D models (primary and discretized) presented in *Rhinoceros*, for both series 60 and AMECRC ship, are given. Visually, surfaces appear to be satisfactorily smooth.

5.2 AMECRC High Speed Monohull Model # 1

In this section, comparison of the mathematical model of AMECRC high speed monohull model # 1 with a reference drawing has been performed.

5.2.1 Principal Properties

Table 5.3 shows the comparison of geometric properties. In this case, the block coefficient was expected to be higher than the values provided. This is because of the difference in the aft region of the provided model data and drawing. The body plan comparison will be explained later.

The coordinates of B-spline surface net, in this case, are again the same as the given information. Therefore, repetition of the long table for coordinates' comparison has been avoided at this point.

Table 5.3: AMECRC Model # 1: Geometric Properties Comparison

	Grid Generation Scheme # 1: 31×53 Panels				
Type	L/B	B/T	C_b	C_p	$L/\nabla^{1/3}$
Doctors (2006)	7.990	3.995	0.394	0.620	8.649
Shipflow Data	8.000	4.000	0.396	0.624	8.653
Calculated Ship Hull	7.992	4.001	0.396	0.626	8.627
	Grid Generation Scheme # 2: 20×60 Panels				
Type	L/B	B/T	C_b	C_p	$L/\nabla^{1/3}$
Doctors (2006)	7.990	3.995	0.394	0.620	8.649
Shipflow Data	8.000	4.000	0.396	0.624	8.653
Calculated Ship Hull	7.991	4.001	0.400	0.631	8.608

5.2.2 Body Plan and Centerline Profile

Figure 5.3 compares the body plan of mathematical and original ship hull. The difference in the basic information of the drawings are:

- the original drawing is not developed based on the coordinate information given for the model,
- the mathematical hull is completely based on the given coordinate information, and
- the bottom center point on the stern according to given offsets is lower than the provided ship hull drawing used in shipflow project.

Therefore, the transom stern's surface area is comparatively higher for the nearby sections. But, as it proceeds forward, the bottom part of the sectional curve closes to the original one. This difference also explains the discrepancy in table 5.3. The rest of the hull is the same for both original and mathematical ship hull, which demands establishment of the applicability of the ship hull generation method convincingly.

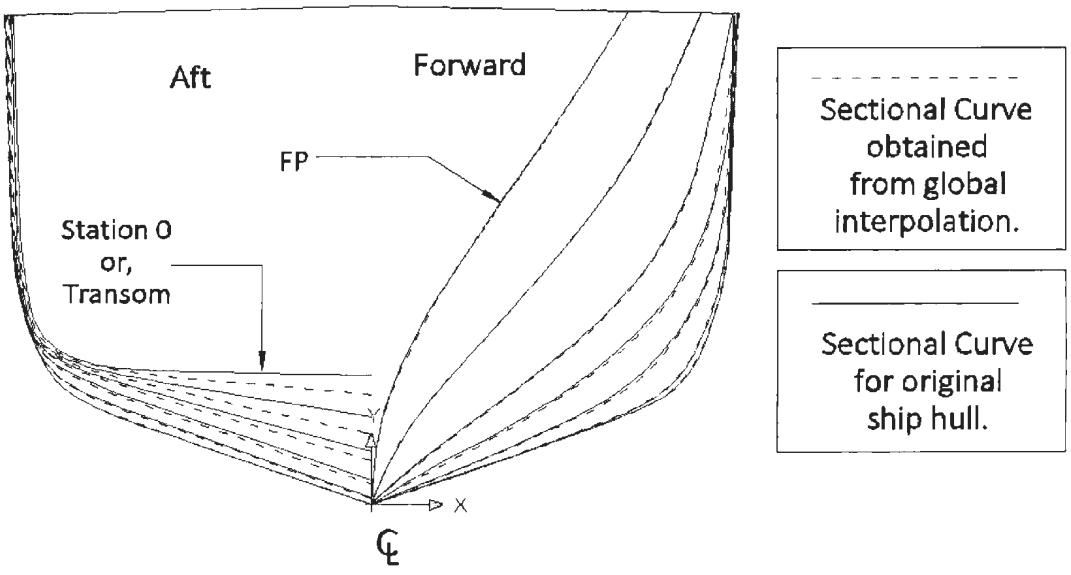

Figure 5.3: AMECRC Model # 1 Body Plan Comparison.

Again, figure 5.4 shows the forward end profile curve for the AMECRC Model # 1 ship.

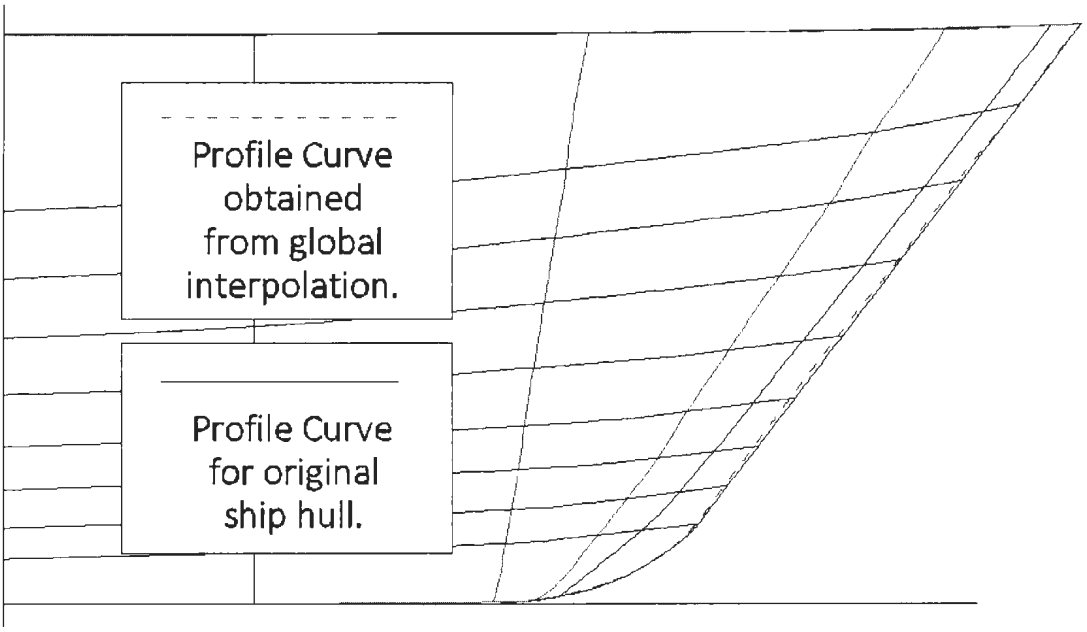

Figure 5.4: AMECRC Model # 1 Forward Profile Curve Comparison.

5.3 Wigley Hull: Principal Properties, Body Plan, and Centerline Profile

For an additional investigation, Wigley hull has been chosen as an objective ship hull. Wigley hull is a mathematically defined hull shape, expressed by the following equation.

$$\frac{y(x,z)}{L} = \pm 2 \times \frac{B}{L} \times \left\{ \frac{x}{L}\left(1 - \frac{x}{L}\right) \right\} \times \left\{ 1 - \left(\frac{L\,z}{T\,L} \right)^2 \right\} \tag{5.1}$$

Here, x-y plane on waterline, origin on forward perpendicular. x-positive towards after end, y-positive starboard and z-positive upward. L is length between perpendicular, B is maximum breadth at midship and T is the draft. $\frac{x}{L} \epsilon [0, 1]$, $\frac{z}{L} \epsilon [0, -\frac{T}{L}]$. Freeboard is extended

from design waterline upward constantly. The mostly used Wigley hull is given by $\frac{L}{B} = 10$ and $\frac{L}{T} = 16$ and block coefficient, $C_b = \frac{4}{9}$.

The following table shows the comparison of principal properties between the original hull and B-spline hull surfaces. The following figure (Fig. 5.5) shows the body plan

Table 5.4: Wigley Hull: Geometric Properties Comparison

	Grid Generation Scheme # 1: 30×60 Panels				
Type	L/B	B/T	C_b	C_p	$L/\nabla^{1/3}$
Original	10.000	1.600	0.444	0.665	8.980
Calculated Ship Hull	10.002	1.589	0.444	0.665	8.965
	Grid Generation Scheme # 2: 20×60 Panels				
Type	L/B	B/T	C_b	C_p	$L/\nabla^{1/3}$
Original	10.000	1.600	0.444	0.665	8.980
Calculated Ship Hull	10.000	1.600	0.443	0.664	8.982

comparison between wigley hull developed by the program and a manual drawing of wigley hull. Apparently, for a simple hull form like Wigley hull, the program develops a perfectly matched hull form. Profile comparison is not provided as they are just straight perpendicular lines. A set of different 3D view of wigley hull is given in the appendix E.

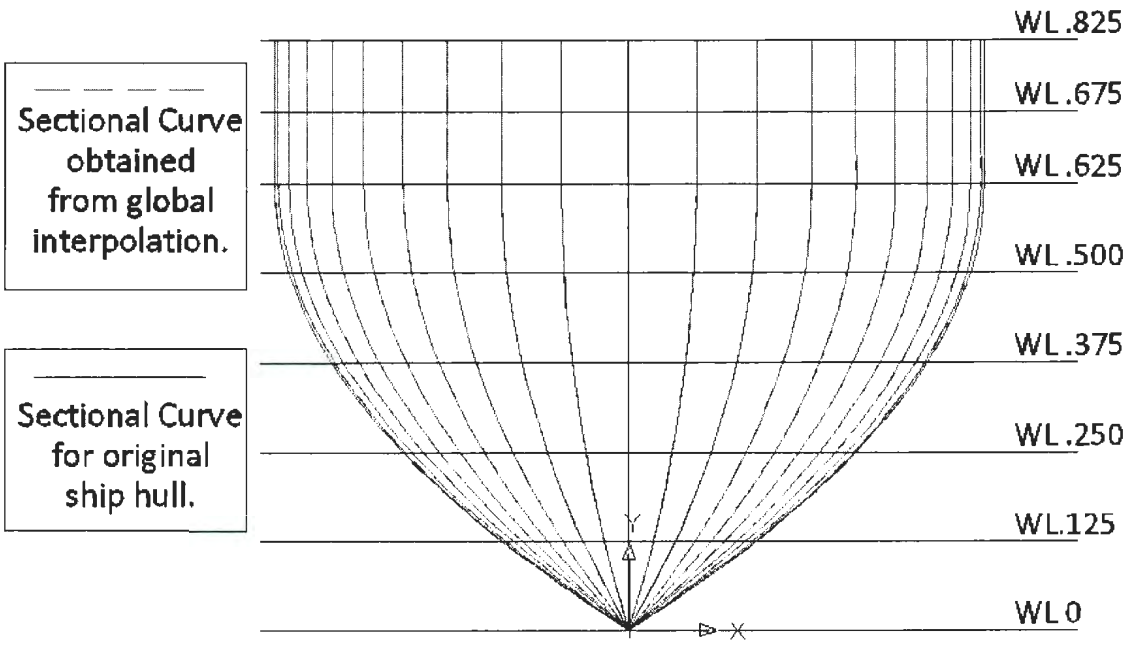

Figure 5.5: Wigley Hull: Body Plan Comparison

5.4 US Navy Combatant DTMB 5415

In order to investigate the applicability of the hull generation method to a ship with bulbous bow, DTMB 5415 has been selected. She is an US Navy Combatant with transom stern and bulbous, and her details, and an IGES file showing a manual drawing of ship hull are available online. This ship hull has few sharp change on her geometry which are not possible to represent with a single B-spline surface. As pointed in the figure 5.6, at the connection of the bulb, and at the after region, the sharp change in hull are not feasible to construct with B-spline surface, as B-spline is a continuous function which does not tolerate any sharp corner. The geometry in the provided IGES file is developed with polyline surfaces and separate overlapping patches. The hull form is still developable with the current method with a slight change is the geometry where the sharp corners are smoothened to curvilinear lines and integrated to main hull patch

as shown in the figure 5.7.

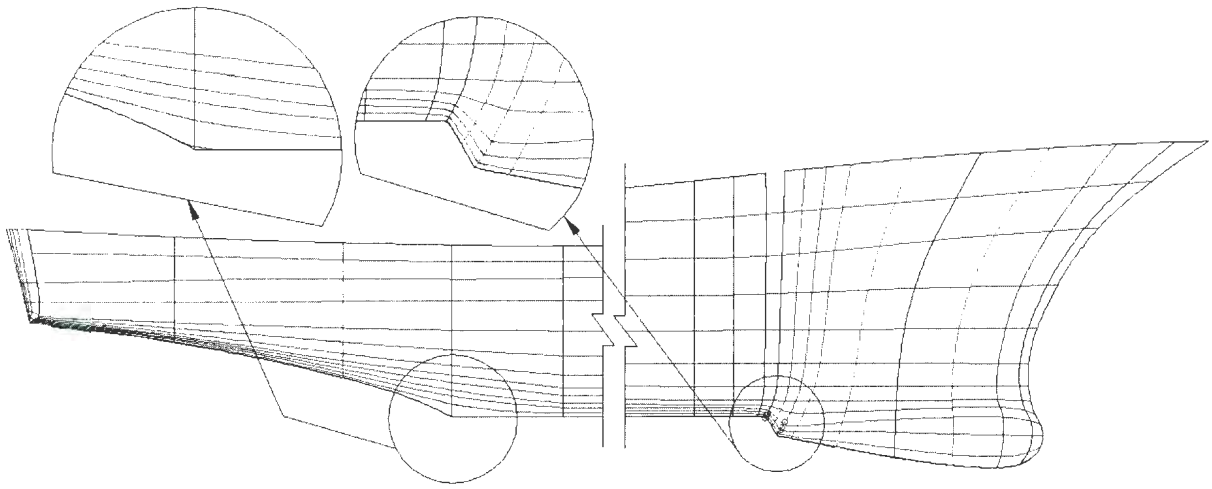

Figure 5.6: DTMB 5415 Sharp Change in Geometry

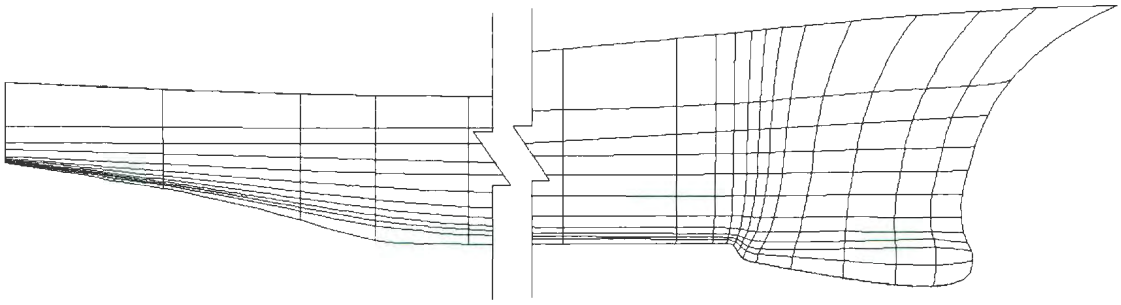

Figure 5.7: DTMB 5415: Geometric Output with Smoothened Sharp Corners

In this case, the input file format with generalized x-y-z information has been used. The transom stern of this hull has been considered as a flat area. Figure 5.7 and 5.8 show the output geometry of the DTMB 5415 ship hull, and table 5.5 shows the comparison of principal properties, and figure 5.9 shows the body plan comparison. Appendix E shows few 3D view of the output geometry.

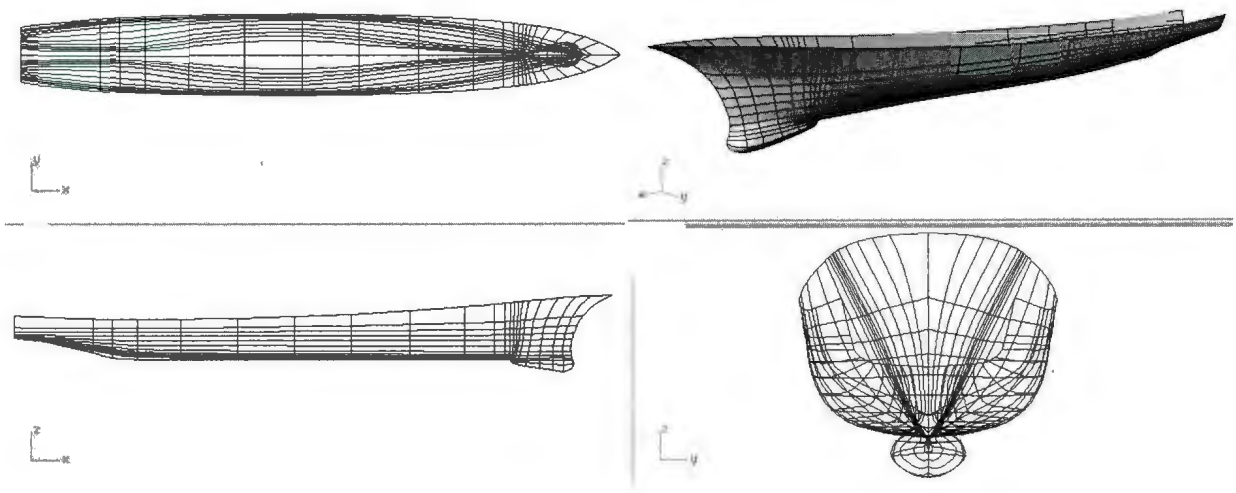

Figure 5.8: DTMB 5415: Geometric Output

Table 5.5: DTMB 5415: Geometric Properties Comparison

	Grid Generation Scheme # 1: 40×80 Panels				
Type	L/B	B/T	C_b	C_p	$L/\nabla^{1/3}$
Original	7.459	3.100	0.507	0.624	6.988
Calculated Ship Hull	7.448	3.102	0.502	0.619	7.034
	Grid Generation Scheme # 2: 20×60 Panels				
Type	L/B	B/T	C_b	C_p	$L/\nabla^{1/3}$
Original	7.459	3.100	0.507	0.624	6.988
Calculated Ship Hull	7.453	3.102	0.507	0.626	6.989

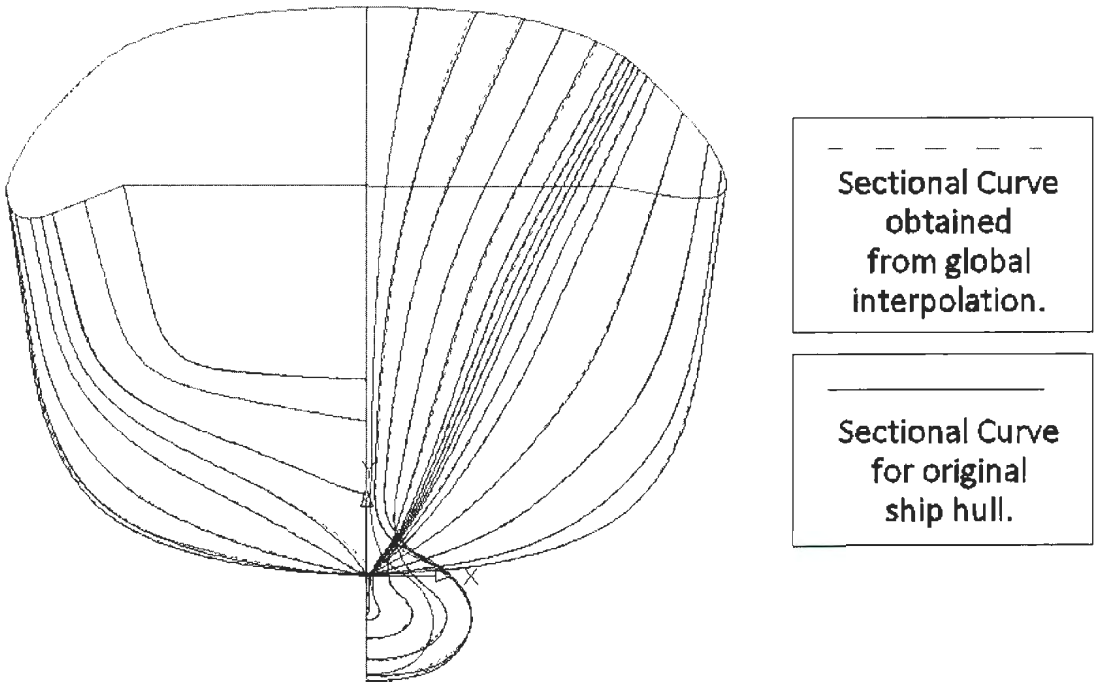

Figure 5.9: DTMB 5415: Body Plan Comparison

In the input file, the z or x coordinates are not necessarily the same for a particular waterline or station (respectively). To describe the bulbous bow or the complicated change in the stern and bow geometry, the best suitable lines have been chosen. Therefore, if the coordinates are given in a table of offsets, it is preferable to transform the input file into the generalized x-y-z format and include stations in the forward region next to bow profile line, for this kind of complicated ship hull. In the original drawing, the bulb in this hull form does not seem to be completely integrated with the ship hull. It seems to be added as an appendix at the bow region (probably for better resistance performance). For a longer bulb integrated with the main hull with a smooth continuity in the geometry (specially at the connecting region with main hull), general table of offsets is good enough to represent the geometry.

Chapter 6

Modified Hull and Wave Resistance

This chapter discusses the output from the optimization process, i.e., the modified ship hull with improved wave resistance. Two different conventional ship hulls, Series 60 (C_b = 0.6) and Wigley hull, were investigated to examine the results due to optimization processes. In the following sections, the results are represented separately for these two hulls.

For each ship hull, first, the wave resistance characteristics at different speeds are compared with few published results. Then, if there is a complete optimization loop, the optimum hull form is represented with her principal properties and resistance performances. If there is not a complete loop, the intermediate modified hulls are investigated. A record of wave resistance coefficients and geometric properties of all modified hulls during an optimization process are provided for each ship. Each optimization process is categorized based on the ship hull form modification strategy.

6.1 Series 60, $C_b = 0.6$

Series 60 (C_b = 0.6) ship hull is one of the mostly embraced hulls among researchers. A lot of publications adopted series 60 hulls in their investigations, regardless of the applications of the studies. Applicability of the grid generation scheme 2 (see 5.1.1 and 3.2) in the resistance

evaluation will be checked first. A set of wave resistance coefficients with respect to Froude numbers provided in Tarafder and Suzuki (2007) has been utilized to compare the results. These values are for the ship hull with fixed sinkage and trim. Another set of wave resistance coefficients found in the same publication has been compared also, which is from the experimental measurements conducted at Ishikawajima-Harima Heavy Industries Co., Ltd. (IHHI). In this study, for the series 60 ship model, load waterline length (LWL) = 20 meters, breadth = 2 meters and draft = 1 meter, and the volume or wetted surfaces given in next sections are calculated for the half of the ship.

Figure 6.1 shows the comparison as mentioned above. Here, the ship hull has been discretized into 20×50 grids (row×column). Results from MAPS Resistance using the discretized ship generated from this program show a good convergence with the trend of the coefficients from Tarafder and Suzuki (2007) and IHHI.

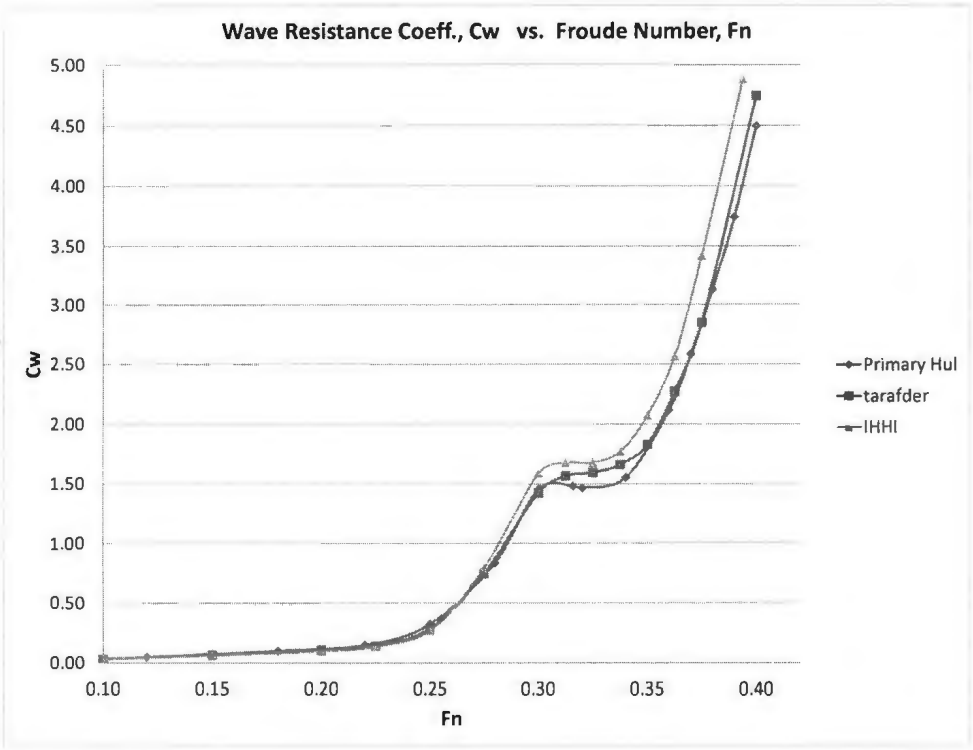

Figure 6.1: Series 60 C_b = 0.6 Wave Resistance Coefficient, C_w

In the optimization process a particular Froude number $F_n = 0.316$ has been chosen, and entire procedure continues based on hull form modification methods. Each process follows a particular modification method and evaluate the output based on the method. In the structure, there will be different iterations, where modified hull forms will experience improved wave resistance performances. In each iteration, the program will produce "*.in", "*.panelin" and "*.igs" files, which will contain numerical and graphical information on the ship in each iteration. If no further improvement is possible, the process will stopped, and the final output is the optimized hull form. If the iteration continues with further minimized resistance coefficients the optimization can be stopped manually if the ship's volume exceeds more than the tolerance. Following sections will explain results based on three basic modification methods.

6.1.1 Series 60, C_b 0.6: Stations Shift

The complete optimization process completes in two main iterations in this method of modification. It seems that in the first iteration, the optimization process finds the minimum solution for wave making resistance coefficient after the iterations in the Fibonacci search for steepest length of the variables. The variables are explained in section 3.3. In the second main iteration, the coefficient's value decreases by an insignificant amount of $4.17874E-010$. Changes in resistance coefficients and principal properties are listed as below in table 6.1

Table 6.1: Series 60, $C_b = 0.6$: Longitudinal Shift - Changes in Properties

Iteration	Volume of Displacement (m^3)	Wetted Surface Area (m^2)	Block Coeff., C_b	Resistance Coeff., $C_w \times 10^3$	Max. Change in Properties (%)
Primary	11.9976	28.5716	0.5998	1.4792	
Iteration 1	11.9424	28.4399	0.5971	1.4438	0.46071
Iteration 2	11.9424	28.4399	0.5971	1.4438	0.46071

The optimization procedure for this particular modification method appears to reduce the

coefficient of resistance by 2.4% in this particular case of series 60 ship hull at Froude number 0.316.

The final hull has been evaluated based on the wave resistance performance for other Froude numbers. In this method of modification, the comparison with modified hull and primary hull on a body plan will not show any difference as it performs only shift of stations longitudinally along the same center line. Figures 6.2, 6.3 and 6.4 show the changes in the load waterplane on the half breadth plan showing the new positions of the stations, zoomed at forward, middle and aft region of the ship respectively. In these figures, broken lines (dashed lines) represent the primary hull and the solid lines represent the new stations (or waterline).

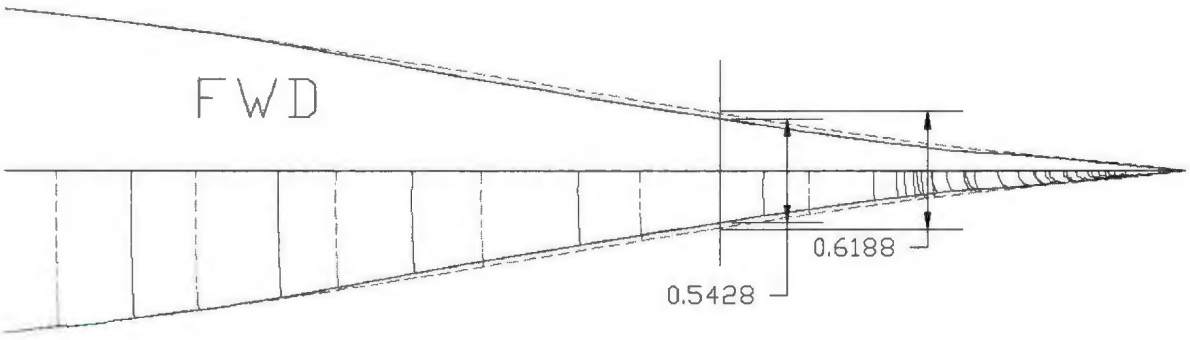

Figure 6.2: Series 60: Longitudinal Shift- Forward.

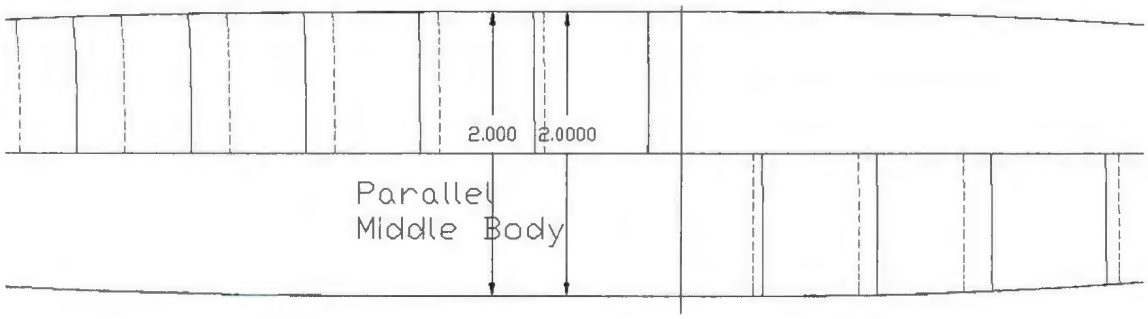

Figure 6.3: Series 60: Longitudinal Shift- Middle.

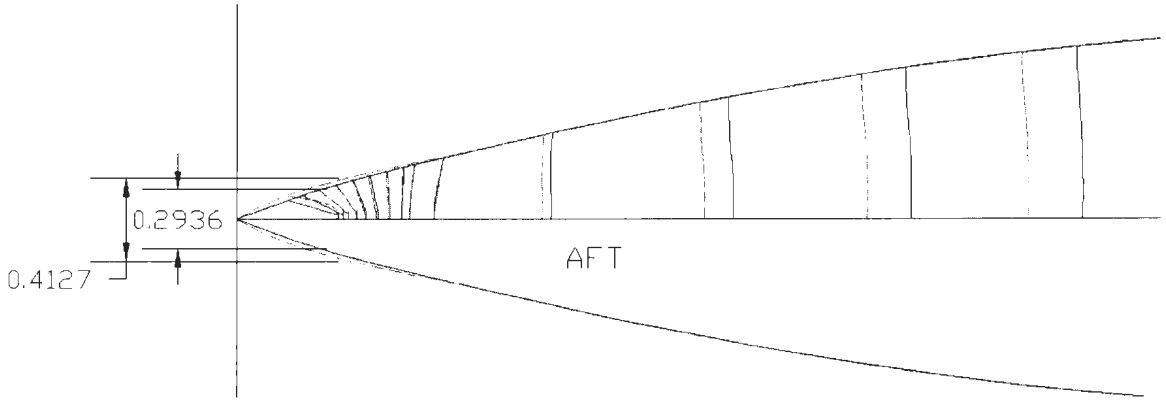

Figure 6.4: Series 60: Longitudinal Shift- Aft.

The optimization procedure shifts the stations (variables) at the forward and after region towards the inners side of the ship longitudinally. This sharpens the angles of entrance and run, which is logical and expected. There are shifts of stations in the middle body, which are not expected to make significant changes as it is inside the parallel middle body region.

6.1.2 Series 60, C_b 0.6: Change in y-coordinates of Stations

In this scheme of modification, all the discretized waterlines are modified along the y-direction. In this case for series 60 ship hull, after 21 main loops, the optimization process finds out an optimized hull form with 35.5% reduction in C_w and 1.3007% less volume of displacement. Yet, depending on the particular project this may not be the final required ship geometry, any other intermediate ship hull could be selected based on necessary objectives. However, the following table (table 6.2) lists all the 21 iterations.

Up to iteration 10 the objective value gradually reduces, but at iteration 11 it picks up, and again gradually reduces to 21 iteration. The objective value at 10 is the lowest value of C_w among all the iterations. At this point, the changes in volume of displacement is the lowest. Therefore, choice of the best suitable hull is still a case-dependent decision.

Table 6.2: Series 60, C_b = 0.6: Change in y-coordinates- Changes in Properties.

Iteration	Volume of Displacement (m^3)	Wetted Surface Area (m^2)	Block Coeff., C_b	Resistance Coeff., $C_w \times 10^3$	Max. Change in Properties (%)
Primary	11.9976	28.5716	0.5998	1.4792	
Iteration 1	11.8657	28.5535	0.5933	1.2540	0.4561
Iteration 2	11.8037	28.5483	0.5902	1.0326	0.9757
Iteration 3	11.7559	28.5470	0.5878	0.9635	1.3771
Iteration 4	11.7299	28.5490	0.5865	0.9215	1.5954
Iteration 5	11.7027	28.5530	0.5851	0.8806	1.8236
Iteration 6	11.6834	28.5564	0.5842	0.8582	1.9854
Iteration 7	11.6635	28.5604	0.5832	0.8329	2.1524
Iteration 8	11.6389	28.5594	0.5819	0.8125	2.3585
Iteration 9	11.6340	28.5781	0.5817	0.7806	2.3994
Iteration 10	11.6092	28.5730	0.5805	0.4461	2.6074
Iteration 11	11.5950	28.5767	0.5798	2.7555	2.7264
Iteration 12	12.0594	28.6495	0.6029	1.7815	1.1694
Iteration 13	12.0657	28.6542	0.6033	1.6762	1.2222
Iteration 14	12.0392	28.6335	0.6020	1.6184	0.9997
Iteration 15	12.0076	28.6124	0.6004	1.5658	0.7349
Iteration 16	11.9741	28.5941	0.4534	1.5055	1.33745
Iteration 17	11.9357	28.5778	0.5968	1.4260	0.1313
Iteration 18	11.8902	28.5630	0.5945	1.3003	0.2500

continued on next page...

...continued from previous page					
Iteration	Volume of Displacement (m^3)	Wetted Surface Area (m^2)	Block Coeff., C_b	Resistance Coeff., $C_w \times 10^3$	Max. Change in Properties (%)
Iteration 19	11.8304	28.5511	0.5915	1.1045	0.7521
Iteration 20	11.7722	28.5468	0.5886	0.9708	1.2406
Iteration 21	11.7650	28.5468	0.5883	0.9690	1.3007

It appears that, in some cases the resistance coefficients are higher than the primary ones, though the differences in volumes are less than 5%. In an optimization process, the algorithm searches for an optimum set of variables where the objective function value is lower than the previous one. But, to maintain some particular constraints of the variables, the original predicted changes of them are altered in few cases. For an example, if an expansion in aft region and a contraction in the waterlines' widths produce a reduction in objective value, logically it will proceed for further extension and contraction on the respective regions. But, for a ship geometry this will not be a standard process. Ship has to maintain a smooth and continuous change in her geometry. Larger angle of run or higher partial derivatives between two consecutive points will possibly lead her to higher resistance force. Whenever any loop reaches higher resistance, it learns from it and changes the variable in next loops.

Figure 6.5 shows the body plans comparison between the intermediate hull at iteration 15 and 21 with the primary hull. For clarity few lines (stations) from forward and after ends have been omitted. Stations at the after end at iteration 21 narrows towards the centerline with visually significant amount. At iteration 15, there has been expansion in both after and forward region which increase the angle of entrance and run.

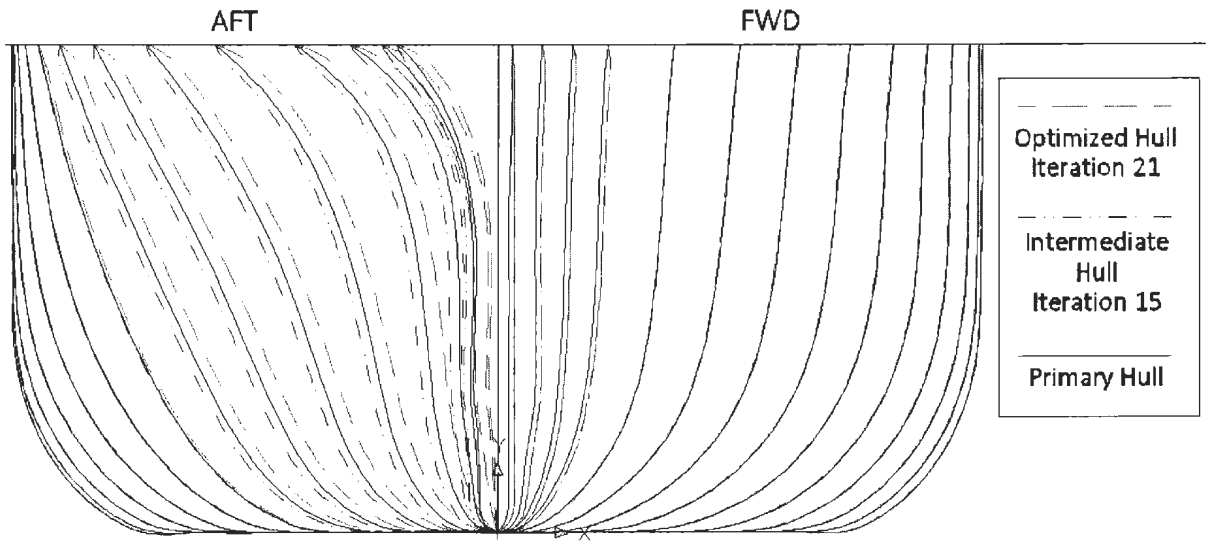

Figure 6.5: Series 60: Variation of Y- Body Plan Comparison.

If the after region sectional areas of a ship is not the main concern compared to improved resistance, intermediate hulls from iteration 1 to 10 can be investigated. Figure 6.6 presents another comparison of intermediate ship hulls at iteration 5 and 10 with primary hull. It is clear from the figure that, the numerical minimization of C_w has been performed by almost converting the lower after part of the ship into a single plate (cross sectional area with very low width). Physically, the hull form in iteration 10 cannot be a good solution.

6.1.3 Series 60, C_b 0.6: Changing the Vertical Location of Nodes on Stations

In fact, this method performs shift of waterplanes in vertical ($\pm z$) direction. In the algorithm for Fibonacci search for optimal step length for the variables, sometimes the Fibonacci number could be much higher, which may slow down the process. If there is a possibility of achieving a higher Fibonacci number, the step length is considered as 1, which transforms the BFGS

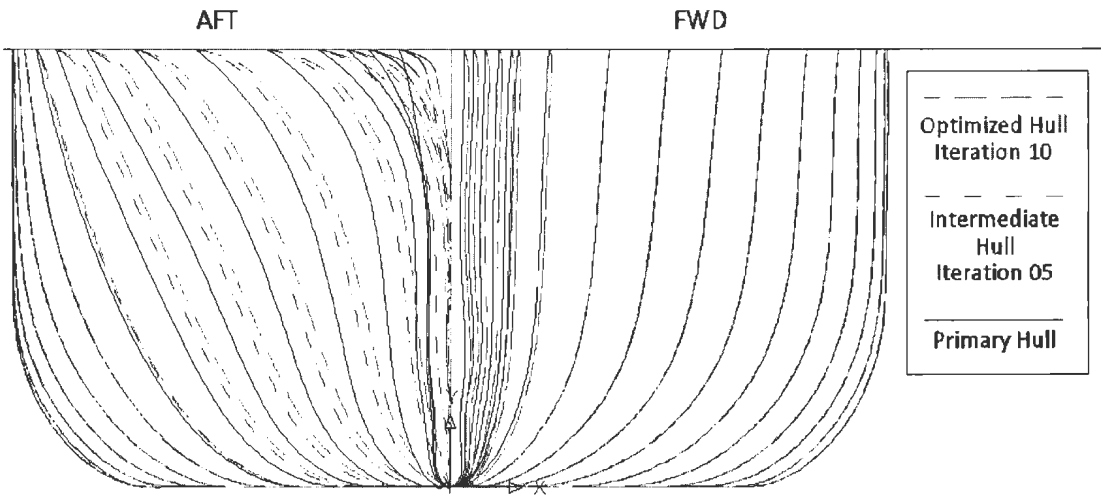

Figure 6.6: Series 60: Variation of Y- Body Plan Comparison.

optimization procedure to a classical quasi-Newton optimization process, still, the Hessian Matrix (see section 3.5) is being updated by the BFGS method.

In the case of waterplane shifting, the Fibonacci interval search (see appendix A) seems to utilize higher Fibonacci numbers. Therefore, in this case, the step length is changed to 1.00. For, most of main optimization loop same process repeats. In consequence, the decrease in the objective function value (C_w) is more continuous, and so, numbers of main optimization loops are higher. The computational time is compensated by the lower number intermediate iterations. The optimization process has been stopped at seventh iteration where the percentage in the difference of volumes of displacement reaches 3.10. The following table shows results recorded at these iterations.

Figure 6.7 shows the bodyplan comparison and figure 6.8 shows aft profile view of modified hull at iteration 7 and primary hull. Few waterplanes are shifted close enough to produce an uneven shape in the neighborhood of the load waterplane (clouded part). From body plan it appears that the flat bottom (clouded part) has been shifted up (about 30 mm of draft 1000 mm) from the tangent line (or, baseline). The center bottom line is fixed at the baseline which numerically keeps the draft unchanged.

Table 6.3: Series 60, $C_b = 0.6$: Vertical Shift of Waterplanes - Changes in Properties

Iteration	Volume of Displacement (m^3)	Wetted Surface Area (m^2)	Block Coeff., C_b	Resistance Coeff., $C_w \times 10^3$	Max. Change in Properties (%)
Primary	11.9976	28.5716	0.5998	1.4792	
Iteration 1	11.8438	28.4800	0.5922	1.4147	0.6396
Iteration 2	11.8233	28.3987	0.5911	1.3723	1.4530
Iteration 3	11.8230	28.2721	0.5911	1.362493	1.4550
Iteration 4	11.7362	28.2690	0.5867	1.351076	2.1789
Iteration 5	11.7349	28.5461	0.5867	1.342575	2.1898
Iteration 6	11.6251	28.1439	0.5812	1.32324	3.1049
Iteration 7	11.62801	28.1417	0.5813	1.332075	3.0800

This new hull may not be accepted for an alternative of the primary hull, even though it gives out a wave resistance reduction by 9.98%. In these circumstances, those modified hulls in other iterations can be compared to each other. In fact, all the modified hulls in every main iteration can be investigated and selected depending on whatever requirements a certain party possesses.

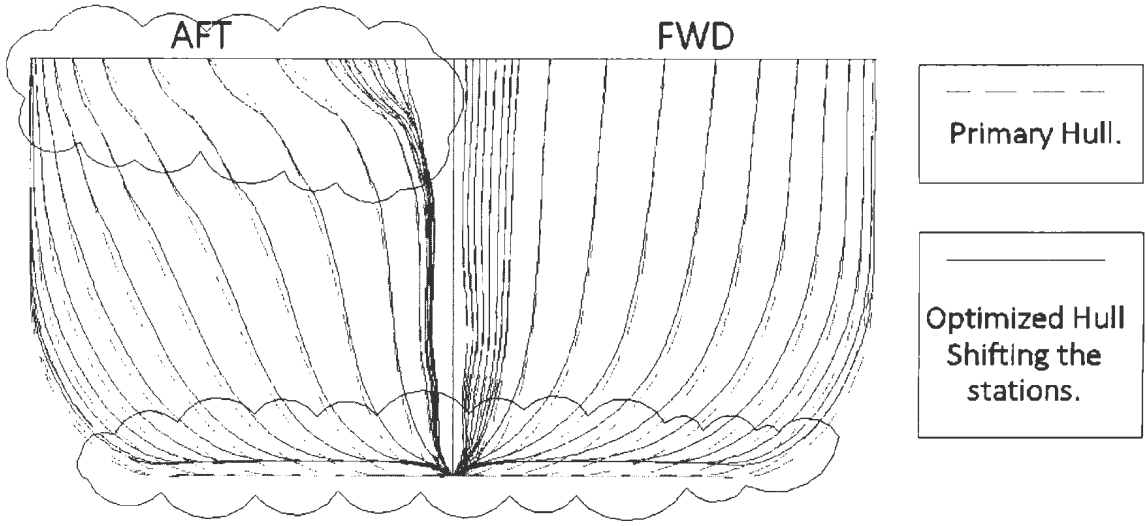

Figure 6.7: Series 60: Shift of Waterplanes - Body Plan Comparison.

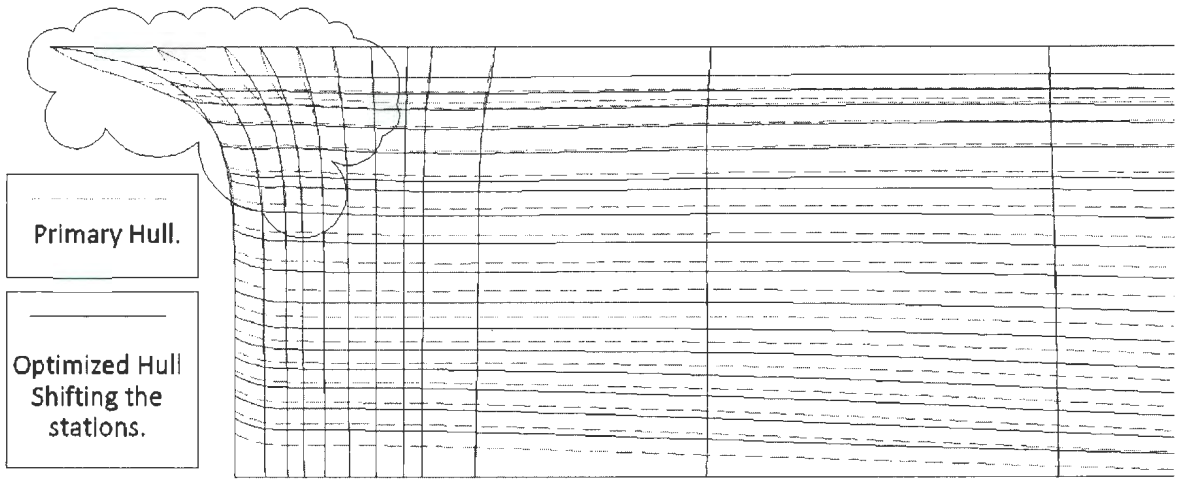

Figure 6.8: Series 60: Shift of Waterplanes - Profile Aft.

Finally, Figure 6.9 shows the comparison of C_w between the original ship hull and the optimized ship hulls for different Froude numbers. New modified ship hull forms have again been evaluated for other speeds. For most of the speeds wave making resistance coefficients appear to be lower than the primary ship hulls. In figure 6.9, St._Shift shows the curve for modified hull at iteration 2 for modification scheme 1, Y-Shift shows for iteration 21, modification scheme 21 and WL_Shift stands for iteration 7 modification scheme 3.

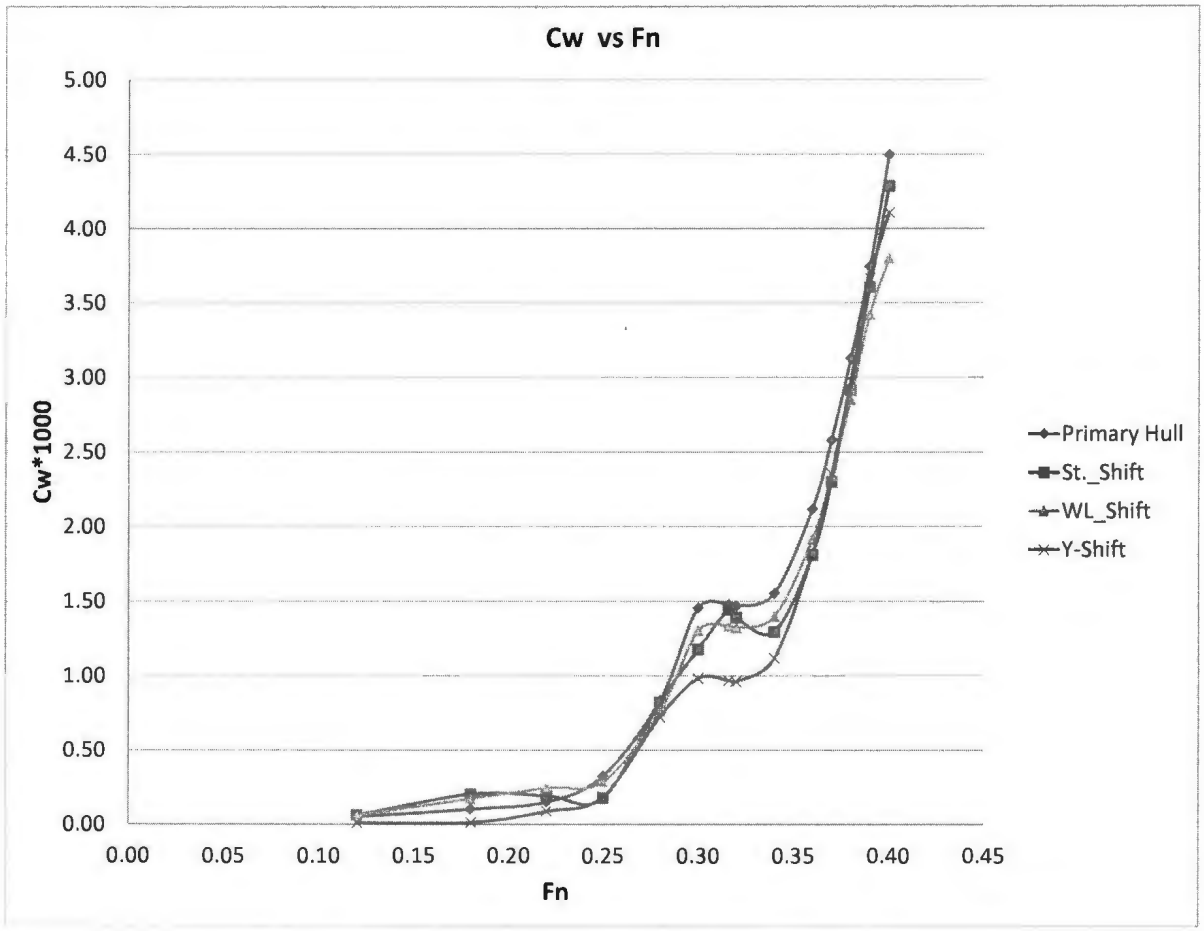

Figure 6.9: Series 60: C_w comparison - Various Modification Methods.

6.2 Wigley Hull, L/B = 10 and L/T = 16

As like the series 60 hull, this section for Wigley hull also starts with the comparison of the behavior of C_w at different Froude numbers (Fn). Figure 6.10 represents a plot of wave resistance coefficients, C_w against Froude number, Fn. This plot compares performance of the primary hull generated by the program of the present study with published data by Tarafder and Suzuki (2007) and experimental results carried out by Shearer and Cross (1965). The result seems to

be convergent with the experimental result except the last point. Next three sections presents results obtained from similar modification methods utilized for series 60 hull form. In this case, the optimization loops run for the Froude number, 0.34.

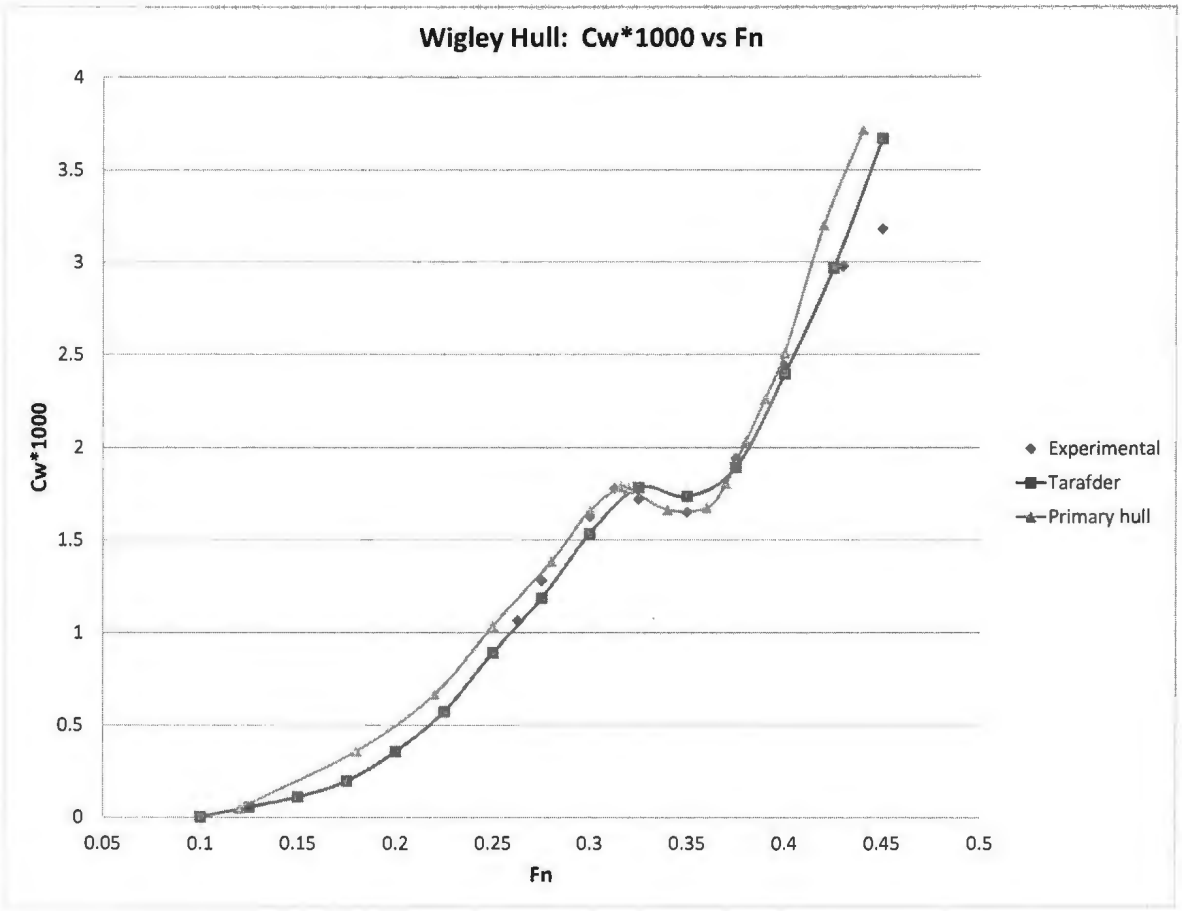

Figure 6.10: Wigley Hull: Wave Making Resistance Coefficient, C_w

6.2.1 Wigley Hull: Stations Shift

Minimization in C_w approaches gradually with slight divergences in two consecutive iterations. At 23rd iteration there is only 0.6008% and the wave resistance is reduced by 3.88%. The optimization procedure may continue for more iterations for further improvement in wave resistance by reducing the value in the stopping criteria. As there is a continuous change in

each iteration throughout the process, the first and last six iterations have been shown in the following table 6.4.

Table 6.4: Wigley Hull: Longitudinal Shift - Changes in Properties

Iteration	Volume of Displacement (m^3)	Wetted Surface Area (m^2)	Block Coeff., C_b	Resistance Coeff., $C_w \times 10^3$	Max. Change in Properties (%)
Primary	1.38318	7.4010	0.44262	1.6419	
Iteration 1	1.3801	7.3984	0.4416	1.6353	0.2227
Iteration 2	1.3799	7.3982	0.4416	1.6325	0.2401
Iteration 3	1.3796	7.3980	0.4415	1.6297	0.2575
Iteration 4	1.3794	7.3978	0.4414	1.6269	0.2748
Iteration 5	1.3791	7.3975	0.4413	1.6241	0.2921
Iteration 6	1.3789	7.3973	0.4413	1.6214	0.3093
⋮	⋮	⋮	⋮	⋮	⋮
Iteration 18	1.3760	7.3946	0.4403	1.5902	0.5160
Iteration 19	1.3758	7.3944	0.4403	1.5878	0.5330
Iteration 20	1.3756	7.3942	0.4402	1.5853	0.5501
Iteration 21	1.3753	7.3940	0.4401	1.5829	0.5670
Iteration 22	1.3751	7.3937	0.4400	1.5806	0.5839
Iteration 23	1.3749	7.3935	0.4399	1.5783	0.6008

As there is no changes in widths of this parabolic hull stations, body plan comparison will not show any difference among the stations. Figures 6.11, 6.12 and 6.13 compares the changes in load waterplane shapes and the shift of stations at forward, middle and after regions of the ship respectively, for the modified ship at iteration 23 with the primary hull. In these

figures few stations have been omitted for clarity. It appears that this modification method shifts stations from forward and after zone towards the midship region narrowing forward and after areas and eventually reduces the wave resistance.

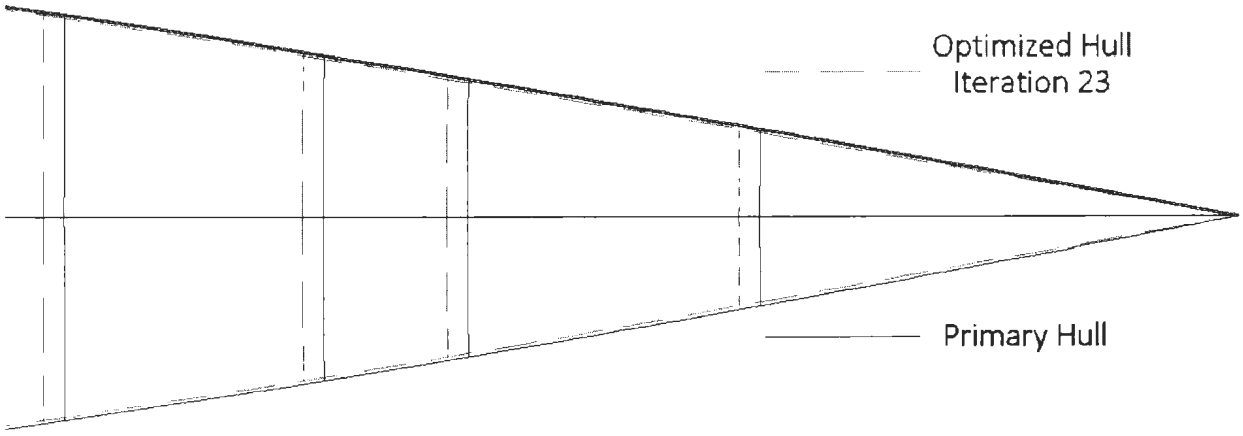

Figure 6.11: Wigley: Longitudinal Shift - Forward.

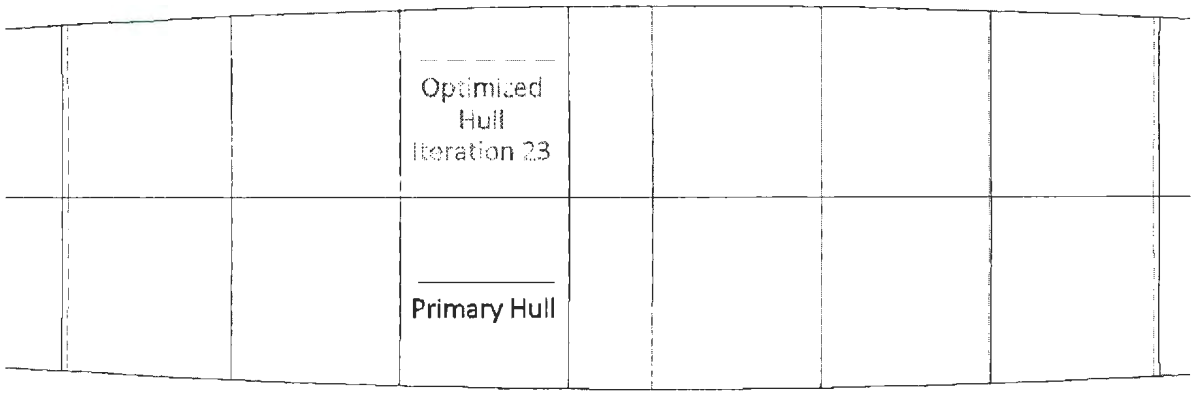

Figure 6.12: Wigley: Longitudinal Shift - Middle.

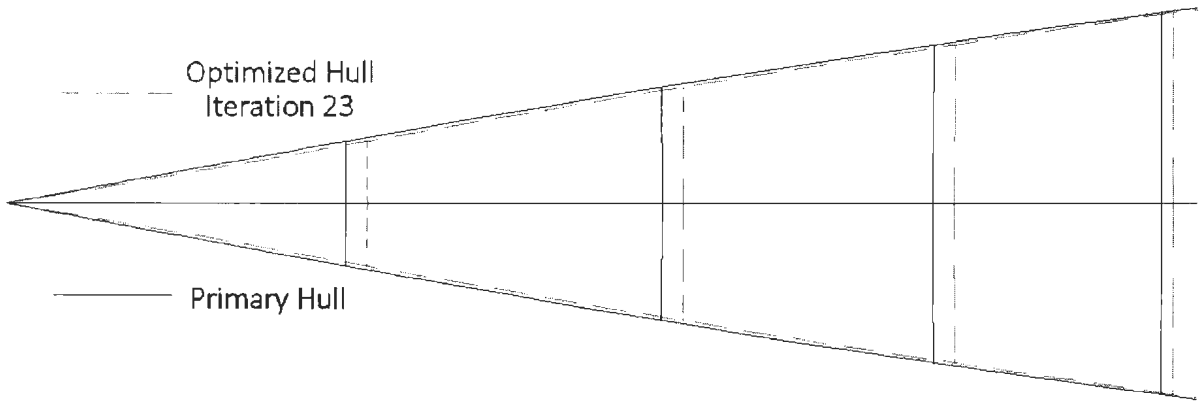

Figure 6.13: Wigley: Longitudinal Shift - Aft.

6.2.2 Wigley Hull: Change in y-coordinates of Stations

In this modification method, for the wigley hull, values for the objective function do not vary in any gradual decreasing pattern. At iteration eight, the new volume of displacement exceeds 5% than the primary one. 5% has been set as the tolerance limit[1] in the case of wigley hull. After 11th iteration the volume seems to expand more. The optimization loop was stopped at 12th iteration. Mostly, the hull form modification was expansion in one region and contraction on other, eventually reducing resistance. However, table 6.5 lists all the iteration, and the different properties.

The following figure (figure 6.14) compares body plans of few modified hulls with lower C_w and tolerance in volume with the primary hull. For visual clarity few stations has been omitted in the drawing. A set of 3D figures of these ship hulls are also presented afterwards.

[1]Tolerance limit is completely case dependent. Depending on the ship type or, volume or, goal of a certain project, one can set the tolerance limit to any suitable amount. For this study, tolerance limit is primarily based on the volume difference (%) in the iterations. For higher initial volume of displacement, it will be lower. For instance, the tolerance is 3.5 for Series 60 and 5.0 for Wigley hull.

Table 6.5: Wigley Hull: Change in Y-coordinates - Changes in Properties

Iteration	Volume of Displacement (m^3)	Wetted Surface Area (m^2)	Block Coeff., C_b	Resistance Coeff., $C_w \times 10^3$	Max. Change in Properties (%)
Primary	1.38318	7.4010	0.44262	1.6419	
Iteration 1	1.4191	7.4692	0.4541	1.3969	2.5957
Iteration 2	1.3694	7.4360	0.4382	1.2027	0.9966
Iteration 3	1.4456	7.5156	0.4626	2.4903	4.5139
Iteration 4	1.3566	7.3856	0.4341	1.4273	1.9212
Iteration 5	1.3190	7.3927	0.4221	1.1764	4.6423
Iteration 6	1.4173	7.5004	0.4536	2.3825	2.4689
Iteration 7	1.3346	7.3851	0.4271	1.3971	3.5162
Iteration 8	1.3018	7.3950	0.4166	1.1696	5.8869
Iteration 9	1.3880	7.4772	0.4442	2.2184	0.3453
Iteration 10	1.3190	7.3914	0.4221	1.3623	4.6376
Iteration 11	1.2915	7.4007	0.4133	1.1649	6.6316
Iteration 12	1.2746	7.4130	0.4079	1.0546	7.8479

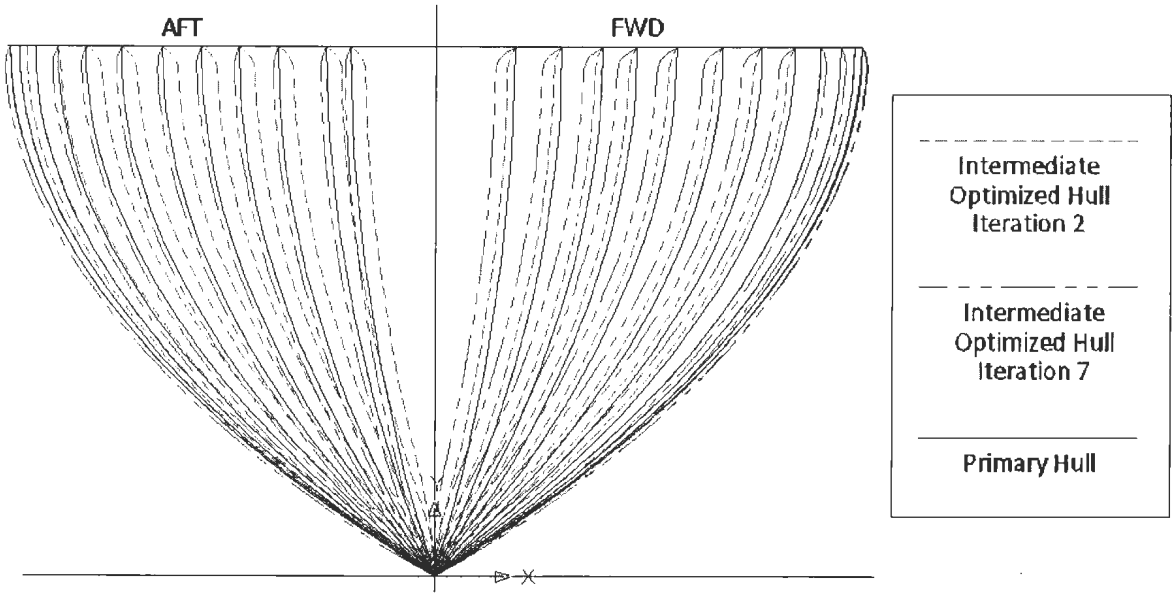

Figure 6.14: Wigley: Variation of Y- Body Plan Comparison.

6.2.3 Wigley Hull: Changing the Vertical Location of Nodes on Stations

Table 6.6 shows the output from the iterations in the optimization program. In this case, there were twelve iterations, and again, the step length was converted to 1.00. In each iteration wave resistance coefficient reduced gradually. As the reduction in volume of displacement was going higher in each iteration, the process was stopped at iteration 12.

Table 6.6: Wigley Hull: Vertical Shift of Waterplanes - Changes in Properties

Iteration	Volume of Displacement (m^3)	Wetted Surface Area (m^2)	Block Coeff., C_b	Resistance Coeff., $C_w \times 10^3$	Max. Change in Properties (%)
Primary	1.38318	7.4010	0.44262	1.6419	
Iteration 1	1.3791	7.3978	0.4413	1.6355	0.2971
Iteration 2	1.3749	7.3948	0.4400	1.6293	0.5985
Iteration 3	1.3708	7.3921	0.4386	1.6232	0.8983
Iteration 4	1.3666	7.3895	0.4373	1.6168	1.2024
Iteration 5	1.3623	7.3872	0.4359	1.6103	1.5135
Iteration 6	1.3580	7.3850	0.4346	1.6037	1.8235
Iteration 7	1.3537	7.3831	0.4338	1.5972	2.1341
Iteration 8	1.3494	7.3814	0.4318	1.5904	2.4462
Iteration 9	1.3450	7.3800	0.4304	1.5837	2.7583
Iteration 10	1.3407	7.3787	0.4290	1.5768	3.0723
Iteration 11	1.3363	7.3777	0.4276	1.5698	3.3906
Iteration 12	1.3319	7.3768	0.4262	1.5628	3.7106

Figure 6.15 and 6.16 compare the body plans of ships at iteration 6 and 12 with primary hull, respectively. For clarity, few stations has been omitted. In each iteration the bottom region seems to be pressed up decreasing the sectional area at the bottom region. This lifts the centroid of the sectional areas and reduces the tangent angle of entrance and run. Eventually, these reduces wetted surface area providing improved performance based on wave resistance. In this case, the resistance coefficient at iteration 12 is 4.82% lower than the primary one, where wetted surface area is reduced by only 0.368%.

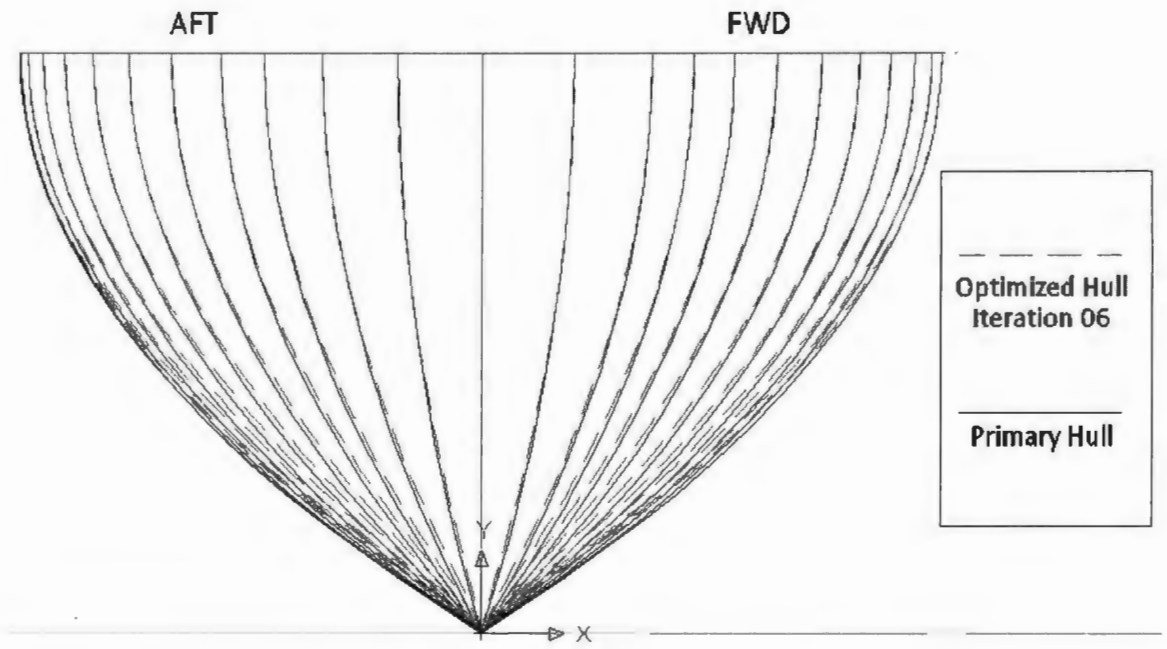

Figure 6.15: Wigley: Shift of Waterplanes - Body Plan Comparison, Iteration 6.

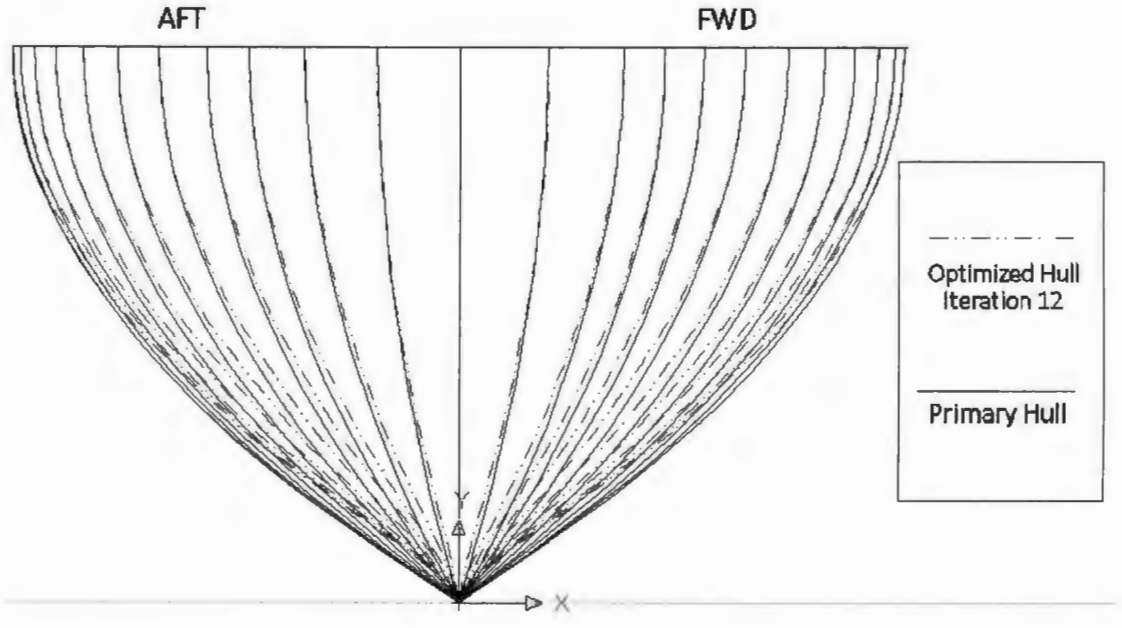

Figure 6.16: Wigley: Shift of Waterplanes - Body Plan Comparison, Iteration 12.

Again, figure 6.17[2] compares C_w for modified hull from different modification methods at various Froude numbers. At most of the speeds, modified hull forms performs better based on resistance point of view. Therefore, it appears that the optimization process is capable to produce new modified ship hulls with improve wave resistance. Based on any particular case of study, one can play with the process to produce a several number of different ship hulls, and select any ship hull satisfying the best interest.

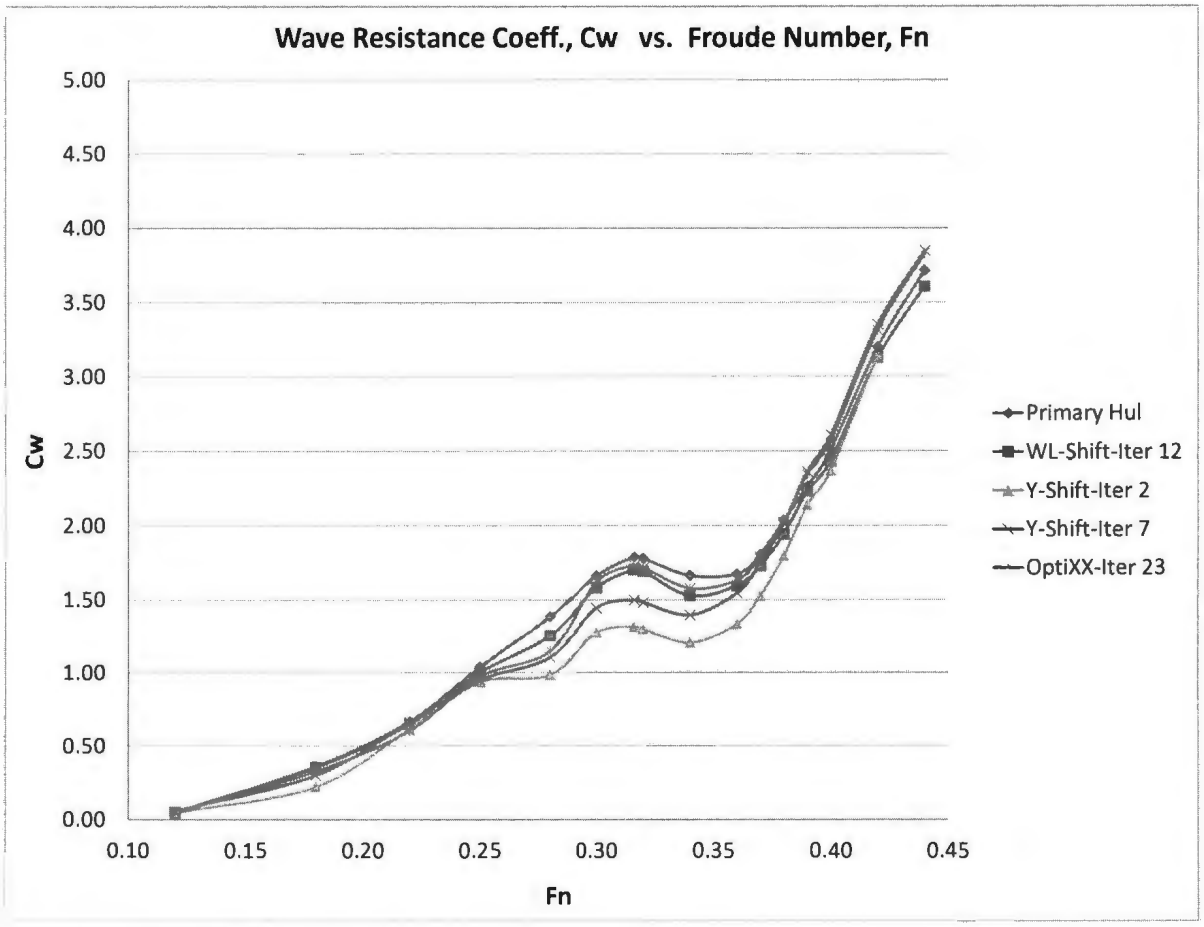

Figure 6.17: Wigley: C_w comparison - Various Modification Methods.

[2]In figure 6.17, Y-Shift-Iter 2 and Y-Shift-Iter 7 represent the curves for modified ship hulls for second modification method at iteration 2 and 7, WL-Shift-Iter 12 represents hull from for the third method at iteration 12, and St.-Shift 23 is the same for first method at iteration 23.

Chapter 7

Conclusions and Recommendations

This study started with an automatic ship hull generation algorithm. A set of appropriate coordinates describing the geometry of a conventional ship is required as the input. Global curve and surface interpolation method were implemented to develop the ship hull form mathematically applicable to any numerical analyses. IGES file format prepared the hull data to represent graphically. Based on geometric properties and visual inspection, the method appears to be validated by showing convincing convergence to original ship hull geometries. Few different types of ship geometries have been investigated, and the method produced satisfactory output. Complicated ship hull like SWATH, Catamaran or ships with sharp corners in hull geometry, may not be generated efficiently by using this method as it uses single B-spline surface patch for one symmetric half of the hull.

Discretization of the primary hull surface was performed to facilitate numerical analysis requiring surfaces described by grids. As the ship hull geometry is also represented with aid of an IGES formatted file, any CFD or CAD or Similar type of softwares capable to read IGES file can utilize the hull for necessary analysis. Although the grid generation was required for the hull up to load waterline, the grid generation scheme can be applied to the total hull including freeboard.

An individual optimization process approaches with an integrated hull modification method and continuous check for constraints violation. Iterative solution sections in the MAPS-Resistance program take the longest time in the whole system. The total time of all optimization loops is completely dependent on the number of variables, ship types, dimensions, number of grids and the course for step length calculation. If the Fibonacci search method is employed for the optimal step length search, for a single standard computing system, one optimization loop requires around 60 minutes. If the step length is set to 1.00, it will take about $\frac{1}{25}$-th of the time. Therefore, a faster objective function calculation system will speed up the complete process.

The optimization procedure does not claim to provide definite single result. This is maintained to serve the best practical case-based interests. There could be several number of suggestions for modified hull forms which provide improved wave resistance. This seems to be a judicious feature considering diversity of users' requirements.

There are several possibilities of improvement in different steps of the total system. There are always scopes for investigating few selective hulls with model testing. Preparation of a model will also correct any possible local bump or discontinuity on the ship geometry.

There cannot be any definite and standard method of hull form modification as well as optimization. It is completely case dependent and decisive to its best interest. Those three methods adopted here are simple methods based on control points, which find suitable applicability in the optimization procedure. Different local and global form parameters, e.g. C_m, C_p, angle of entrance and run, sectional area curve, etc., can be accepted as variables. These parameters can be applied directly as modification variables if the ship design process is parametric.

Modification methods in this study can directly be applied to primary hull stations and waterlines. In that case, discretization will be performed inside the optimization algorithm everytime before the hydrodynamic analysis. This modification will provide extensive local changes in all regions of the geometry. But, it will increase the number of variables inside the

optimization loop giving rise to the computational time.

In case of ship hull development, parametric design can be considered as further study, where inputs will be simpler and lesser in number. Then, precalculation of parameters will be required, if not available. Approximation methods or local interpolation methods for B-spline surface generation can also be investigated, where fairing process will find modest applicability. NURBS surface may also be applied in geometry development. In that case, the differences between the effect on ship geometries due to variable weights in NURBS and unit weights in B-splines can be observed.

Various optimization methods can be applied and variances can be investigated, specially response surface method (RSM) can provide appealing opportunities. Finally, the present optimization system can be applied in search for optimality of other objective functions related to ship design. In that case, an algorithm performing the evaluation of the function has to be integrated or, called inside the system. If more than one objectives are desired to be explored simultaneously, a multi-objective multivariable optimization strategy needs to replace the present optimization procedure.

Bibliography

(1996). *"Initial Graphics Exchange Specification (IGES 5.3)"*. U.S. Product Data Association, Trident Research Center, Suite 204; N. Charleston, SC 29418, first edition.

Abt, C., Bade, S. D., Birk, L., and Harries, S. (2001). "Parametric hull form design - a step towards one week ship design". *8th International Symposium on Practical Design of Ships and Other Floating Structures. PRADS.*

Abt, C. and Schellenberger, G. (2007). "An integrated approach for hydrodynamic optimization of SWATH hull fomrs". 10th International Symposium on Practical Design of Ships and Other Floating Structures, Houston, Texas, USA.

Bao-ji, Z., Kun, M., and Zhuo-shang, J. (2009). "The optimization of the hull form with the minimum wave making resistance based on Rankine source method". *Journal of Hydrodynamics*, 21(2):pp. 277 – 284.

Branke, J., Deb, K., Miettinen, K., and Słowiński(Eds.), R. (2008). *"Multiobjective Optimization (Interactive and Evolutionary Approaches)"*. Springer-Verlag Berlin Heidelberg, first edition.

Çalişal, S. M., Gören, Ö., and Danişman, D. B. (2002). "Resistance reduction by increased beam for displacement-type ships". *Journal of Ship Research*, 46(3):pp. 208 – 213.

Cang, V. T. and Le, T.-H. (2011). "Modeling of ship surface with non uniform B-spline". International MultiConference of Engineers and Computer Scientists 2011, Hong Kong.

Dawson, C. W. (1977). "A practical computer method for solving ship-wave problem". 2nd International Conference on Numerical Ship Hydrodynamics, University of California, Berkeley, USA, pages pp. 30 – 38.

Doctors, L. J. (2006). "A numerical study of the resistance of transom-stern monohulls". 5th International Conference on High Performance Marine Vehicles, Australia.

Esping, B., Clarin, P., and Romell, O. (1990). "OCTOPUS-a tool for distributed optimization of multi-disciplinary objectives". ALFGAM Optimering, AB, Stockholm, Sweden.

Grigoropoulos, G. J. (2004). "Hull form optimization for hydrodynamic performance". *Marine Technology*, 41(4):pp. 167 – 182.

Harries, S. (1998). *"Parametric Design and Hydrodynamic Optimization of Ship Hull Forms"*. PhD thesis, Technischen Universität, Berlin.

Harries, S. and Abt, C. (1997). "Parametric curve design applying fairness criteria". International Workshop on Creating Fair and Shape-Preserving Curves and Surfaces, Network Fairshape, Berlin/Potsdam. Published at Teubner, 1998.

Harries, S., Abt, C., and Hochkirch, K. (2004). "Modeling meets simulations - process integration to improve design". Honorary Colloquium for Prof. Hagen, Prof. Schlüter and Prof. Thiel.

Hilleary, R. R. (1966). "Tangent search method of constrained minimization". Technical Report/Res. Paper No. 59, Naval Postgraduate School, Monterey, CA, USA.

Hollister, S. M. (1996). "Automatic hull variation and optimization". Meeting of the New England Section of The Society of Naval Architects and Marine Engineers.

Hooke, R. and Jeeves, T. A. (1961). "Direct search solution of numerical and statistical problems". *Journal of the Association for Computing Machinery*, 8(4).

Hsiung, C.-C. (1981). "Optimal ship forms for minimum wave resistance". *Journal of Ship Research*, 25(2):pp. 95 – 116.

Hu, S. M., Li, Y. F., Ju, T., and Zhu, X. (2001). "Modifying the shape of nurbs with geometric constraints". *Computer Aided Design, ELSEVIER*, 33:pp. 903 – 912.

Hutchison, B. L. and Hochkirch, K. (2007). "CFD hull form optimization of a 12,000 cu. yd. (9175 m^3) dredge". 10th International Symposium on Practical Design of Ships and Other Floating Structures, Houston, Texas, USA.

Janson, C. and Larson, L. (1997). "A method for the optimization of ship hulls from a resistance point of view". Twenty-First Symposium on Naval Hydrodynamics, pages 680–696, `http://www.nap.edu/openbook/0309058791/html/680.html`.

Khamayesh, A. and Hamann, B. (1996). "Eliptic grid generation using NURBS surfaces". *Computer-Aided Geometric Desing, Elsevier*, 13:pp. 369 – 386.

Kim, H. and Yang, C. (2010). "A new surface modification approach for cfd-based hull form optimization". 9th International Conference on Hydrodynamics, Shanghai, China.

Kim, H. and Yang, C. (2011). "Hydrodynamic optimization of multihull ships". 11th International Conference on Fast Sea Transportation, FAST 2011, Honolulu, Hawai, USA.

Kim, H., Yang, C., Löhner, R., and Noblesse, F. (2008). "A practical hydrodynamic optimization tool for the design of a monohull ship". International Offshore and Polar Engineering Conference (ISOPE), Vancouver, BC, Canada.

Kim, H., Yang, C., and Noblesse, F. (2010). "Hull form optimization for reduced resistance and improved seakeeping via practical design-oriented cfd tools". GCMS '10, Ottawa, Canada.

Kouh, J. S. and Chau, S. W. (1993). "Computer-aided geometric design and panel generation for hull forms based on rational cubic Béizer curves". *Computer Aided Design, ELSEVIER Science Publishers B.V.*, 10:pp. 537 – 549.

Kracht, A. M. (1978). "Design of bulbous bows". *SNAME Transactions*, 86:pp. 197 – 217.

Lackenby, H. (1950). "On systematic geometrical variation of ship forms". RINA, *Originally published for written discussion. (Based on the work of the British's Shipbuilding Research Association)*.

Larsson, L. (1997). "SHIPFLOW user's manual and theoretical manual". FLOTECH Int. AB, Gothenburg.

Legriel, J., Guernic, C. L., Cotton, S., and Maler, O. (2010). "Approximating the Pareto front of multi-criteria optimization problem". VERIMAG, France and French MINLOGIC project ATHOLE.

Majumder, M., Akitürk, A., and Çalişal, S. M. (2002). "Optimized design of small craft". *Marine Technology*, 39(2):pp. 67 – 76.

Makkar, J. (2002). "Commercial aspects of shipping - voyage estimation". `http://www.pfri.uniri.hr/~bopri/documents/11VoyageEstimation_000.pdf`.

Manisonneuve, J. J., Harries, S., Marzi, J., Raven, H. C., Viviani, U., and Piippo, H. (2003). "Toward optimal design of ship hull shapes". IMDC 8-th International Marine design Conference, Athens.

Markov, N. E. and Suzuki, K. (2000). "Fundamental studies on Rankine source panel method fully based on b-splines". *Journal of the Society of Naval Architects of Japan*, 187.

Markov, N. E. and Suzuki, K. (2001). "Hull form optimization by shift and deformation of ship functions". *Journal of Ship Research*, 45(3):pp. 197 – 204.

Martineli, L. and Jameson, A. (2007). "An adjoint method for design optimization of ship hulls". 9th International Conference of Numerical Ship Hydrodynamics.

Michell, J. H. (1898). "The wave resistance". *Philosophical Magazine*, 5(45):pp. 106 – 123.

Ni, S., Qiu, W., and Peng, H. (2011). "MAPS-resistance version 2.0". Technical Report (INT2010-001), Ocean and Naval Architectural Engineering, Memorial University, St. John's, NL, Canada.

Nowacki, H. (1993). "Hull form variation and evaluation". *The Japan Society of Naval Architects and Ocean Engineers*, (219):pp. 173 – 184.

Nowacki, H., Bloor, M., and Oleksiewicz, B. (1995). *"Computational Geometry for Ships"*. World Scientific Publishing Co. Pte. Ltd., second edition.

Pérez, F., A., J., Clemente, J. A., and Souto, A. (2007). "Geometric modeling of bulbous bows with the use of non-uniform rational B-spline surfaces". *J Mar Sci Technol*, 12:pp. 83 – 94.

Pérez-Arribas, F. and Clemente, J. A. (2011). "Constrained design of simple ship hulls with b-spline surfaces". *Computer-Aided Desing, Elsevier*, 43:pp. 1829 – 1840.

Pérez-Arribas, F., Clemente, J. A., Suárez, J. A., and González, J. M. (2008). "Parametric generation, modelling, and fairing of simple hull lines with the use of non-uniform rational b-spline surfaces". *Journal of Ship Research*, 52(1):pp. 01 – 15.

Pérez-Arribas, F., Suárez-Suárez, J. A., and Fernández-Jambrina, L. (2006). "Automatic surface modeling of a ship hull". *Computer-Aided Design, Elsevier*.

Piegl, L. (1989). "Modifying the shape of rational b-splines. part 2 : Surfaces". *Computer Aided Design, ELSEVIER*, 21(9):pp. 538 – 546.

Piegl, L. and Tiller, W. (1997). *"The NURBS Book"*. Springer-Verlag Berlin Heidelberg, second edition.

Pike, R. W. (2001). *"Optimization for Engineering Systems"*. Louisiana State University, `www.mpri.lsu.edu/bookindex.html`, first edition.

Press, W. H., Teukolsky, S. A., Vetterling, W. T., and Flannery, B. P. (1988). *"Numerical recipes in C"*. Cambridge University Press, New York, NY, USA, second edition.

Rao, S. S. (2009). *"Engineering Optimization - Theory and Practice"*. John Wiley & Sons, Inc., fourth edition.

Ravindran, A., Ragsdell, K. M., and Reklaitis, G. V. (2006). *"Engineering Optimization - Methods and Applications"*. John Wiley & Sons, Inc., second edition.

Rogers, D. F. and Satterfield, S. G. (1980). "B-spline for ship hull design". SIGGRAPH '80 Proceedings of the 7th annual conference. ACM, New York, USA.

Sahoo, P. K., Peng, H., Won, J., and Sangarasigamany, D. (2011). "Re-evaluation of resistance prediction for high-speed round bilge hull forms". 11th International Conference on Fast Sea Transportation, FAST 2011, Honolulu, Hawaii, USA.

Saoyu, N., Qiu, W., and Peng, H. (2012). "User's manual of MAPS-resistance version 2.0". Ocean and Naval Architectural Engineering, Memorial University, St. John's, NL, Canada.

Shearer, J. J. and Cross, J. R. (1965). "The experimental determination of the components of ship resistance for a mathematical model". Transactions of INA 107.

Tarafder, M. S. and Suzuki, K. (2007). "Numerical calculation of free-surface potential flow around a ship using the modified rankine source panel method". *Ocean Engineering, ELSEVIER*, 35:pp. 536 – 544.

Thompson, J. F., Soni, V. K., and Weatherill, N. P., editors (1999). *"Handbook of Grid Generation"*. CRC Press LLC, first edition.

Todd, F. H. (1963). "Series 60, methodical experiments with models of single-screw merchant ships ". Research and Development Report, Defense Documentation Center for Scientific and Technical Information, Cameron Station, Alexandria, Virginia.

Valorani, M., Peri, D., and Campana, E. F. (2003). "Sensitivity analysis methods to design optimal ship hulls". *Optimization and Engineering*, 4(3):pp. 337 – 364.

Wen, A. S., Shamsuddin, S. M. H., and Samian, Y. (2006). "Optimized NURBS ship's hull fitting using simulated annealing". International Conference on Computer Graphics, Imaging and Visualisation (CGIV'06), Leeds, UK.

Yang, C., Kim, H., Löhner, R., and Noblesse, F. (2008). "Practical hydrodynamic optimization of ship hull forms". GCMS '08, Edinburgh, UK.

Yoshimoto, F., Harada, T., and Yoshimoto, Y. (2003). "Data fitting with a spline using a real-coded genetic algorithm". *Computer Aided Design, ELSEVIER*, 35:pp. 751 – 760.

Zalek, S. D., Parsons, M. G., and Beck, R. F. (2009). "Naval hull form multicriterion hydrodynamic optimization for conceptual design phase". *Journal of Ship Research*, 53(4):pp. 199 – 213.

Appendix A

Fibonacci Search Method

This search technique is considered to be the best one of the minimax methods. It has the largest interval reduction of all of the procedures, but it requires that the number of experiments be specified in advance. The algorithm begins by placing the last two experiments optimally in the interval preceding the final interval of uncertainty. This is simultaneous search with two experiments or evaluations of target function. Then the development determines the location of each preceding experiment to arrive at the location of the first two experiments.

The Fibonacci search method is based on the Fibonacci numbers $\{F_k\}_{k=0}^{\infty}$ defined by the equation A.1,

$$F_o = o, F_1 = 1$$
$$F_n = F_{n-1} + F_{n-2} \tag{A.1}$$

for $n = 2, 3, \ldots$. Thus the Fibonacci numbers are $0, 1, 1, 2, 3, 5, 8, 13, 21, 34, 55, \ldots$.

In the search method total number of Fibonacci numbers should be chosen, which in this algorithm has been chosen as 50. To move from first set of two evaluations to next set of experiments/ evaluations, a fraction or ratio needs to be chosen. In general Fibonacci search, an irrational number is taken as this fraction, which is known as the golden ratio, $\varphi = 1.618034$. The Fibonacci search algorithm to find the optimum step length, inside the main optimization

algorithm, is given in the following.

```
 f(x) = function of evaluation
Lower Bound, HB = 0.0
Higher Bound, LB = 1.0
Test Value, T = 1.0
Tolerance = 0.00001
Golden Ratio, GR = 1.618034
L = 1
!!  -- Searching the interval for Fibonacci Search -- !!
!!  Test Value for Lower Bound ------
10    TVLB = f(T)
!!  Test Value for Higher Bound ------
TVHB = f(HB)
L = L + 1
if (L > 6) Then
StepLength = 1.0
goto 111
else
endif
if (TVLB > TVHB) go to 20
else
endif
TLower = T; T = HB
HB = HB × GR
go to 10
20    continue
!!  -- Determination of Bounds and Delta for Fibonacci Search -- !!
!!  Delta, δ is the fractional resolution based on the final
!!  interval of uncertainty .  !!
!!  ------------------------------------------------------------ !!
if (T ≠ 1.0) LB = TLower
else
endif
Interval = HB − LB; Delta = T − LB; TestLB = T; TestHB = HB − Delta
if (TestLB < TestHB) go to 30
else
endif
TLower = TestLB; TestLB = TestHB; Delta = TestLB − LB
TestHB = HB − Delta
30    Continue
Interval = HB − LB; Ratio = Interval ÷ GR
!!  -- Determination of the Number of Evaluations Required to have !!
!!  Tolerance = 0.00001 -- !!
```

```
!!  --- Fibonacci Number --- !!
Fibonacci[1] = 1.0
Fibonacci[2] = 1.0
Do 50 I = 3, 50
!!  Running a loop from 3 to 50, with increment 1.  !!
Fibonacci[I] = Fibonacci[I − 1] + Fibonacci[I − 2]
if (Fibonacci[I] < Ratio) ExpNo = I + 1
!!  ExpNo = total number of evaluations experiments needed.
else
endif
!!  -- Closed Bound Fibonacci Search -- !!
TVLB = f(TestLB)
TVHB = f(TestHB)
if (TVLB ≥ TVHB) go to 40
else
endif
LB = TestLB; Interval = HB − LB; Delta = Interval − Delta
TestLB = TestHB; TestHB = HB − Delta
Flag = 1     !!  Declaring the possible location of optimal step length
go to 50
40    Continue
HB = TestHB; Interval = HB − LB; Delta = Interval − Delta
TestHB = TestLB; TestLB = LB + Delta
Flag = 2     !!  Declaring the possible location of optimal step length
50    Continue
if (Flag = 1) StepLength = TestLB
elseif (Flag = 2) StepLength = TestHB
else
endif
111    Continue
END
```

Appendix B

Input Files

B.1 Offset Table Format in Excel

Sample view:

Hull Offset in Full scale

Name:	Series 60, Cb = 0.6
Total No. of Stations:	25
Total No. of Waterlines:	9
Ship Length (LWL)	20.00000
Breadth	1.00000
Draft	1.00000

Center Buttocline/ Profile Information (First row : Waterlines; Second row: Stations or distance form FP) :

	0	0	0.075	0.25	0.5	0.75	1	1.25	1.5
	0.19300	0.19300	0.12903	0.09677	0.09032	0.05645	0.00000	-0.07097	-0.15163
	19.61613	19.61613	19.61613	19.61613	19.61613	19.65161	20.04516	20.50000	20.56452
St. ↓/ WL →									
	0	0	0.075	0.25	0.5	0.75	1	1.25	1.5
0	0.00000	0.00000	0.00000	0.00000	0.00000	0.00000	0.00000	0.02000	0.04200
0.5	0.00000	0.00639	0.02771	0.04137	0.04100	0.04300	0.05100	0.07600	0.12000
1	0.00000	0.00923	0.05542	0.08077	0.08700	0.09000	0.10200	0.13300	0.19800
1.5	0.00000	0.01349	0.08227	0.12411	0.14100	0.14800	0.16000	0.19500	0.27800
2	0.00000	0.01704	0.10998	0.17533	0.20400	0.21300	0.22800	0.27000	0.36000
3	0.00000	0.03905	0.16974	0.28959	0.34600	0.36800	0.39100	0.44000	0.53100
4	0.00000	0.09514	0.27192	0.42946	0.50200	0.53500	0.56200	0.60700	0.68300
5	0.00000	0.19525	0.40356	0.58017	0.66000	0.69100	0.71800	0.75400	0.80400
6	0.00000	0.33299	0.54558	0.72201	0.80200	0.82400	0.84100	0.86200	0.88900
7	0.00000	0.47286	0.67461	0.84119	0.90600	0.91700	0.92600	0.93600	0.94600
8	0.00000	0.59001	0.77767	0.92098	0.97100	0.97700	0.97900	0.98100	0.98200
9	0.00000	0.67095	0.83482	0.96432	0.99600	1.00000	1.00000	1.00000	1.00000
10	0.00000	0.71000	0.86600	0.98500	1.00000	1.00000	1.00000	1.00000	1.00000
11	0.00000	0.68515	0.85041	0.97515	1.00000	1.00000	1.00000	1.00000	1.00000
12	0.00000	0.62622	0.79845	0.94363	0.99400	1.00000	1.00000	1.00000	1.00000
13	0.00000	0.54457	0.71532	0.87862	0.96200	0.98700	0.99400	0.99700	1.00000
14	0.00000	0.44162	0.60707	0.76929	0.88400	0.94300	0.97500	0.99000	0.99900
15	0.00000	0.32873	0.48496	0.62942	0.75400	0.85700	0.93700	0.97700	0.99400
16	0.00000	0.21939	0.35766	0.47576	0.59200	0.72800	0.85700	0.93300	0.97500
17	0.00000	0.11928	0.23122	0.32505	0.41300	0.54100	0.72500	0.84400	0.92400
18	0.00000	0.04615	0.13163	0.19011	0.23600	0.32100	0.53600	0.70900	0.83400
18.5	0.00000	0.02272	0.08833	0.12805	0.15600	0.21600	0.42500	0.62600	0.76900
19	0.00000	0.00894	0.05023	0.07486	0.08500	0.11600	0.30800	0.53000	0.68600
19.5	0.00000	0.00610	0.01732	0.01970	0.02200	0.04100	0.19300	0.41800	0.57900
20	0.00000	0.00000	0.00000	0.00000	0.00000	0.00000	0.08200	0.27000	0.42000

Figure B.1: *.xls File: Offset Table Format

B.2 *.csv File for Offset Table Format

```
Hull Offset in Full scale,,,,,,,,,,
Name:,"Series 60, Cb = 0.6",,,,,,,,,
Total No. of Stations: ,,,25,,,,,,,
Total No. of Waterlines: ,,,9,,,,,,,
Ship Length (LWL),,,20.00000,,,,,,,
Breadth,,,1.00000,,,,,,,
Draft,,,1.00000,,,,,,,
,,,,,,,,,,
Center Buttocline/ Profile Information   (First row : Waterlines; Second row:  Stations
,0,0,0.075,0.25,0.5,0.75,1,1.25,1.5,,
,0.19300,0.19300,0.12903,0.09677,0.09032,0.05645,0.00000,-0.07097,-0.15163,,
,19.61613,19.61613,19.61613,19.61613,19.61613,19.65161,20.04516,20.50000,20.56452,,
St. ?/ WL  ?,,,,,,,,,,
,0,0,0.075,0.25,0.5,0.75,1,1.25,1.5,,
0,0.00000,0.00000,0.00000,0.00000,0.00000,0.00000,0.00000,0.02000,0.04200,,
0.5,0.00000,0.00639,0.02771,0.04137,0.04100,0.04300,0.05100,0.07600,0.12000,,
1,0.00000,0.00923,0.05542,0.08077,0.08700,0.09000,0.10200,0.13300,0.19800,,
1.5,0.00000,0.01349,0.08227,0.12411,0.14100,0.14800,0.16000,0.19500,0.27800,,
2,0.00000,0.01704,0.10998,0.17533,0.20400,0.21300,0.22800,0.27000,0.36000,,
3,0.00000,0.03905,0.16974,0.28959,0.34600,0.36800,0.39100,0.44000,0.53100,,
4,0.00000,0.08514,0.27192,0.42946,0.50200,0.53500,0.56200,0.60700,0.68300,,
5,0.00000,0.19525,0.40356,0.58017,0.66000,0.69100,0.71800,0.75400,0.80400,,
6,0.00000,0.33299,0.54558,0.72201,0.80200,0.82400,0.84100,0.86200,0.88900,,
7,0.00000,0.47286,0.67461,0.84119,0.90600,0.91700,0.92600,0.93600,0.94600,,
8,0.00000,0.59001,0.77767,0.92038,0.97100,0.97700,0.97900,0.98100,0.98200,,
9,0.00000,0.67035,0.83482,0.96432,0.99600,1.00000,1.00000,1.00000,1.00000,,
10,0.00000,0.71000,0.86600,0.98500,1.00000,1.00000,1.00000,1.00000,1.00000,,
11,0.00000,0.68515,0.85041,0.97515,1.00000,1.00000,1.00000,1.00000,1.00000,,
12,0.00000,0.62622,0.79845,0.94363,0.99400,1.00000,1.00000,1.00000,1.00000,,
13,0.00000,0.54457,0.71532,0.87862,0.96200,0.98700,0.99400,0.99700,1.00000,,
14,0.00000,0.44162,0.60707,0.76929,0.88400,0.94300,0.97500,0.99000,0.99300,,
15,0.00000,0.32873,0.48496,0.62942,0.75400,0.85700,0.93700,0.97700,0.99400,,
16,0.00000,0.21939,0.35766,0.47576,0.59200,0.72800,0.85700,0.93300,0.97500,,
17,0.00000,0.11928,0.23123,0.32505,0.41300,0.51100,0.72500,0.81400,0.92400,
```

Figure B.2: *.csv file: Offset Table Format

B.3 *x-y-z* Format in Excel

	A	B	C	D	E
1					
2	Number of Stations		27		
3	Number of Horizontal points		21		
4	Length =		52.1166664		
5	Half Beam =		3.257292		
6	Draft =		1.628125		
7					
8	If it has a transom hull please write TR = 1, if not, write TR = 0				
9	TR =		1		
10	If there is a bulbous bow, write bulb = 1, if not, write bulb = 0				
11	bulb =		0		
12					
13	2.035349433	0.000000	0.044000		
14	1.547700818	0.000000	0.208333		
15	1.121600086	0.000000	0.418667		
16	0.859296339	0.000000	0.625000		
17	0.695499354	0.000000	0.833333		
18	0.526378306	0.000000	1.041667		
19	0.362731981	0.000000	1.250000		
20	0.184178475	0.000000	1.458333		
21	0.056348256	0.000000	1.628125		
22	-0.13302985	0.000000	1.875000		
23	-0.29636846	0.000000	2.083333		
24	-0.46444153	0.000000	2.291667		
25	-0.63014737	0.000000	2.500000		
26	-0.8025935	0.000000	2.708333		
27	-0.97458172	0.000000	2.916667		
28	-1.15282061	0.000000	3.125000		

Figure B.3: *.xls file: *x-y-z* Format

B.4 *.csv File for *x*-*y*-*z* Format

```
Number of Stations,,27,,,,,,,
Number of Horizontal points,,21,,,,,,,
Length =,,52.1166664,,,,,,,
Half Beam =,,3.257292,,,,,,,
Draft =,,1.628125,,,,,,,
,,,,,,,,,
"If it has a transom hull please write TR = 1, if not, write TR
= 0",,,,,,,,,
TR =,1,,,,,,,,
"If there is a bulbous bow, write bulb = 1, if not, write bulb =
0",,,,,,,,,
bulb =,0,,,,,,,,
,,,,,,,,,
2.035349433,0.000000,0.044000,,,,,,,
1.547700818,0.000000,0.208333,,,,,,,
1.121600086,0.000000,0.418667,,,,,,,
0.859296339,0.000000,0.625000,,,,,,,
0.695499354,0.000000,0.833333,,,,,,,
0.526378306,0.000000,1.041667,,,,,,,
0.362731981,0.000000,1.250000,,,,,,,
0.184178475,0.000000,1.458333,,,,,,,
0.056348256,0.000000,1.628125,,,,,,,
-0.133029847,0.000000,1.875000,,,,,,,
-0.296368461,0.000000,2.083333,,,,,,,
-0.464441528,0.000000,2.291667,,,,,,,
-0.630147368,0.000000,2.500000,,,,,,,
-0.802593499,0.000000,2.708333,,,,,,,
-0.974581721,0.000000,2.916667,,,,,,,
-1.152820608,0.000000,3.125000,,,,,,,
-1.407149928,0.000000,3.541667,,,,,,,
-1.594769918,0.000000,3.750000,,,,,,,
-1.886623237,0.000000,3.958333,,,,,,,
-2.15762989,0.000000,4.266667
```

Figure B.4: *.csv file: *x*-*y*-*z* Format

Appendix C

Cubic Spline Interpolation Code

```
  Subroutine SPLINEint(N,XI,FI,X,F)

!! This subroutine performs cubic spline interpolation
!! with natural cubic spline.
!! X = The point where the interpolation occurs.
!! F = Interpolated value of the function (output)
!! XI = Input value of the independent variable
!! FI = Dependent function, FI = f(XI)
!! N = Number of points or variables used to interpolate
!! P2 = Second order derivative.

  IMPLICIT NONE
  INTEGER, PARAMETER :: M=100
  INTEGER, INTENT (IN) :: N
  INTEGER :: I, K
  DoublePrecision :: F, DX, H, ALPHA, BETA, GAMMA, ETA
  DoublePrecision, INTENT (IN) :: X, XI(N+5), FI(N+5)
  DoublePrecision, INTENT (OUT) :: P2(N+5)

  CALL Cubic(N, XI, FI, P2)

! Finding the approximation of the function
  H = (XI(N+1)-XI(1))/M
  X = XI(1)
  DO I = 1, M-1
    X = X + H
```

```
! Searching the interval where X is located
    K = 1
    DX = X-XI(1)
    DO WHILE (DX .GE. 0)
      K = K + 1
      DX = X-XI(K)
    END DO
    K = K - 1

! Finding the value of function f(X)

    DX = XI(K+1) - XI(K)
    ALPHA = P2(K+1)/(6*DX)
    BETA = -P2(K)/(6*DX)
    GAMMA = FI(K+1)/DX - DX*P2(K+1)/6
    ETA = DX*P2(K)/6 - FI(K)/DX
    F = ALPHA*(X-XI(K))*(X-XI(K))*(X-XI(K)) &
       +BETA*(X-XI(K+1))*(X-XI(K+1))*(X-XI(K+1)) &
       +GAMMA*(X-XI(K))+ETA*(X-XI(K+1))
  END DO

  Return
END Subroutine SPLINEint


SUBROUTINE Cubic (N, XI, FI, P2)
!
! Function to carry out the cubic-spline approximation
! with the second-order derivatives returned.
!
  INTEGER :: I
  INTEGER, INTENT (IN) :: N
  DoublePrecision, INTENT (IN) :: XI(N+5), FI(N+5)
  DoublePrecision , INTENT (OUT) :: P2(N+5)
  DoublePrecision :: G(N), H(N),D(N-1), B(N-1), C(N-1)


! Assigning the intervals and function differences

  DO I = 1, N
    H(I) = XI(I+1) - XI(I)
    G(I) = FI(I+1) - FI(I)
  END DO
```

```
!  The coefficient matrix elements

  DO I = 1, N-1
    D(I) = 2*(H(I+1)+H(I))
    B(I) = 6*(G(I+1)/H(I+1)-G(I)/H(I))
    C(I) = H(I+1)
  END DO

! Calculating the second-order derivatives

  CALL Tridiagonal_LE (N-1, D, C, C, B, G)
  P2(1) = 0
  P2(N+1) = 0
  DO I = 2, N
    P2(I) = G(I-1)
  END DO


  Return
END SUBROUTINE Cubic


SUBROUTINE Tridiagonal_LE (L, D, E, C, B, Z)

! Subroutine to solve the tridiagonal linear equation system.

  INTEGER, INTENT (IN) :: L
  INTEGER :: I
  DoublePrecision, INTENT (IN), DIMENSION (L):: D, E, C, B
  DoublePrecision, INTENT (OUT), DIMENSION (L):: Z
  DoublePrecision, DIMENSION (L):: Y, W
  DoublePrecision, DIMENSION (L-1):: V, T

! Evaluating the elements in the LU decomposition

  W(1) = D(1)
  V(1)  = C(1)
  T(1)  = E(1)/W(1)
  DO I = 2, L - 1
    W(I) = D(I)-V(I-1)*T(I-1)
    V(I) = C(I)
    T(I) = E(I)/W(I)
```

```
  END DO
  W(L) = D(L)-V(L-1)*T(L-1)

! Forward substitution to obtain Y

  Y(1) = B(1)/W(1)
  DO I = 2, L
    Y(I) = (B(I)-V(I-1)*Y(I-1))/W(I)
  END DO

! Backward substitution to obtain Z
  Z(L) = Y(L)
  DO I = L-1, 1, -1
    Z(I) = Y(I) - T(I)*Z(I+1)
  END DO

  Return
END SUBROUTINE Tridiagonal_LE
```

Appendix D

Transom Stern Discretization

```
      !!  TY = y-coordinate of transom grid points.
     !!  Bisection = half of total vertical grid points (integer)
     !!  MVerNo = total number of vertical grid points on each station.
     Bisection = Int(MVerNo/2)
     !!!!  Transom information.....
     KL = 0
     Do I = 1, Bisection + 1 !!!  Running a loop from I = 1 to Bisection+1
     KL = KL+1
     If ((2*Bisection = MVerNo) .and.  (I = Bisection+1)) Then
     Y1 = (GVY(I,1) + GVY(I-1,1))/2.d0
     Z1 = ((GVZ(I,1) + GVZ(I-1,1))/2.d0)
     Print*, GVX(I,1),Y1,Z1 !!!  Here GVX = x-coordinates of the trnasom grid
points.
     goto 146
     Else
     EndIf
     Print*, GVX(I,1), GVY(I,1), GVZ(I,1)
     146 End Do
     Do J = 2, Bisection + 1
     KL = KL + 1
     Do I = 1, Bisection+1
     If (I == 1) Then
     TY(I,J) = GVY(1,1) - TY1*(Dble(J-1))
     Print*, GVX(I,1), TY(I,J), GVZ(1,1)
     goto 147
```

```
Else
EndIf
If (I = Bisection) Then
TY(I,J) = GVY(Bisection,1) - TYB*Dble(J-1)
Print*, GVX(I,1), TY(I,J), GVZ(Bisection,1)
goto 147
Else
EndIf
If (I = Bisection + 1) Then
Prin*, GVX(I,1), GVY(KL,1), GVZ(KL,1)
goto 147
Else
EndIf
!!!  Finding the intermediate points on the transom between LWL and
!!!  Bisection-th WL.
!!!  Linear Interpolating.......
!!!  y = y0 + (x - x0) × (y1 - y0)/(x1 - x0)
TY(I,J) = (GVY(1,1)-(TY1*(Dble(J-1)))) + ((GVZ(I,1)-GVZ(1,1))*
((GVY(Bisection,1)-(TYB*(Dble(J-1))))-(GVY(1,1)-
(TY1*(Dble(J-1)))))/(GVZ(Bisection,1) - GVZ(1,1)))
Print*, GVX(I,1), TY(I,J), GVZ(I,1)
147 End Do
End Do
END
```

Appendix E

3D Model Sample Views

E.1 Series 60, $C_b = 0.6$

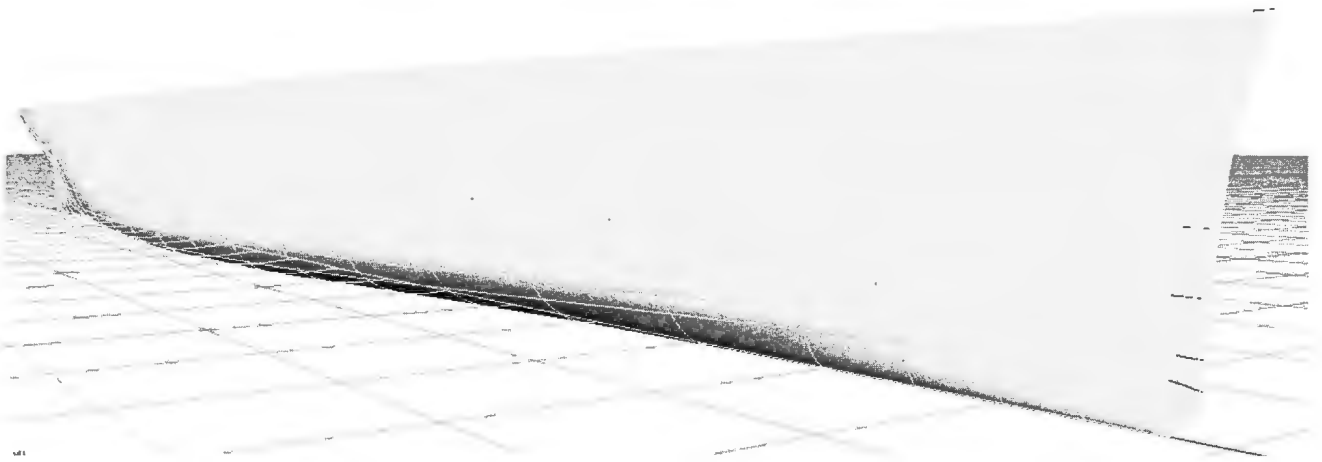

Figure E.1: Series 60, $C_b = 0.6$, 3D Model, View 1

Figure E.2: Series 60, $C_b = 0.6$, 3D Model, View 2

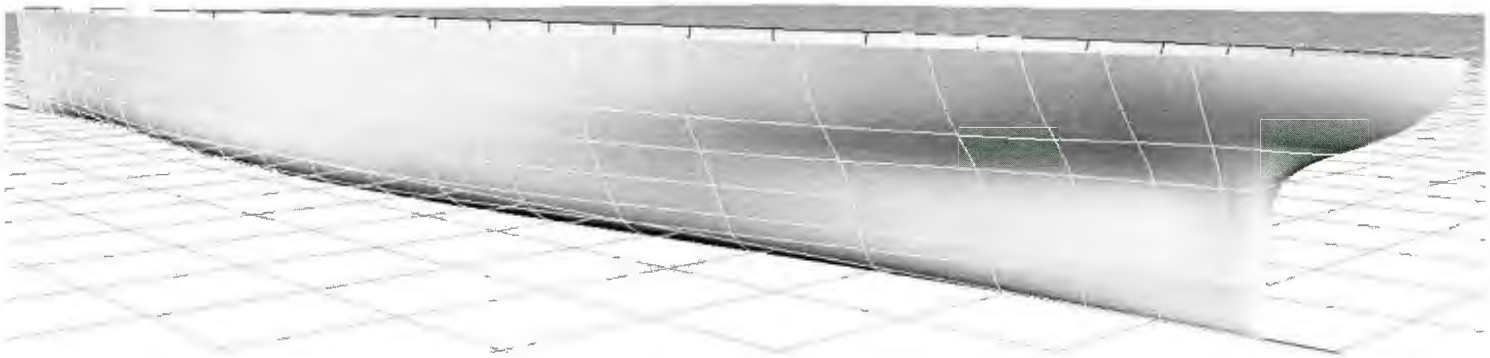

Figure E.3: Series 60, $C_b = 0.6$, 3D Model, View 3

Figure E.4: Series 60, $C_b = 0.6$, 3D Model, View 4

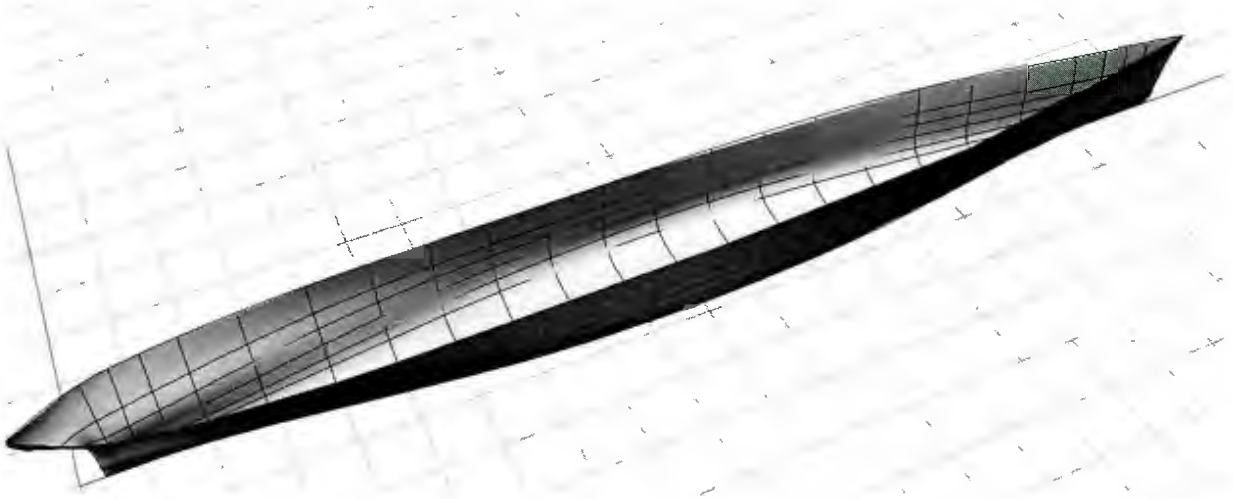

Figure E.5: Series 60, C_b = 0.6, 3D Model, View 5

Figure E.6: Series 60, C_b = 0.6, 3D Model, View 6

Figure E.7: Series 60, C_b = 0.6, 3D Model, View 7 (flat bottom)

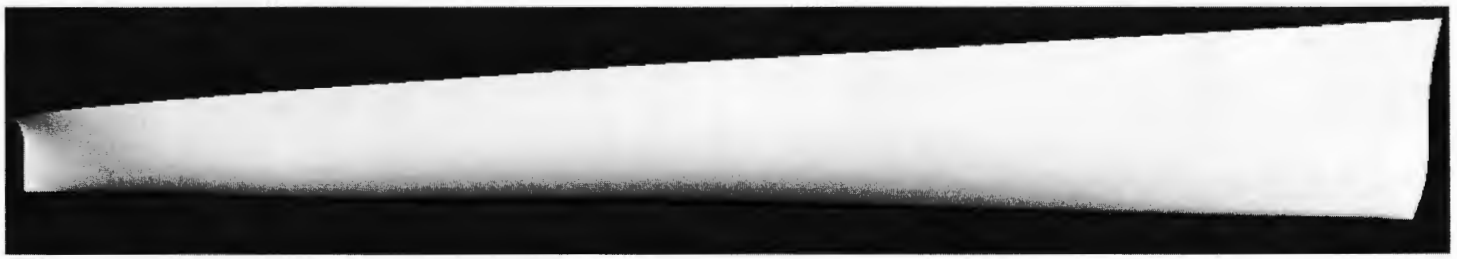

Figure E.8: Series 60, C_b = 0.6, 3D Model, View 8

E.2 AMECRC Series: Model # 1

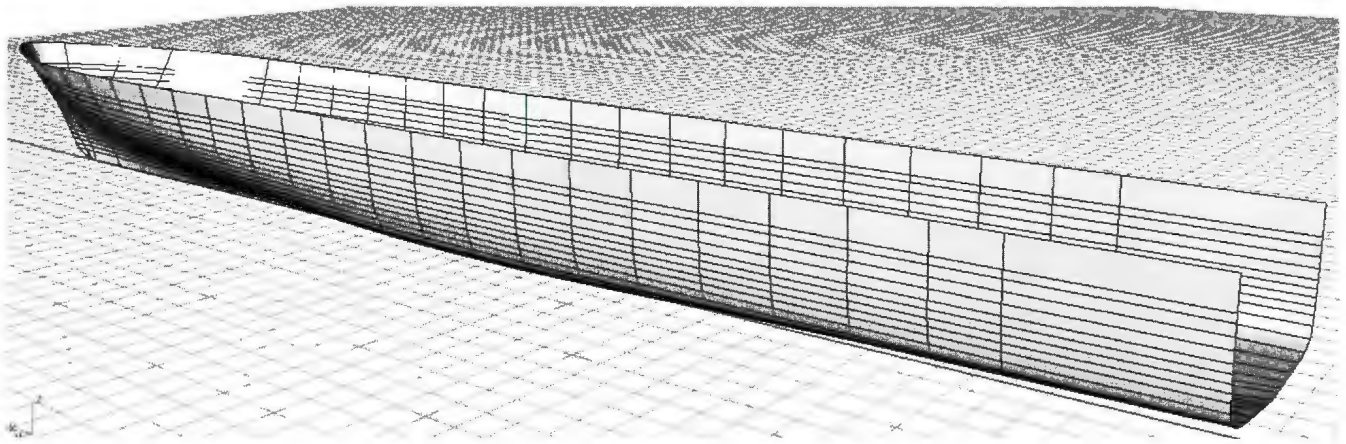

Figure E.9: AMECRC Model # 1, 3D Model, View 1

Figure E.10: AMECRC Model # 1, 3D Model, View 2

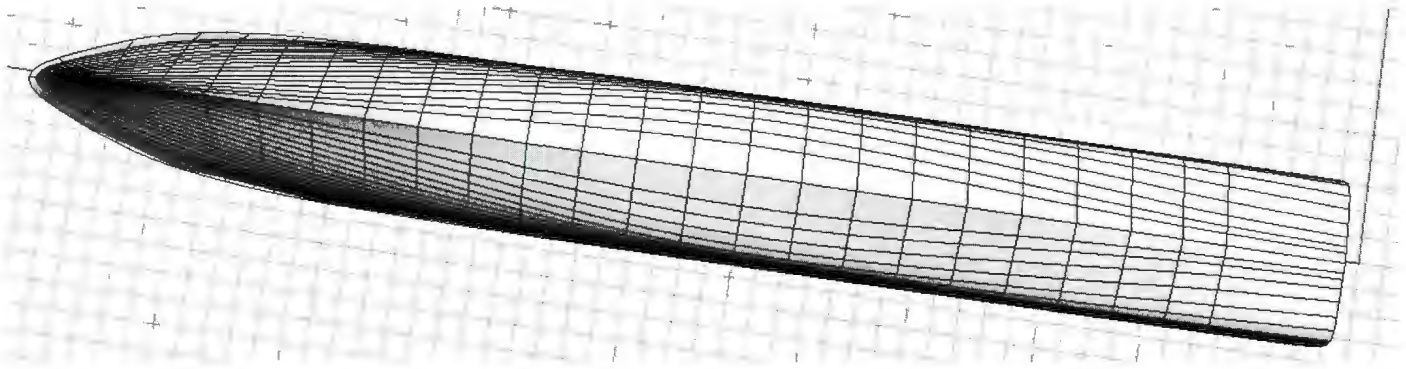

Figure E.11: AMECRC Model # 1, 3D Model, View 3 (bottom)

Figure E.12: AMECRC Model # 1, 3D Model, View 4 (bottom)

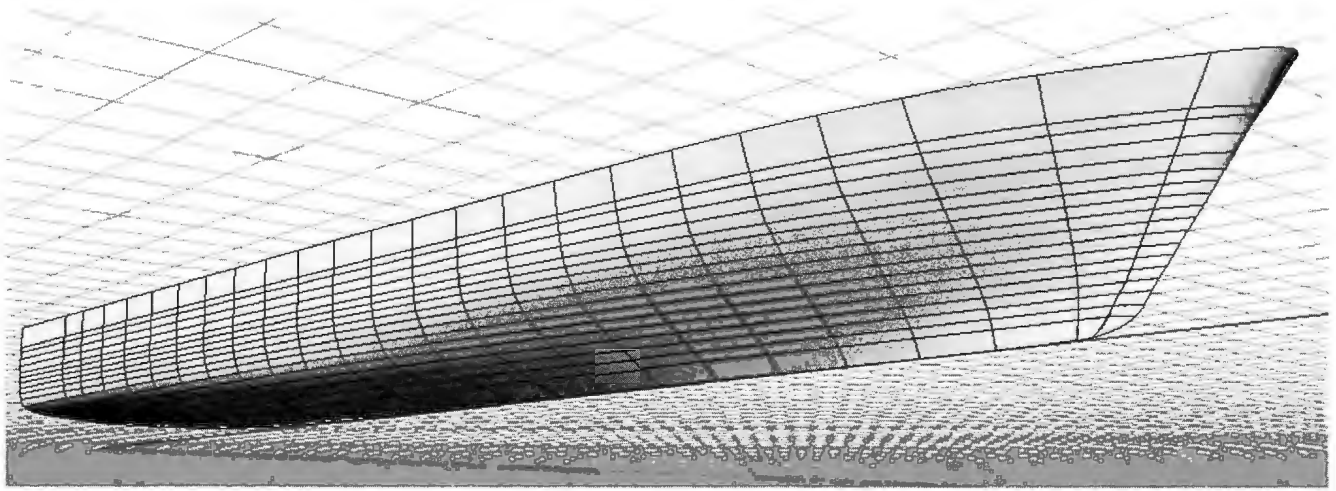

Figure E.13: AMECRC Model # 1, 3D Model, View 5

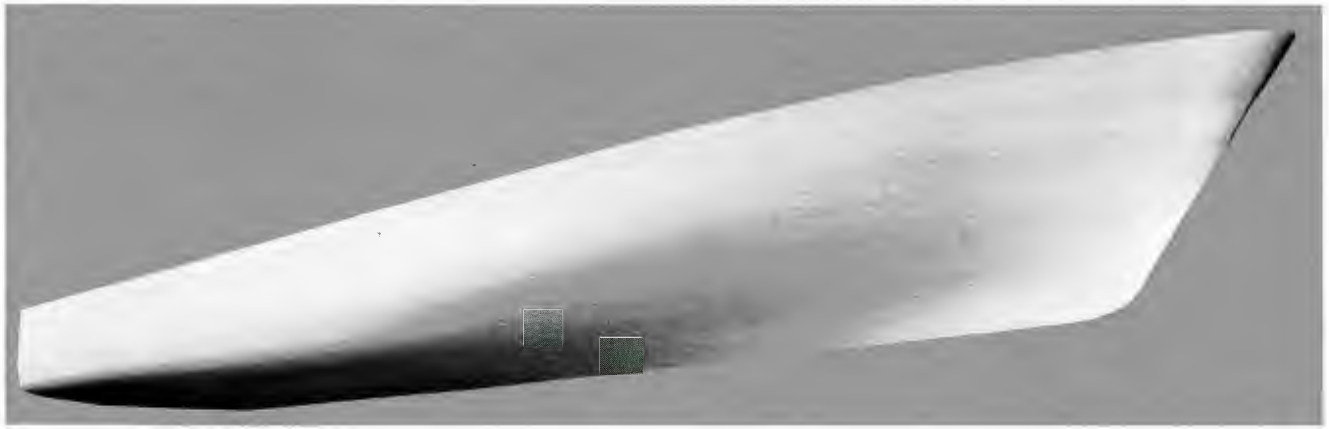

Figure E.14: AMECRC Model # 1, 3D Model, View 6

E.3 Wigley Hull: L/B = 10, L/T = 16

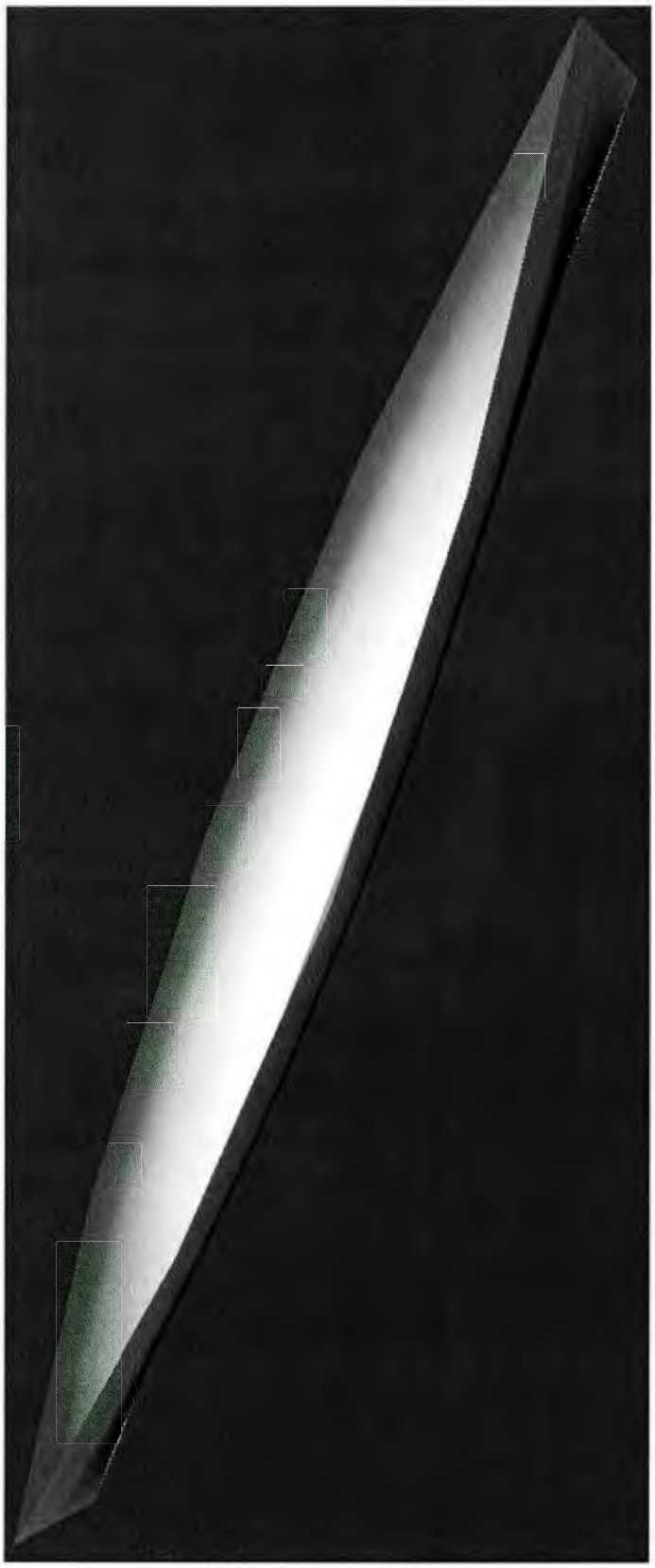

Figure E.15: Wigley Hull: L/B = 10, L/T = 16; 3d Model View 1

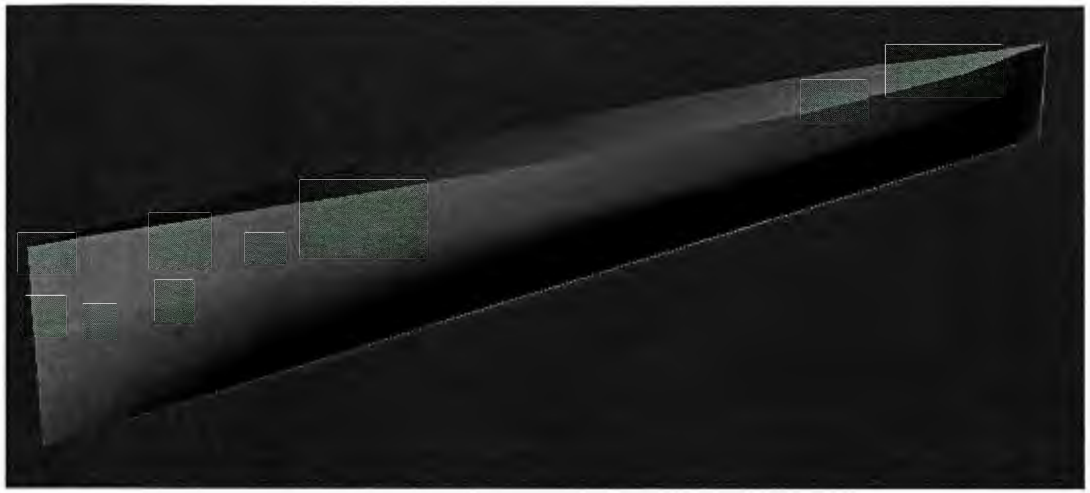

Figure E.16: Wigley Hull: L/B = 10, L/T = 16; 3d Model View 2

Figure E.17: Wigley Hull: L/B = 10, L/T = 16; 3d Model View 3 (bottom)

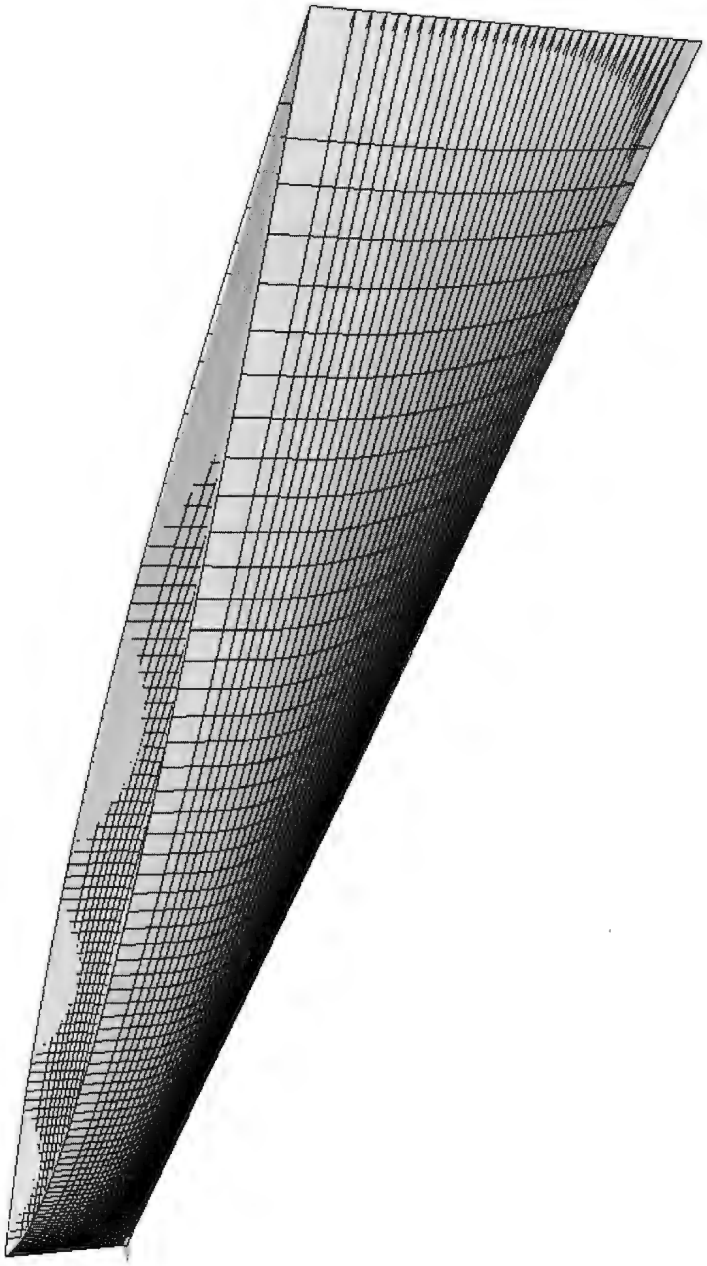

Figure E.18: Wigley Hull: L/B = 10, L/T = 16; 3d Model View 4

E.4 US Navy Combatant DTMB 5415

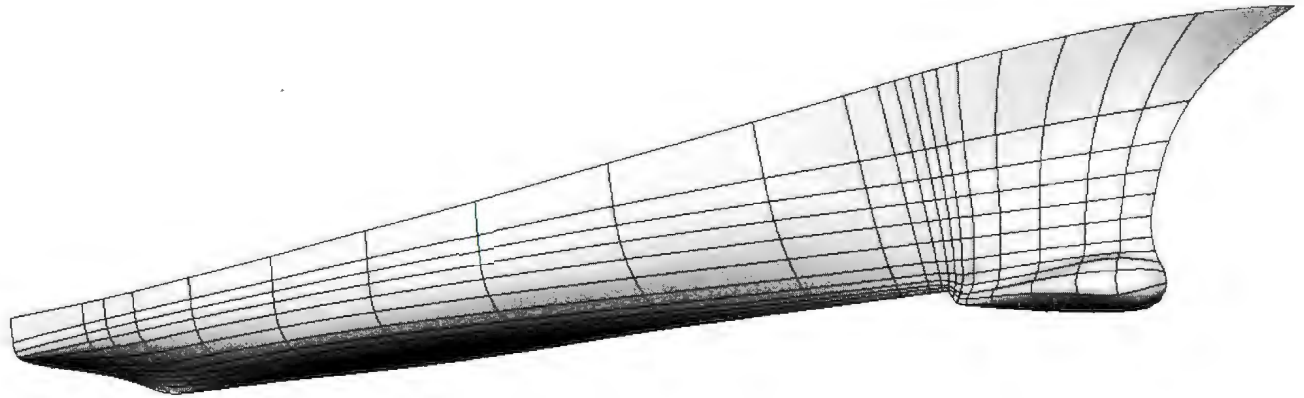

Figure E.19: DTMB 5415; 3d Model View 1

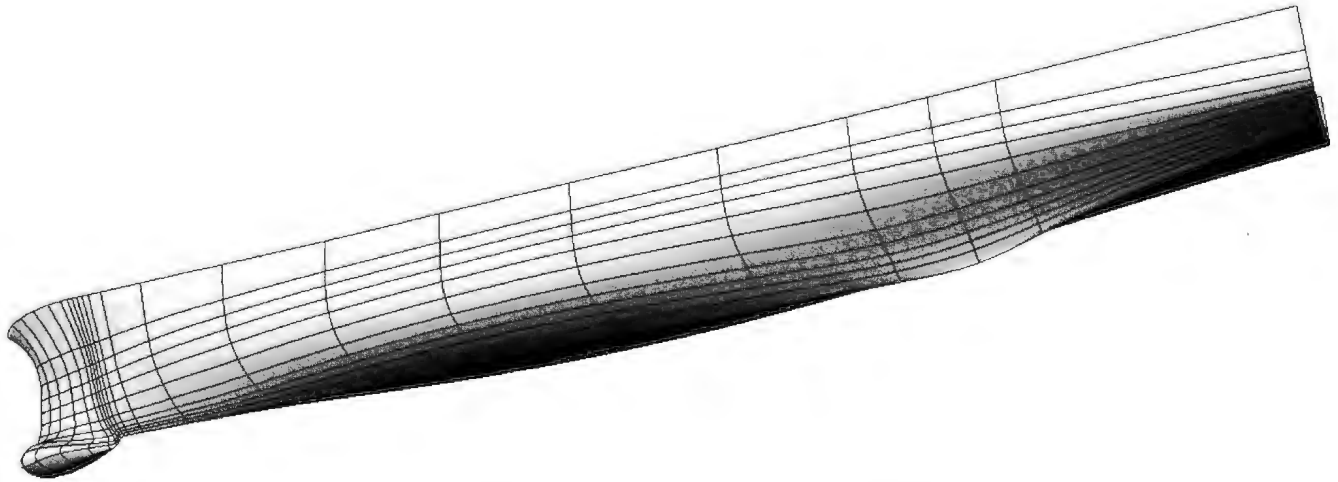

Figure E.20: DTMB 5415; 3d Model View 2

Figure E.21: DTMB 5415; 3d Model View 3

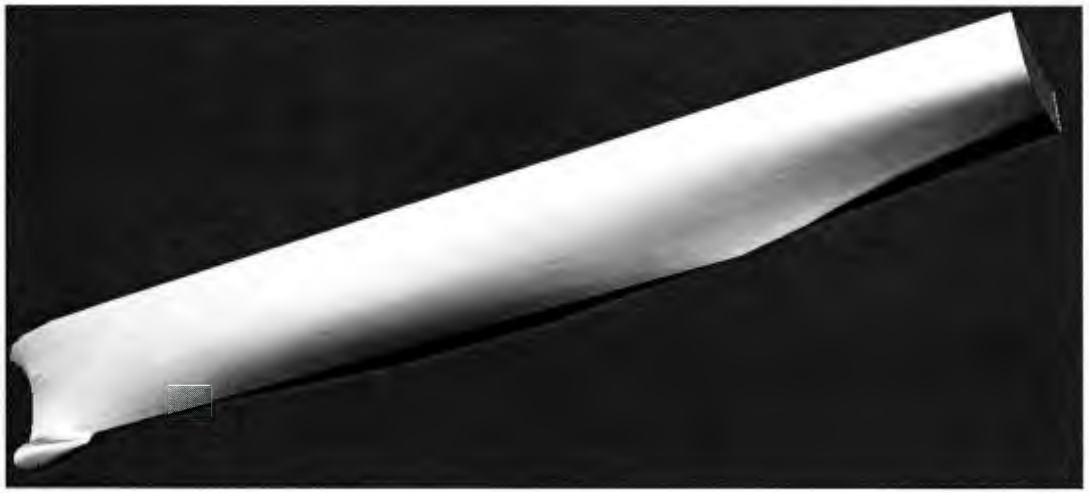

Figure E.22: DTMB 5415; 3d Model View 4

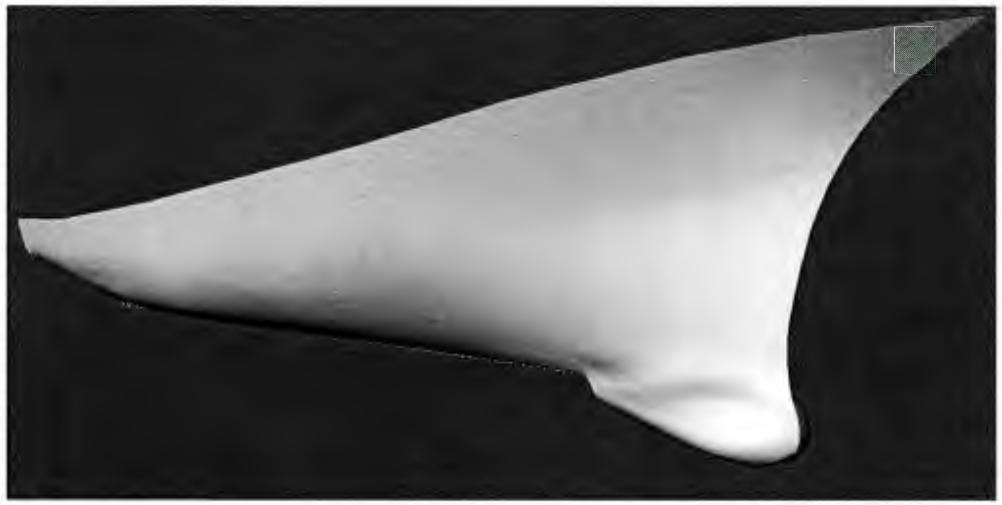

Figure E.23: DTMB 5415; 3d Model View 5

Figure E.24: DTMB 5415; 3d Model View 6